

INDIRECT DETECTION OF *BACILLUS ANTHRACIS*
(ANTHRAX) USING AMPLIFIED GAMMA
PHAGE-BASED ASSAYS

by
Robert W. Reiman

ARTHUR LAKES LIBRARY
COLORADO SCHOOL OF MINES
GOLDEN, CO 80401

ProQuest Number: 10797167

All rights reserved

INFORMATION TO ALL USERS

The quality of this reproduction is dependent upon the quality of the copy submitted.

In the unlikely event that the author did not send a complete manuscript and there are missing pages, these will be noted. Also, if material had to be removed, a note will indicate the deletion.



ProQuest 10797167

Published by ProQuest LLC (2019). Copyright of the Dissertation is held by the Author.

All rights reserved.

This work is protected against unauthorized copying under Title 17, United States Code
Microform Edition © ProQuest LLC.

ProQuest LLC.
789 East Eisenhower Parkway
P.O. Box 1346
Ann Arbor, MI 48106 – 1346

A thesis submitted to the Faculty and the Board of Trustees of the Colorado School of Mines in partial fulfillment of the requirements for the degree of Doctor of Philosophy (Applied Chemistry).

Golden, Colorado

Date 18 Dec 2006

Signed: Robert W. Reiman

Robert W. Reiman

Approved: Kent J. Voorhees

Dr. Kent J. Voorhees

Thesis Advisor

Golden, Colorado

Date 18 Dec 2006

Daniel M. Knauss

Dr. Daniel Knauss

Interim Department Head
of Chemistry and Geochemistry

ABSTRACT

The need for a simple, specific, sensitive, inexpensive, accurate, and rapid method to identify *Bacillus anthracis* became apparent during the Fall 2001 anthrax attacks which caused widespread panic and ultimately killed five individuals. The Centers for Disease Control and Prevention currently employs agar plate lysis by gamma phage and direct fluorescence assay to confirm the presence of *Bacillus anthracis*. These confirmatory methods require isolation of individual colonies from an overnight culture, are time consuming, and are best suited for laboratory environments.

The research described in this dissertation focused on applying the highly specific gamma phage lytic replication cycle to indirectly detect *Bacillus anthracis*. The production of progeny gamma phage only occurs in the presence of a suitable host, so the detection of increasing concentrations, or amplification, of progeny gamma phage implies the presence of viable *Bacillus anthracis* cells. Four unique gamma phage-based detection assays using real-time polymerase chain reaction, matrix-assisted laser desorption/ionization time-of-flight mass spectrometry, and two different designs of hand-held immunoassays based on this gamma phage amplification phenomenon were designed, developed, and experimentally tested for indirectly detecting viable *Bacillus anthracis*.

This research demonstrated that vegetative *Bacillus anthracis* was required to produce the gamma phage amplification event. Real-time polymerase chain reaction was used to detect the increased amount of gamma phage DNA produced by gamma phage amplification, and thereby indirectly detect a starting concentration of four *Bacillus anthracis* cells in less than five hours. The other three gamma phage-based detection assays were unable to indirectly detect *Bacillus anthracis*, but three of the four assays demonstrated gamma phage detection capabilities. Real-time polymerase chain reaction detected gamma phage at 1.30×10^3 pfu/mL (26 particles), matrix-assisted laser

desorption/ionization time-of-flight mass spectrometry detected gamma phage at 6.0×10^7 pfu/mL (3.0×10^4 particles), and one of the hand-held immunoassays detected gamma phage at 4.6×10^4 pfu/mL (3.4×10^3 particles). A new hand-held immunoassay will be developed using monoclonal antibodies to correct for the cross reactivity problems identified in this research.

TABLE OF CONTENTS

ABSTRACT.....	iii
LIST OF FIGURES	viii
LIST OF TABLES.....	x
LIST OF ABBREVIATIONS.....	xi
ACKNOWLEDGEMENTS.....	xiv
CHAPTER 1 INTRODUCTION.....	1
1.1 Background.....	1
1.2 Review of Anthrax Outbreaks and Attacks	3
1.3 Threat from <i>B. anthracis</i> as a Weapon of Mass Destruction.....	5
1.4 Thesis Overview	8
CHAPTER 2 CURRENT LABORATORY RESPONSE NETWORK (LRN) METHODS OF DETECTING <i>BACILLUS ANTHRACIS</i>	10
2.1 Introduction.....	10
2.2 Cell Culture/Lysis by Gamma Phage.....	11
2.3 Microscopy	12
2.4 Direct Fluorescence Assay (DFA).....	13
2.5 Real-Time Polymerase Chain Reaction (RT-PCR).....	16
2.6 Hand-Held Immunoassay (HHA).....	20
CHAPTER 3 CHARACTERIZATION OF <i>BACILLUS ANTHRACIS</i>	24
3.1 Background on <i>B. anthracis</i>	24
3.2 Morphology, Physiology and Taxonomy of <i>B. anthracis</i>	27
3.3 Safe Handling Methods	31
3.4 Growth Conditions.....	32
3.4.1 Introduction.....	32
3.4.2 Materials and Methods	34

3.4.3 Results	35
3.4.4 Discussion and Conclusions	39
3.5 Determining Titer of <i>B. anthracis</i>	40
3.5.1 Introduction.....	40
3.5.2 Materials and Methods	41
3.5.3 Results	41
3.5.4 Discussion and Conclusions	43
CHAPTER 4 CHARACTERIZATION AND AMPLIFICATION OF GAMMA PHAGE.....	44
4.1 Introduction to Bacteriophage	44
4.2 Morphology, Physiology and Taxonomy of Gamma Phage.....	45
4.2.1 Introduction.....	45
4.2.2 Materials and Methods	46
4.2.3 Results	47
4.2.4 Discussion and Conclusions	47
4.3 Propagation of Gamma Phage	48
4.3.1 Introduction.....	48
4.3.2 Materials and Methods	48
4.3.3 Results	50
4.3.4 Discussion and Conclusions	51
4.4 Concentrating and Purifying Gamma Phage	52
4.4.1 Introduction.....	52
4.4.2 Materials and Methods	52
4.4.3 Results	54
4.4.4 Discussion and Conclusions	56
4.5 Determining Titer of Gamma Phage.....	57
4.5.1 Introduction.....	57
4.5.2 Materials and Methods	58
4.5.3 Results	59
4.5.4 Discussion and Conclusions	60
4.6 Bacteriophage Amplification.....	61

CHAPTER 5 INDIRECT DETECTION OF <i>BACILLUS ANTHRACIS</i> USING REAL-TIME POLYMERASE CHAIN REACTION (RT-PCR) TO DETECT GAMMA PHAGE DNA	63
5.1 Introduction.....	63
5.2 Materials and Methods.....	64
5.3 Results.....	69
5.4 Discussion and Conclusions	74
CHAPTER 6 INDIRECT DETECTION OF <i>BACILLUS ANTHRACIS</i> USING MATRIX-ASSISTED LASER DESORPTION/IONIZATION TIME-OF-FLIGHT MASS SPECTROMETRY (MALDI-TOF-MS) TO DETECT GAMMA PHAGE PROTEINS	78
6.1 Introduction.....	78
6.2 Materials and Methods.....	80
6.3 Results.....	84
6.4 Discussion and Conclusions	89
CHAPTER 7 INDIRECT DETECTION OF <i>BACILLUS ANTHRACIS</i> USING HAND-HELD IMMUNOASSAYS TO DETECT GAMMA PHAGE	91
7.1 Introduction.....	91
7.2 Hand-Held Immunoassay 1 (HHA 1: Versions 1 and 2).....	94
7.2.1 <i>Materials and Methods</i>	97
7.2.2 <i>Results</i>	105
7.2.3 <i>Discussion and Conclusions</i>	116
7.3 Hand-Held Immunoassay 2 (HHA 2).....	118
7.3.1 <i>Materials and Methods</i>	119
7.3.2 <i>Results</i>	121
7.3.3 <i>Discussion and Conclusions</i>	123
CHAPTER 8 PROJECT ASSESSMENT AND FOLLOW-ON WORK	125
8.1 Project Overview	125
8.2 Assessment of Project.....	126
8.3 Recommended Follow-on Work.....	128
REFERENCES CITED.....	130

LIST OF FIGURES

Figure 1.0 Probability of infection versus dose for inhalation anthrax.....	7
Figure 2.0 DFA staining of <i>B. anthracis</i> cells (magnification 400x)	15
Figure 2.1 Schematic of RT-PCR process	18
Figure 2.2 RT-PCR spectra.....	19
Figure 2.3 Individual HHA cassette.....	21
Figure 2.4 HHA ticket after removal from plastic cassette	21
Figure 2.5 Possible HHA results.....	23
Figure 3.0 Model of anthrax toxin entry into eukaryotic cells	26
Figure 3.1 Gram stained colonies of <i>B. anthracis</i> Sterne	28
Figure 3.2 <i>B. anthracis</i> Sterne streak culture on TSA	29
Figure 3.3 Pasteur Institute TEM of <i>Bacillus</i> surface.....	30
Figure 3.4 Typical bacterial population growth curve.....	34
Figure 3.5 <i>B. anthracis</i> Sterne growth curve in BHI at 37 °C.....	38
Figure 3.6 <i>In vitro</i> <i>B. anthracis</i> Sterne growth	39
Figure 3.7 <i>B. anthracis</i> on 5% SBA to determine cfu/mL.....	42
Figure 4.0 TEM of CsCl purified CSM gamma phage.....	47
Figure 4.1 Propagation of gamma phage on 5% SBA plate	50
Figure 4.2 Sterile-filtered gamma phage	54
Figure 4.3 PEG purified gamma phage.....	55

Figure 4.4 CsCl purified gamma phage	56
Figure 4.5 Gamma phage plaque assay.....	59
Figure 5.0 R.A.P.I.D. [®] RT-PCR spectrum of a pure gamma phage dilution series	70
Figure 5.1 Flash Gel™ cassette-DNA marker of RT-PCR amplicons	74
Figure 6.0 MALDI-MS spectrum of CsCl purified gamma phage in Milli-Q water.....	85
Figure 6.1 MALDI-MS spectra of gamma phage dilution series for detection limit	87
Figure 6.2 MALDI-MS spectra of gamma phage dilution series for detection limit	88
Figure 7.0 Characteristic Y-shape of IgG antibody	92
Figure 7.1 EM of gamma phage particles on <i>B. anthracis</i> Sterne surface.....	95
Figure 7.2 HHA 1 version 1.....	96
Figure 7.3 HHA 1 version 2.....	96
Figure 7.4 SDS-PAGE on rabbit-anti gamma phage antibodies.....	109
Figure 7.5 Protein ladder (standards) used in SDS-PAGE	110
Figure 7.6 Isoelectric focusing gel on rabbit-anti-gamma phage antibodies	111
Figure 7.7 Colloidal gold-conjugated to gamma phage.....	113
Figure 7.8 Design of HHA 2.....	119

LIST OF TABLES

Table 3.0 <i>B. anthracis</i> growth data in TSB at 27 °C, 37 °C, and 47 °C.....	36
Table 3.1 <i>B. anthracis</i> growth data in BHI at 37 °C.....	37
Table 3.2 <i>B. anthracis</i> serial dilutions for viable plate count.....	42
Table 4.0 Gamma phage serial dilutions for plaque assay.....	60
Table 5.0 Concentrations of <i>B. anthracis</i> and gamma phage for RT-PCR.....	68
Table 5.1 Dilution series in attograms (ag) of gamma phage DNA.....	71
Table 5.2 Results of <i>B. anthracis</i> DL and MOI experiments.....	72
Table 6.0 Reaction components for gamma phage amplification (method one).....	83
Table 6.1 Reaction components for gamma phage amplification (method two).....	84
Table 7.0 Polyclonal antibody production schedule	98
Table 7.1 ELISA results on rabbit anti-gamma phage antibodies (pre and 1 st bleeds).....	106
Table 7.2 ELISA results on rabbit anti-gamma phage antibodies (final bleeds).....	107
Table 7.3 ICP-MS Au analysis of HHA strips.....	115
Table 7.4 Test HHA 2 with gamma page dilution series (5.8×10^8 pfu/mL)	122
Table 7.5 Test HHA 2 with gamma phage dilution series (2.3×10^7 pfu/mL).....	122
Table 7.6 Test HHA 2 with gamma phage dilution series (5.6×10^7 pfu/mL).....	123

LIST OF ABBREVIATIONS

Ab	antibody
ABTS	2,2'-azino-bis(3-ethyl-benzthiazoline-6-sulfonic acid)
AFIP	Armed Forces Institute of Pathology
ATCC	American Type Culture Collection
a.u.	arbitrary units
BHI	brain heart infusion
bp	base pair
BSA	bovine serum albumin
BSL	biosafety level
BW	biowarfare
CDC	Centers for Disease Control and Prevention
cDNA	complementary DNA
cfu	colony-forming unit
CSM	Colorado School of Mines
C _T	threshold cycle
Da	dalton (equivalent to atomic mass unit)
DFA	direct fluorescent assay
DL	detection limit
DNA	deoxyribonucleic acid
dNTP	deoxyribonucleotide triphosphate
DoD	U.S. Department of Defense
EDC	1-ethyl-3-(3-dimethylaminopropyl)-carbodiimide hydrochloride
EF	edema factor
ELISA	enzyme-linked immunosorbent assay
EPA	U.S. Environmental Protection Agency

FDA	Food and Drug Administration
GAO	government accountability office
GE	genome equivalent
HEPA	high-efficiency particulate air
HHA	hand-held immunoassay
HHS	U.S. Department of Health and Human Services
HRP	horseradish peroxidase
ICP-MS	inductively coupled plasma mass spectrometry
ID	identification
IEF	isoelectric focusing
Ig	immunoglobulin (another name for antibody)
LD ₅₀	lethal dose, 50% (50 percent probability of causing death)
LF	lethal factor
LFI	lateral flow immunochromatography
LRN	Laboratory Response Network
MAb	monoclonal antibody
MALDI	matrix-assisted laser desorption/ionization
MDx	Millenia Diagnostics, Inc.
MOI	multiplicity of infection
MS	mass spectrometry
MW	molecular weight
MWCO	molecular weight cutoff
m/z	mass-to-charge ratio
NASBA	nucleic acid sequence-based amplification
NIOSH	National Institute for Occupational Safety and Health
NMRC	Naval Medical Research Center
NTC	no template control
OD	optical density

PA	protective antigen
PAb	polyclonal antibody
PBS	phosphate-buffered saline
PCR	polymerase chain reaction
PEG	polyethylene glycol
pfu	plaque forming unit
pH	negative 10-base log of the positive hydrogen ion concentration
Phage	abbreviation for bacteriophage
pI	isoelectric point; the pH at which the net charge on a particle is zero
QDL	quantification detection limit
RNA	ribonucleic acid
RT-PCR	real-time polymerase chain reaction
SASP	small, acid-soluble spore protein
SBA	sheep's blood agar
SDS-PAGE	sodium dodecyl sulfate-polyacrylamide gel electrophoresis
SM	suspension medium
TEM	transmission electron microscopy
TMTC	too many to count
TOF	time-of-flight
TSA	tryptic soy agar
TSB	tryptic soy broth
USAFA	United States Air Force Academy
USAMRIID	United States Army Medical Research Institute of Infectious Diseases
USDA	United States Department of Agriculture
USPS	United States Postal Service
UV	ultraviolet
WMD	weapons of mass destruction

ACKNOWLEDGEMENTS

First and foremost I thank our God who said, “I am the vine; you are the branches. If a man remains in me and I in him, he will bear much fruit; apart from me you can do nothing” (John 15:5). If anything good comes from these three years of labor, Jesus owns the credit for providing me just enough strength and perseverance.

Second, I thank the Air Force and the Air Force Academy. They provided my initial college academic foundation, and then showed their continued confidence in me by sponsoring my Ph.D. program. I gave my best academic effort in honor of my “brothers-in-arms” who deployed around the world, away from loved ones, so I could pursue this academic endeavor. This academic achievement pales compared with their daily heroic efforts and sacrifices.

Third, I thank my family. My wife Linda and my three daughters Jessica, Heather and Samantha are the great loves of my life. I appreciate the sacrifices you all have made throughout my career. The military life has not been easy, but returning home to “my four girls” has always made the difficulties and absences seem insignificant. To my mother Rita and stepfather Bob who died 18 July 2006, I appreciate you both cheering my academic and military accomplishments. I only wish I could have one more round of golf and another beer with Bob, but I know you are smiling from heaven. To my dad Stewart who once asked, “What are you going to do with a chemistry degree?” I still do not know where these chemistry degrees will ultimately take me, but it has been an incredible ride so far. I thank you and my stepmother Terri for the love, support and discipline you both provided me growing up. To my parents-in-law, Jack and Elizabeth, thank you for sharing your daughter with me and for making the effort to visit us wherever the Air Force sent us. Besides being family, we will always be connected by our service in the greatest Air Force ever.

Fourth, I thank the people at CSM that made my learning experience so positive. Thank you, Dr. Voorhees for taking me into your research group under very challenging time constraints. You provided sound advice, strong mentorship, listened to many practice presentations, and never gave up on me throughout this journey. I was honored to work for you. Thank you, Dr. MacCarthy for always having a few minutes to talk throughout my time at CSM. You were a major influence in my selecting CSM and an inspiration to me while I was there. Thank you, George Klinger and John Dane for the helpful suggestions you both made during all my practice presentations. John, I hope you keep working out at the gym without me; it will pay lasting dividends to both your health and your sanity. I also thank my committee, Dr. Bird, Dr. Cowley, Dr. Eberhart, Dr. MacCarthy, and Dr. Voorhees. You all molded and mentored me into a lean, mean chemistry machine. Maybe not, but you all devoted your time and expertise to me. I cannot thank you enough for that voluntary gift.

Last, but definitely not least, I thank Lt. Col. (Dr.) Dan Atchley. I entered into a field of research that I had no prior experience in, except for getting stuck with the anthrax vaccine. The heavy emphasis on microbiology and biochemistry made me feel extremely vulnerable. You stepped in as a mentor, a friend, and an “expert” in the field that I could always rely on. You never really had the free time, but you made yourself available for me. I am thankful that you and your family came into our lives back in 1993 and now am greatly indebted to you for helping me become proficient in another area of chemistry.

CHAPTER 1

INTRODUCTION

1.1 Background

Bacteria are small free-living organisms called microorganisms or microbes that have been around for billions of years and are given a two-part scientific name; the first being the genus and the second being the species. Bacteria are prokaryotes, organisms that lack a membrane enclosed nucleus, which can usually be grown on solid and/or in liquid culture media. These prokaryotic microorganisms have structures consisting of nuclear material (nucleoid and plasmids), cytoplasm, cytoplasmic membrane, and possibly a cell wall; these structures are composed primarily of proteins, nucleic acids, lipids and polysaccharides. The cell wall gives bacteria their characteristic shapes of spherical, rod-shaped, or spiral. As living microorganisms, bacteria utilize environmental nutrients, transform them and eliminate waste (metabolism), and reproduce by simple binary division. Bacteria are about one-tenth the diameter (0.2 μm to 750 μm) of most cells in our body. Antoni van Leeuwenhoek, an amateur microscope builder, was the first documented person to see bacteria in 1676; however, it would be through Robert Koch's Postulates published in 1884 that the link between specific bacteria and a specific infectious disease was definitively established [1].

Bacillus anthracis, the etiologic agent of anthrax, is an endospore-forming gram-positive bacillus that affects both animals and humans. The need for a simple, specific, sensitive, inexpensive, accurate, and rapid method to identify *B. anthracis* became apparent during the Fall 2001 anthrax attacks which caused widespread panic and ultimately killed five individuals. Tragically, the two critical questions that needed to be answered quickly - were the discovered powders *B. anthracis* and were the spores viable

- took days to answer. The events of 2001 resulted in a national urgency directed towards preventing, or at least minimizing, the consequences of any future bioterrorist attack by improving our early detection and identification methods. The Centers for Disease Control and Prevention (CDC), a national laboratory in the Laboratory Response Network (LRN), employed confirmatory tests for *B. anthracis* require isolation of individual colonies from an overnight culture. Suspect colonies of *B. anthracis* are then confirmed either via a direct fluorescence assay (DFA) for a *B. anthracis*-specific capsular protein and plate lysis by gamma phage or via a capsular DFA and a *B. anthracis*-specific cell wall component DFA [2]. These tests require highly skilled technicians, can take 16 to 20 hours beyond the time required for initial isolation culture for plate lysis by the gamma phage, require special handling of reagents, and are not well suited for field environments.

The overall goal of the application-based research described in this dissertation was to design, develop, and assess gamma phage amplification assays to indirectly identify *B. anthracis*. The objectives used to achieve this goal were: 1) to characterize the gamma phage/*B. anthracis* system in terms of morphology, physiology and optimal growth conditions; 2) to propagate and highly purify gamma phage for antibody development; 3) to design and develop assays using the gamma phage amplification phenomenon to indirectly identify *B. anthracis*; and 4) to assess the gamma phage-based assays in terms of simplicity of use, cost, speed, specificity, detection limit (DL), and reproducibility. The assays described in this dissertation used real-time polymerase chain reaction (RT-PCR), matrix-assisted laser desorption/ionization time-of-flight mass spectrometry (MALDI-TOF-MS), and two different designs of hand-held immunoassays (HHAs) to indirectly identify *B. anthracis* using its highly selective bacteriophage called gamma phage. These gamma phage-based assays could supplement or, in some cases, replace the assays currently being used to detect *B. anthracis* in a biological incident or attack. The advantages of using gamma phage amplification assays to indirectly detect *B. anthracis* compared with the direct detection of *B. anthracis* should include: 1) more

rapid detection; 2) improved specificity; 3) lower detection limit; 4) no requirement for overnight bacterial culture; and 5) only viable *B. anthracis* is detected.

1.2 Review of Anthrax Outbreaks and Attacks

Anthrax has had a major impact on human history and was even mentioned in early Egyptian, Roman, and Greek writings. For example, two of the ten plagues written about in the Bible (Exodus) had symptoms similar to anthrax. Anthrax was a major human and livestock disease in Europe from the 16th through the 19th centuries with the 1613 pandemic, referred to as “black bane”, killing more than sixty thousand people and a massive number of livestock. During the mid-1880’s, anthrax epidemics became common among workers who processed animal hides and wool, so these outbreaks became known as “woolsorters’ disease”. Both the Germans and the Japanese used anthrax as a biowarfare agent; the Germans targeted livestock in several countries during World War I and the Japanese conducted experiments in Manchukuo Unit 731 that killed over 10,000 Chinese and Soviet prisoners from 1933 to 1945 with anthrax and other infectious diseases [3]. In 1942, the British proved that *B. anthracis* spores survived and maintained their virulence after being detonated in bombs. During World War II, the U.S. military experimented with *B. anthracis* at Camp (now Fort) Detrick and “weaponized” it in the 1950’s and 1960’s before President Nixon halted our offensive biowarfare program in 1969. Approximately 220 pounds of “weaponized” *B. anthracis* was later destroyed. In 1979, an accidental release of *B. anthracis* spores at a Soviet Army biological research facility upwind of the town of Sverdlovsk killed 66 people due to the resulting anthrax outbreak [4]. In 1993, Aum Shinrikyo’s cult members released *B. anthracis* spores around Tokyo using sprayers mounted on vans; luckily, no anthrax was contracted because the cult had used an attenuated unencapsulated strain [3].

The Fall 2001 anthrax attacks in the U.S. started September 18 with letters containing *B. anthracis* spores being sent to Peter Jennings at ABC news, Tom Brokaw at

NBC news, Dan Rather at CBS news, and to the New York Post editor; a total of 12 people including a seven month baby became ill but recovered after medical treatment [3]. Then on October 5, a photo editor at American Media Inc. in Boca Raton, Florida died of inhalation anthrax after *B. anthracis* was isolated from his spinal fluid and blood two days earlier. On October 15, two letters were delivered to the Hart Senate Office Building addressed to Senators Daschle and Leahy; one was opened by an intern of Senate Majority leader Tom Daschle. Subsequently in separate exposures, five postal workers in Washington D.C. became ill; two of those later died of inhalation anthrax. The pattern that developed was the use of letters delivered through the regular mail with return addresses in New Jersey that spilled fine powder. Later tests showed that the white powder was the highly virulent *B. anthracis* Ames strain. On October 31, a New York City hospital worker died from anthrax and on November 21, a 94 year old woman from Oxford, CT also died from anthrax. Both of these individuals had the inhalation form of anthrax that was speculated to have been caused by cross-contaminated mail.

Considering only the Hart Office exposures, over 6,000 nasal swabs were tested in the Capitol physician's office along with thousands of environmental cultures that were taken over several days. The final results of the nasal swabs tests showed that 28 people had been exposed to anthrax [5]. The LRN laboratories were overwhelmed with testing over 125,000 environmental specimens from the Fall 2001 attacks that resulted in more than one million individual tests [6]. All six letters were processed through the United States Postal Service (USPS) processing and distribution center in Trenton, New Jersey and two of the six had been further sorted through the Brentwood mail center in Washington, D.C. The final tallies in the Fall 2001 anthrax attacks were 22 individuals contracted anthrax across four states (eleven each from inhalation and cutaneous); five people, including two Washington D.C. postal workers, died from inhalation anthrax.

The agencies involved in collecting samples used a variety of methods to collect samples including dry swab, wet wipes, premoistened synthetic (noncotton) swabs, and high-efficiency particulate air (HEPA) vacuums [6]. The Hart Senate Office Building

and several postal facilities were closed, sealed, and decontaminated with chlorine dioxide to kill the *B. anthracis* spores at a cost of over \$35 million [7]. Last year on March 14 2005, the Department of Defense (DoD) had preliminary false positive *B. anthracis* detections at the Pentagon's Defense Post Office in Fairfax County, resulting in facility closures and interagency confusion [6]. Senator Bill Frist, in "When Every Moment Counts", recounts some lessons learned from our Fall 2001 anthrax attacks. He says, "We learned that every moment counts when terrorists turn a deadly agent into a weapon against us...Gaps in our public health system-the result of twenty years of neglect and underinvestment - became glaringly apparent" [5].

1.3 Threat from *B. anthracis* as a Weapon of Mass Destruction

Biological, chemical, and nuclear weapons are collectively called Weapons of Mass Destruction (WMD) because of the indiscriminate large-scale casualties these weapons are capable of producing. A study conducted in 1993 by the U.S. Congressional Office of Technology Assessment determined that 100 kg of *B. anthracis* spores delivered by a single airplane over a city like Washington, D.C. on a clear and calm night would cause between one and three million deaths [8]. President George W. Bush said in the National Security Strategy of the United States of America dated September 17, 2002 [9]:

The gravest danger our Nation faces lies at the crossroads of radicalism and technology. Our enemies have openly declared that they are seeking weapons of mass destruction, and evidence indicates that they are doing so with determination. The United States will not allow these efforts to succeed. We will build defenses against ballistic missiles and other means of delivery. We will cooperate with other nations to deny, contain, and curtail our enemies' efforts to acquire dangerous technologies. And, as a matter of common sense and self-defense, America will act against such emerging threats before they are fully formed. We cannot defend America and our friends by hoping for the best. So we must be prepared to defeat our enemies' plans, using the best intelligence and proceeding with deliberation. History will judge harshly those who saw this coming

danger but failed to act. In the new world we have entered, the only path to peace and security is the path of action.

Although nuclear weapons took center stage focus during the Cold War with the Soviet Union and chemical weapons were used extensively by Iraq during the Iran-Iraq War from 1980-1988, it was a biological weapon that was used in the Fall 2001 U.S. anthrax attacks. The risk of *B. anthracis* being used as a WMD had been assessed by our national leadership as high based on high availability, high stability, medium for deliverability, and high for lethality [5]. Easy access to *B. anthracis* had been curtailed in the U.S. after the discovery that the American Type Culture Collection (ATCC) shipped several strains of *B. anthracis* to Iraq in the 1980's [10]; however, foreign microorganism banks were unaffected and *B. anthracis* spores could still easily be obtained from any previously contaminated site. *B. anthracis* can be prepared and used in either liquid or dry form; although the liquid form is easier to produce, it is much more difficult to disseminate into small aerosol droplets.

For maximum effectiveness, *B. anthracis* would be “weaponized” and delivered as an aerosol with particles 1 to 5 microns in diameter to penetrate the lungs most effectively [6]. “Weaponized” *B. anthracis* means it has been specially processed to maximize lethality and is identified by its properties that include: exceptional purity, highly virulent strain, high spore concentration (millions of spores per gram), uniform and very small particle size, low electrostatic charge, and treated with silica to reduce clumping [11]. Reaerosolization studies in the Hart Senate Building showed 80% of the spores were 0.95 um to 3.5 um [12]. One could hold trillions of “weaponized” spores in your hand if they were 1 to 5 microns with no electrostatic charge [6]. The U.S. Army Medical Research Institute of Infectious Diseases (USAMRIID) studies using aerosol *B. anthracis* Ames to infect monkeys found that 8,000 to 50,000 spores caused the inhalation form of the anthrax disease and resulted in death; these numbers of spores can be inhaled in a single breath [10]. Referring to these monkey studies with an assumption that untreated inhalation anthrax results in death, DoD reports a human LD₅₀ (lethal dose,

50%) of 8,000 to 10,000 spores for inhalation anthrax as shown graphically in Figure 1.0 [13] below.

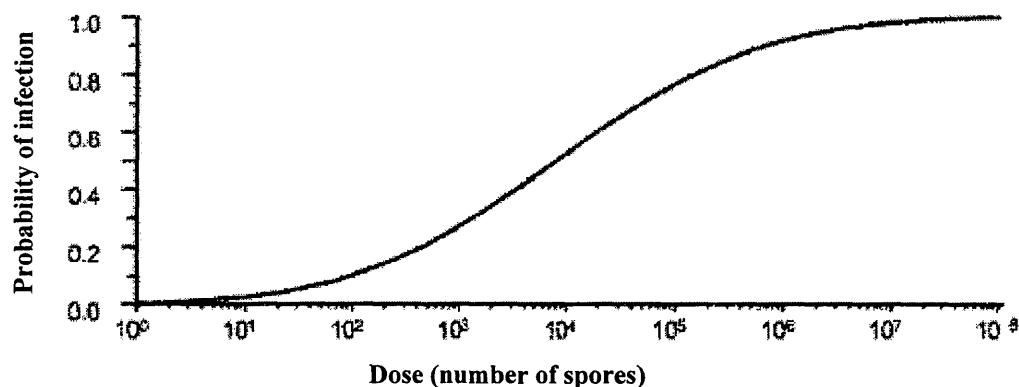


Figure 1.0 Probability of infection versus dose for inhalation anthrax

The LD₅₀ is the dose of spores required to kill half the people that are exposed. The probability of infection, shown on the y-axis in Figure 1.0, at 0.5 is used as the LD₅₀ because inhalation anthrax is generally 100% fatal without previous vaccination or aggressive antibiotic treatment after exposure.

The CDC now “regulates the possession, use, and transfer of select agents and toxins”; these agents and toxins are classified as “select” if they “have the potential to pose a severe threat to public health and safety” [14]. *B. anthracis* is on both the U.S. Department of Health and Human Services (HHS) and the U.S. Department of Agriculture (USDA) lists of select biological pathogens and toxins. Fortunately anthrax is not a contagious disease, so it cannot be passed from person to person; however, *B. anthracis* is one of six pathogens classified by the CDC as Category A or high-priority biological threat agents that include organisms that pose a risk to national security because they [15]:

- can be easily disseminated or transmitted from person to person;
- result in high mortality rates and have the potential for major public health impact;
- might cause public panic and social disruption; and
- require special action for public health preparedness.

“Weaponized” *B. anthracis* has now been used in a bioterrorist attack here in the U.S. Luckily for many Americans, this was a very limited scale attack meant to cause panic and confusion more than mass casualties.

1.4 Thesis Overview

After firmly establishing what anthrax is and the threat that *B. anthracis* poses to the world as a WMD, current LRN methods used in detecting *B. anthracis* are reviewed in Chapter 2. LRN methods directly detect *B. anthracis* as either a presumptive or a confirmatory identification. Any positive presumptive test must be followed up with a confirmatory test. Next, in Chapters 3 and 4 respectively, the *B. anthracis* bacterium and the gamma phage bacteriophage are characterized by their morphology, physiology and taxonomy. Additional information covered includes: anthrax disease-causing mechanism, safe handling methods, determining titers, growth or propagation conditions, concentration and purification methods, and gamma phage amplification procedures. In Chapters 5 through 7, four unique gamma phage-based detection assays based on the bacteriophage amplification phenomenon are introduced, experimentally tested, and assessed for their effectiveness in indirectly detecting viable *B. anthracis*. The usefulness of the four gamma phage-based detection assays are addressed in terms of their simplicity, cost, speed, specificity, DL, and reproducibility as well as through comparisons with current LRN methods that directly detect *B. anthracis*. Assay specificity is the ability to accurately discriminate between *B. anthracis*, or gamma phage, and other antigens. Assay cross reactivity with other antigens could produce either false positive or false negative results, so additional sample matrices and

microorganisms were tested to determine the proposed assay specificity. Host range experiments are typically conducted to ensure all *B. anthracis* strains are detected with a particular assay; however, these studies will be conducted at a later date when proper clearances can be obtained that grant access to these dangerous pathogens and the facilities to safely work with them. Assay DL, also referred to as sensitivity in the microbiology field, is the minimum number of microorganisms required to give a positive test result. Achieving low assay DLs is critical, given the small number of microorganisms necessary to cause the anthrax disease, in minimizing the possibility of false negatives that can put people at risk of death and severely hurt the credibility of the assay. Assay reproducibility is ability to produce the same results under the same test conditions. An emphasis was made to run all assays in triplicate, unless material or cost limited, to show reproducibility in all results. Throughout the experimental testing of all four gamma phage-based assays, both negative and positive sample controls were run to ensure the assays were performing as expected. Lastly in Chapter 8, an overview and assessment of the research work is given, followed by recommendations of where further research should be focused.

CHAPTER 2

CURRENT LABORATORY RESPONSE NETWORK (LRN) METHODS OF DETECTING *BACILLUS ANTHRACIS*

2.1 Introduction

This chapter reviews the methods currently utilized by the LRN to detect *B. anthracis*. The LRN was established by the CDC in 1999 as a national network of laboratories that could respond to biological and chemical terrorism. It has since grown to more than 140 laboratories that are designated according to their capabilities and certifications. The “national” laboratories that include the CDC, USAMRIID, and the Naval Medical Research Center (NMRC) conduct definitive characterization of strains; “reference” laboratories confirm the presence of threat agents; and “sentinel” laboratories recognize and refer potential agents to higher level laboratories [16]. Most LRN approved methods to detect *B. anthracis* are considered presumptive tests, meaning they are non-confirmatory tests used to screen for the presence of *B. anthracis*. All presumptive positive samples would then be referred to a qualified laboratory for confirmatory testing that involves cell culture with gamma phage lysis and direct fluorescence assay. LRN detection methods will be described and discussed with an emphasis on how the methods work and providing information on cost, assay speed, false alarms, specificity, DL and reproducibility. Although the LRN supplies critical detection capability, it would be irresponsible to rely exclusively on LRN laboratories and their laboratory-based methods. First responders need the training and the technology to conduct field screening. According to Dr. Charles Gallaway of the Defense Science and Technology Office, the Chemical and Biological Defense Program requires extremely

portable deployable diagnostic capabilities that are easy to operate with minimal logistical requirements.

2.2 Cell Culture/Lysis by Gamma Phage

The CDC culture method with gamma phage lysis is accepted as the “Gold Standard” in positive identification of *B. anthracis* and is currently one of the methods used in confirmatory tests [17]. To conduct the gamma phage lysis assay [18], the bacterial isolates must first be cultured overnight on 5% SBA to select *B. anthracis* colonies from a potentially mixed bacterial population. Both positive (*B. anthracis* Pasteur) and negative (*B. cereus*) controls are run along with samples of the unknown. Approximately one millimeter (mm) bead of cells from an individual bacterial colony, thought to be *B. anthracis*, are then spread on a 5% SBA plate (Petri dish) previously divided into quadrants in close horizontal streaks using a 1 μ L loop in the first plate quadrant of the plate followed by repeating the horizontal streaks in the second quadrant (lower concentration of bacteria) using the same loop. The two other plate quadrants are used for isolation streaks to test for bacterial purity. Five μ L of gamma phage suspension is pipetted on the centers of the horizontal streaks; plates are marked and incubated at $35\text{ }^{\circ}\text{C} \pm 2\text{ }^{\circ}\text{C}$ for 20 ± 4 hours. A positive assay would result in plaque formation seen as a 5 to 10 mm clearing in the confluent bacterial lawn at the site of gamma phage inoculation. Test results are only valid if the positive control plate also produces a 5 to 10 mm clearing after incubation and the negative control produces no clearing.

The cost to run a cell culture with gamma phage lysis is minimal (several dollars), but is very dependent on having reliable gamma phage stocks readily available. These traditional microbiological methods typically require between 18 to 24 hours to obtain results, are highly dependent on bacterial growth rates, and are subject to human error when selecting the growth of *B. anthracis* from the plate [6]. Plaques, or clearings, can sometimes be visible against the opaque bacterial lawn after only 6 hours, but these

clearings typically take between 12 and 16 hours to develop. The culture method requires that the sampled *B. anthracis* spore suspension germinate on 5% SBA to isolate individual colonies prior to the gamma phage lysis test. To germinate, the biological integrity of the sample must be maintained throughout sample collection, transportation, and analysis; failure to preserve the viability of a sample could lead to false negatives. A USAMRIID study screening 51 independent *B. anthracis* (including two known non-susceptible strains) and 49 other *Bacillus* species and strains assayed with plate culture and gamma phage lysis showed 98 % specificity for *B. anthracis* [18]. Theoretically one bacterium, referred to as a colony forming unit (cfu), can produce a colony when streaked on solid growth media so the culture method is potentially more sensitive (lower DL) than most other methods for the detection of *B. anthracis*. DLs are not typically reported with this culture method because the overnight isolation culture allows for additional bacterial growth that is then used to form the confluent bacterial lawn. Studies have shown that various *B. anthracis* strains may differ in their response to gamma phage and are sensitive to bacterial inoculum levels (first quadrant compared with second quadrant); for example, the Sterne strain formed more clearly defined plaques in the first quadrant [18].

2.3 Microscopy

Three types of stains are typically used for preparing samples to be viewed under a microscope; they are the Gram stain, India ink stain and M'Fadyean (polychrome methylene blue) stain. Microscopic methods are considered presumptive identification methods because of the large number of similar looking bacilli. Grown *in vivo*, *B. anthracis* forms short chains while the bacilli form very long strings when grown *in vitro*. To perform a Gram stain, a slide is fixed with an unknown sample either by heat or adding methanol then immersed in a series of solutions that include a purple dye (gentian violet), ethanol, iodine, and a pink dye (safranin). Bacteria that retain the crystal violet

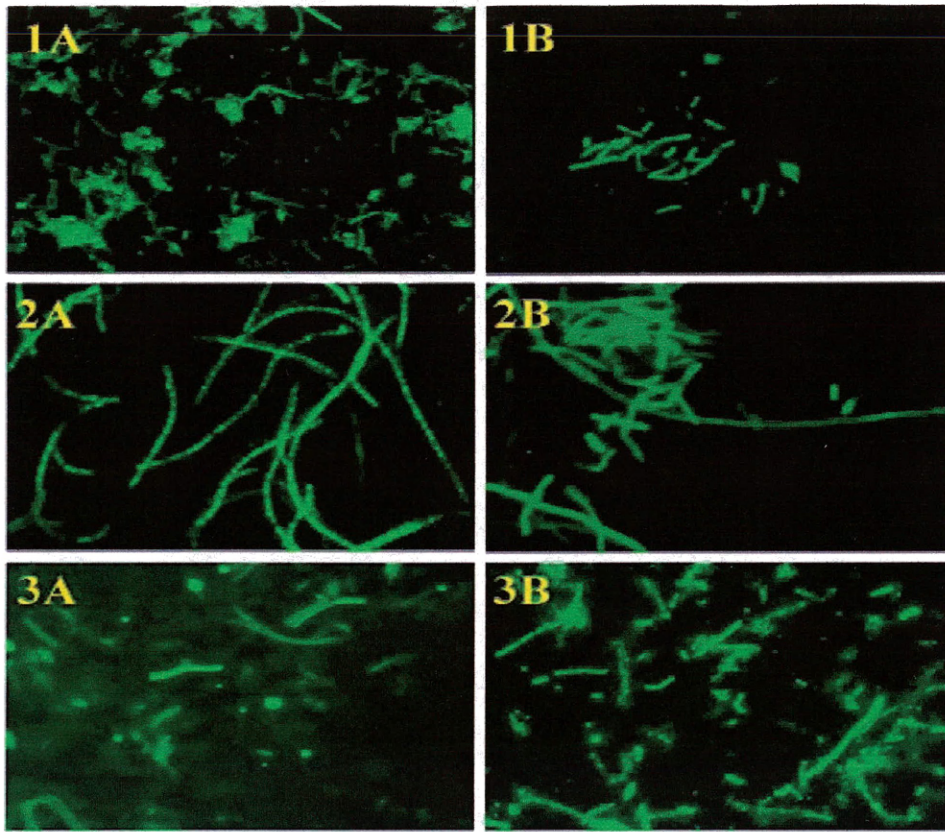
color of the primary Gram stain are considered gram-positive. *B. anthracis* is a gram-positive rod-shaped bacterium that would appear as violet blue rods containing colorless oval spores when viewed under a microscope. The India ink stain is used to view the poly-D-glutamic acid capsule of *B. anthracis*. This capsule is a gel or slime layer that covers the surface of a virulent vegetative *B. anthracis* cell and protects it from the host immune system. The India ink stain is done by transferring 5-10 μL of the unknown sample to a slide, placing a cover slip on the drop, then adding 5-10 μL of India ink to the edge of the cover slip, and then viewing under a 100X oil immersion objective [19]. Since the India ink does not penetrate the capsule, the capsule appears as a well-defined light zone around the cell against a black background. The M'Fadyean stain is conducted similarly to the India ink stain, but stains both the capsule and the bacilli. When viewed under a microscope, the M'Fadyean stain used on blood containing *B. anthracis* would show pink capsules surrounding dark blue 'box-car' bacilli [20].

These microscopic methods require an initial monetary investment of several hundred dollars for equipment, but then require very little money to operate. The three staining processes discussed above, take less than 15 minutes to conduct and results could be available shortly thereafter. Capsules are produced by other bacilli, but the presence of a capsule could be used to distinguish *B. anthracis* from *B. cereus* and *B. thuringiensis* since they are close relatives to *B. anthracis* that do not synthesize a capsule. Although not specific to *B. anthracis*, these microscopic methods are very sensitive in that they only require one microorganism to be stained for presumptive identification (low DL). Using fresh reagents, reproducibility of the staining process is typically considered excellent.

2.4 Direct Fluorescence Assay (DFA)

The CDC employed confirmatory tests require isolation of individual colonies from an overnight culture. Suspect colonies of *B. anthracis* are then confirmed via a

DFA for a *B. anthracis*-specific capsular protein (CAP-DFA) and a *B. anthracis*-specific cell wall component DFA (CW-DFA) [2]. CAP-DFA procedures are conducted as detailed below [2]. A 10 μL loop of suspected *B. anthracis*, *B. anthracis* Pasteur, and *B. cereus* fresh growth from 16 to 20 hour incubated SBA plates are separately suspended in 450 μL heart infusion broth supplemented with horse blood and 0.8% NaHCO_3 then incubated for three hours at 35-37 $^\circ\text{C}$. Forty-five μL of these suspensions are then placed into three microcentrifuge tubes labeled as test sample, positive control (*B. anthracis* Pasteur) and negative control (*B. cereus*). Five μL of fluorescein isothiocyanate (FITC)-labeled monoclonal antibody against the capsule is then added to each tube. The tubes are then gently mixed and incubated at 35-37 $^\circ\text{C}$ for 30 minutes. One mL of phosphate-buffered saline (PBS) containing 0.3% Tween 20 (PBST) is added to each tube which are then inverted and mixed. The samples are then pelleted by centrifugation for three minutes at 14,000 x g. The supernatant is removed and the pellet washed with 900 μL of deionized water. The tubes are gently inverted three times, the supernatant removed, and the pellet resuspended in the residual fluid. Two μL of the suspension is then spread onto a Teflon-coated microscope slide and allowed to air dry for 10 minutes. One drop of fluorescence mounting fluid is added and the samples are sealed with a coverslip. The samples are then examined using a UV microscope with a 40 or 100X objective lens. CAP-DFA detects the poly- γ -D-glutamic acid capsule which is produced in vegetative *B. anthracis* cells in an elevated CO_2 environment. CW-DFA follows a similar procedure as described for the CAP-DFA except that 150 μL PBST is added directly to the colony obtained from the overnight SBA plate instead of adding growth media and incubating. CW-DFA detects the galactose/N-acetylglucosamine cell wall associated polysaccharide expressed by vegetative *B. anthracis* cells. A bright apple-green fluorescence of the cell against a dark background as shown in Figure 2.0 below [21] is reported as a positive for *B. anthracis*. In Figure 2.0, sample one is the positive control (*B. anthracis* Pasteur), sample 2 is from an environmental specimen, and sample 3 is from a clinical lung tissue specimen (both sample 2 and 3 are from the Fall 2001 attacks).



Panel A (CW-DFA) and Panel B (CAP-DFA)

Figure 2.0 DFA staining of *B. anthracis* cells (magnification 400x)

The cost of a UV microscope can run from several hundred to several thousand dollars depending upon the selected capabilities. CAP-DFA procedures take approximately four hours after the overnight isolation cultures whereas CW-DFA can be done in approximately one hour after the overnight isolation culture. Both sensitivity and specificity of DFA were analyzed using 230 *B. anthracis* isolates and 56 non-*B. anthracis* strains. CAP-DFA specificity was 98% and CW-DFA specificity was 78.6%; however, specificity became 100% when positive results from both CAP-DFA and CW-DFA tests were required [21]. The DL of either assay was determined to be approximately 10^4 cells/mL by using 10-fold dilutions of prepared Pasteur strain [21].

2.5 Real-Time Polymerase Chain Reaction (RT-PCR)

Real-time polymerase chain reaction is an extremely sensitive nucleic acid sequence-based amplification (NASBA) technique that amplifies small quantities of DNA [22]; it is used by the LRN to presumptively identify bacteria and viruses. Biologist Kary Mullis invented PCR, described as being to genes as the Gutenberg press was to the written word, in 1983 and for his accomplishments was awarded the Nobel Prize in 1993. The main difference between RT-PCR and PCR is that the amplified DNA is detected as the amplification takes place in RT-PCR while sample post processing must be done prior to amplified DNA detection with PCR. The genetic material of microorganisms has sequences of DNA or RNA that are unique to that microorganism. Two small sections of *B. anthracis* DNA, called primers, are designed and produced that serve as templates to selectively copy portions of the *B. anthracis* gene using a DNA polymerase called Taq polymerase. To design proper primers, a researcher needs to know exact genomic sequence of the target DNA and the sequence must not change. Fortunately, the genome of *B. anthracis* has been shown to be the most genetically uniform bacterial species known to date.

RT-PCR is used to confirm the presence of both the capsule and toxin genes in *B. anthracis* since both genes are required for *B. anthracis* to be fully virulent. The RT-PCR process is shown in Figure 2.1 and is described below. The designed primers, deoxyribonucleotide triphosphates (dNTPs), buffer solution, and Taq polymerase are added to a DNA template. The original DNA template is melted (or denatured) at approximately 95 °C and Taq polymerase is activated (labeled number 1 in Figure 2.1). The primers anneal at 45-60 °C and the Taq polymerase docks (labeled number 2 in Figure 2.1). One primer anneals on the 5' end of the gene and Taq polymerase makes a new strand in that direction while the other primer is made to the opposite strand to go in the opposite direction. The Taq polymerase makes two new strands at around 70 °C thereby doubling the amount of DNA present (labeled number 3 in Figure 2.1). This provides two new templates for the next cycle where the DNA is again melted, primers anneal, and the Taq polymerase makes four new strands. The temperature profile cycles continue which results in logarithmic amplification of the template DNA that exists between the primers, called the amplicon, until it is present in sufficient quantity to detect in real-time using labels, dyes or probes. The RT-PCR reaction conditions must be experimentally optimized because PCR can be sensitive to divalent cations, variations in temperature, amplicon size, as well as nucleotide and primer concentrations. A typical RT-PCR spectrum is shown in Figure 2.2. The temperature profile sequences (temperature on the y-axis and time on the x-axis) are shown on top screen; the fluorescence intensity (y-axis) and number of cycles (x-axis) are shown on bottom screen. PCR can make millions of copies in less than an hour with over million-fold amplification occurring in just 20 cycles.

RT-PCR equipment costs vary from \$5,000 up to over \$40,000 and the reagent costs with other consumable items run approximately \$10 per sample being tested. Depending on sample capacity and reaction conditions, approximately 30 samples can be tested in less than two hours with the actual RT-PCR analysis taking only 15 to 60

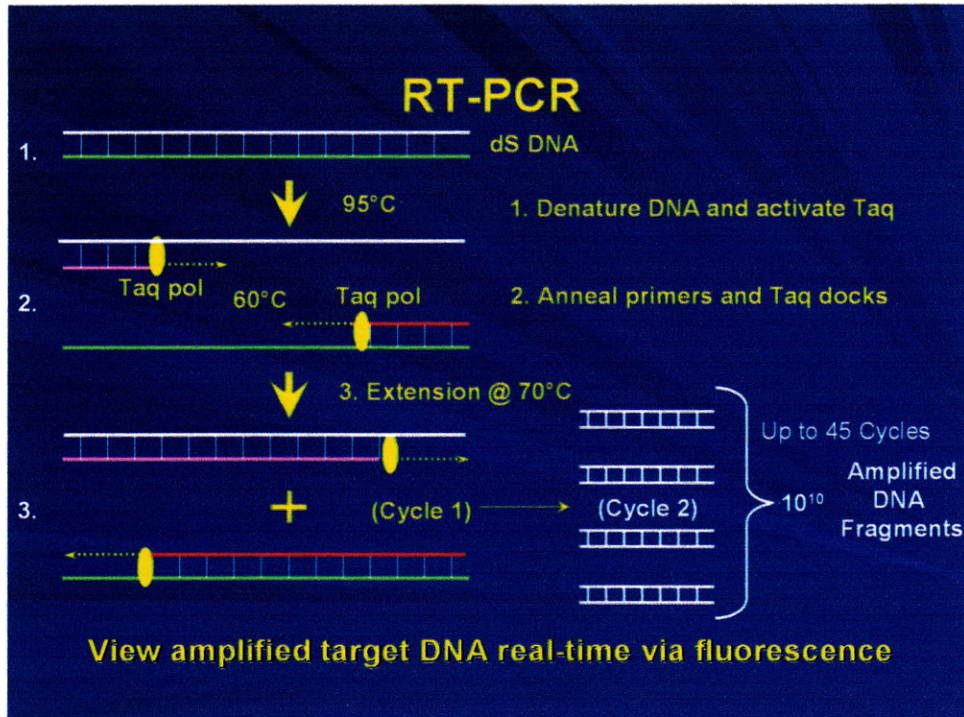


Figure 2.1 Schematic of RT-PCR process

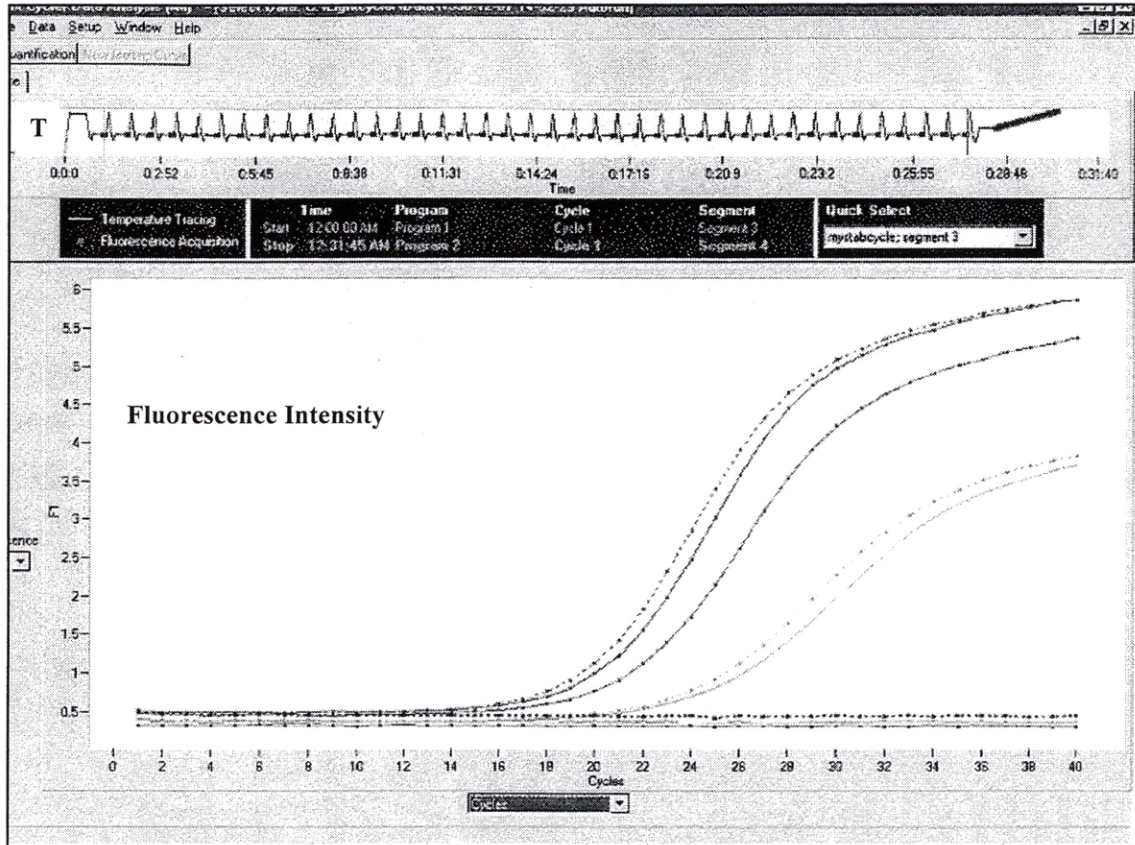


Figure 2.2 RT-PCR spectra

minutes. RT-PCR methods have reported sensitivities (or DLs) as low as 5 cells, typical DLs run from 10 to 100 cells, and have very low false alarm rates of 0.001% for a single template (or target) [13]. Sample contamination is a serious concern when using a very sensitive technique like RT-PCR since a very small amount of template DNA can rapidly be amplified. The potential for contamination is minimized by conducting sample preparation, sample loading, and sample analysis in separate work areas. RT-PCR has been reported to detect 50 fg of genomic *B. anthracis* DNA or approximately 9 genome equivalents (GEs) when testing for one DNA target [23], and 1 pg of genomic *B. anthracis* DNA or approximately 167 GEs when testing for three DNA targets (two plasmid and one chromosomal) [24]. Obtaining high specificity sometimes requires using multiple DNA targets, called multiplexing, to rule out genetically similar non-*anthracis Bacillus* species [25]. To identify *B. anthracis* using RT-PCR, the LRN uses a total of three gene targets located on the chromosome and the two virulence plasmids to achieve high specificity [24]. All three targets have to be present for a positive RT-PCR assay for *B. anthracis*.

Some recognized advantages of RT-PCR over other detection methods are excellent sensitivity (or DL), superb specificity (determined by amplicon/target), real-time cycle-to-cycle analysis, and no post-PCR processing (minimized complexity and potential contamination) [22]. Although RT-PCR has been used extensively in pathogen detection, it amplifies DNA whether the pathogen is dead (nonviable) or alive (viable). Nonviable *B. anthracis* spores that are RT-PCR amplified could produce positive scores for disinfection methods that do not remove nonviable spores and thereby divert response resources away from where they are most critically needed.

2.6 Hand-Held Immunoassay (HHA)

Hand-held immunoassays, also referred to as lateral flow immunochromatography (LFI) strips, are structure-based detectors that rely on molecular recognition by antibodies

in a multi-step immunoassay. These detectors, shown in Figures 2.3 and 2.4, utilize antibodies to selectively bind with epitopes on the surface of pathogens. Figure 2.3 shows the outer protective plastic cassette while Figure 2.4 shows the inner details.



Figure 2.3 Individual HHA cassette

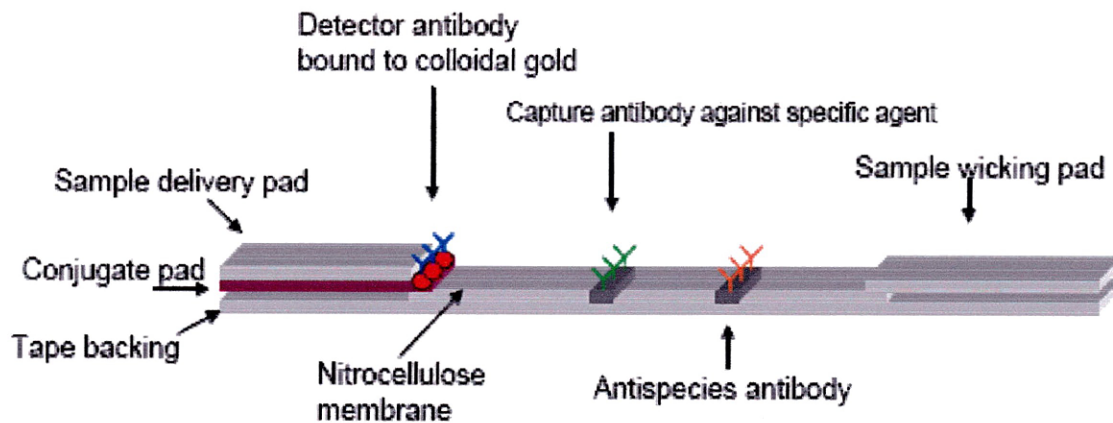


Figure 2.4 HHA ticket after removal from plastic cassette

RedLine Alert™ by Tetracore® was the first immunochromatographic test kit approved by the Food and Drug Administration (FDA) for the detection of *B. anthracis* after an overnight culture on SBA plates. The components of the HHA are described below, proceeding from left to right in Figure 2.4 [26]. Colloidal gold-conjugated murine anti-*B. anthracis* monoclonal antibodies (MAbs), specific for a vegetative *B. anthracis* cell surface protein, are used as the detector antibodies. These gold-conjugated antibodies are not immobilized and are called the detector antibodies because they will be concentrated on the capture (or test) and/or control lines (labeled as capture antibody and antispecies antibody respectively in Figure 2.4) to produce a visible red colored line. Next, the capture (or test) antibodies are rabbit anti-*B. anthracis* polyclonal antibodies (PAbs) for vegetative *B. anthracis*. These capture antibodies are immobilized along the capture (or test) line to concentrate *B. anthracis* if present in the unknown sample. The last antibodies labeled antispecies antibody in Figure 2.4 are anti-murine antibodies immobilized along the control line. The control serves to concentrate the gold-conjugated murine anti-*B. anthracis* MAbs along a line to signify that capillary flow occurred and the reagents were working properly.

To operate a HHA, a dry or wet swab could be used to withdraw a sample from the environment. The sample is then streaked onto 5% SBA plates and incubated at 37 °C for 12 to 24 hours. An isolated 1 to 2 mm diameter colony would then be mixed into approximately 200 µL of a colony buffer solution to maintain the pH around 7.0 to 7.4. Seventy-five to 150 µL of the sample colony in buffer is then applied to the sample delivery pad and allowed to wick down the nitrocellulose membrane by capillary action. A liquid sample could be applied directly without any sample pretreatment. If *B. anthracis* was present in the sample, the colloidal gold-conjugated murine anti-*B. anthracis* MAbs will bind to the *B. anthracis* cells and be wicked down the membrane. At the capture line, the rabbit anti-*B. anthracis* PAbs will bind to the *B. anthracis* cells thereby concentrating the gold particles to produce a visible red line. The colloidal gold serves as the visible detection mechanism by forming a visible red line when

concentrated. The excess colloidal gold-conjugated murine anti-*B. anthracis* MAbs flow to the control line where they are concentrated by the anti-murine antibodies. The resulting red line signifies that capillary flow occurred and the reagents were working properly. A positive (red) control line must be present for the results to be considered. The HHA results should be read at 15 minutes and results after 20 minutes are not considered valid. See Figure 2.5 for possible HHA results. Note: the “S” on the cassette is where sample is loaded, the “T” is the capture (or test) line, and the “C” is the control line.

The cost is between \$7 and \$10 per HHA including the colony buffer solution. HHAs have analysis times of 15 minutes, reported sensitivities (or DLs) of 10^5 cells/mL to 10^8 cells/mL and have false alarm rates of 0.1% [13]. False positives can result from insufficient specificity and/or non-specific binding since antibody binding is very sensitive to pH changes and matrix effects. Testing of the RedLine Alert™ HHA using 145 *B. anthracis* isolates and 101 non-*anthracis Bacillus* species yielded a host range specificity of 98.6% and a cross reactivity of 11.9% [26]. Reproducibility with the RedLine Alert™ HHA was 100% [26], but HHAs typically have reproducibility values between 78% to 100%.

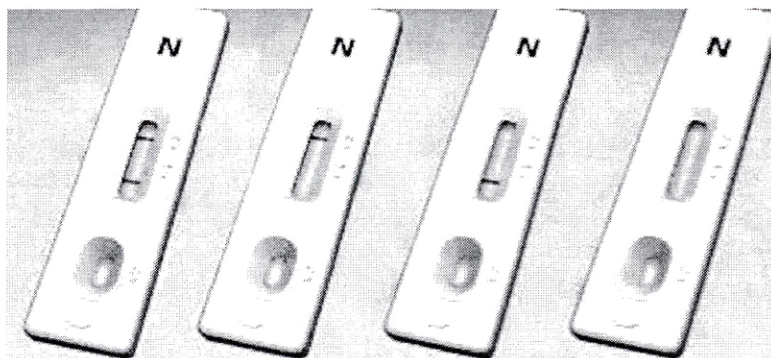


Figure 2.5 Possible HHA results

From left to right: 1) positive 2) negative 3) faulty and 4) faulty

CHAPTER 3

CHARACTERIZATION OF *BACILLUS ANTHRACIS*

3.1 Background on *B. anthracis*

Bacillus anthracis can exist in the actively growing “vegetative” state or the dormant “spore” state which protects the bacterium from drying, UV radiation, extreme temperatures, and other dangerous conditions. In the presence of oxygen, the bacterium encases itself in a thick outer coating called a spore when the cell experiences environmental stress to include temperature extremes as well as a lack of nutrients. The spore is central to the cycle of infection; these viable spores have been known to survive in soil for decades and readily germinate, or become vegetative, in a suitable host when the environmental conditions become favorable again. It is through these environmental spores that most anthrax is contracted and spores would be how “weaponized” anthrax would be delivered.

The mode of spore entry into a human or animal determines the classification of the anthrax and the typical symptoms displayed. Cutaneous anthrax occurs when *B. anthracis* enters a cut or abrasion on the skin and begins as an itchy bump resembling an insect bite, then within several days develops into a vesicle which leads to a painless ulcer with a black dying area in the center. Gastrointestinal anthrax occurs when contaminated food is eaten and leads to nausea, vomiting, fever, severe diarrhea, abdominal pain, and vomiting blood. Inhalation anthrax occurs when spores are inhaled into the lungs and has symptoms similar to the flu or common cold such as fever, fatigue, nonproductive cough, headache, sweats, and chest pain; this quickly progresses to shortness of breath and shock. About 20% of untreated cutaneous anthrax will result in death, 25% to 60% of untreated gastrointestinal anthrax will cause death and inhalation

anthrax is usually always fatal without early and aggressive antibiotic treatment [27]. Early diagnosis and treatment of anthrax is critical to survival as evidenced by the difference between the numbers of deaths in the 1979 Sverdlovsk incident compared with the Fall 2001 anthrax attacks.

Fully virulent strains of *B. anthracis* have two large plasmids (pXO1⁺/pXO2⁺) that contain circular extrachromosomal DNA. Plasmid pXO1 includes genes for the three proteins, protective antigen (83 kDa PA), edema factor (89 kDa EF) and lethal factor (87 kDa LF), that combine to form two toxins; these proteins are produced during the exponential growth phase of *B. anthracis* and are responsible for the characteristic symptoms of anthrax [20]. Plasmid pXO2 has genes for the capsule, a polypeptide of gamma-linked alpha-peptide chains of 50 to 100 D-glutamic acid residues, which makes the cells resistant to phagocytosis (ingestion and degradation by immune system cells). Both capsule and toxin genes are required for fully virulent *B. anthracis* [28], and the production of the toxin proteins and the capsule are in response to increased CO₂ levels over atmospheric that are typically present in mammalian blood and tissues. Any toxin protein intradermally injected by itself has no toxic effect; however, PA injected with LF combines to form lethal toxin that ultimately leads to sudden death from low blood pressure and shock while injection of PA with EF produces edema toxin that results in severe swelling in tissues referred to as edema [29].

The PA-mediated toxin entry into host cells, called intoxication, which damages or kills the cells is shown in Figure 3.0 [30]. The process of toxin entry into a cell is as follows [30]: 1) PA binds to its receptor on the cell; 2) proteolytic activation of PA and dissociation of amino-terminal PA₂₀; 3) self-association of monomeric PA₆₃ to form the heptameric prepore; 4) binding of EF/ LF to the prepore; 5) endocytosis of the receptor/PA₆₃/ligand complex; and 6) pH-dependent insertion of PA₆₃ and the translocation of the ligand. In the case of inhalational anthrax, *B. anthracis* spores enter

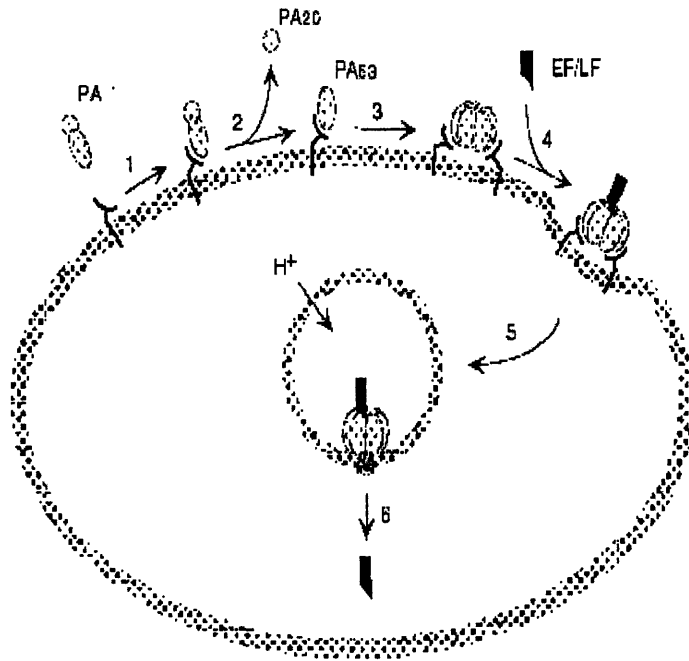


Figure 3.0 Model of anthrax toxin entry into eukaryotic cells

the lungs and into the mucus membrane barrier where they are engulfed by macrophages which are a type of phagocyte (white blood cell) located in the skin and lungs. The macrophages unwittingly transport the spores to the mediastinal lymph nodes in the center of the chest as the *B. anthracis* become vegetative inside and ultimately kill and burst open the macrophages releasing the bacteria, toxins, destructive enzymes, and superoxides into the bloodstream [7]. The bacteria also secrete the same toxins in the bloodstream where they travel and cause tissue and organ damage, massive edema (swelling by accumulation of bodily fluids), and shock caused by reduced blood circulation. Death normally results from septicemia, or blood poisoning, caused by the secreted *B. anthracis* toxins. Most animal species, if untreated with antibiotics, contain between 10 and 100 million *B. anthracis* organisms per milliliter of blood at death but only 1×10^6 cells/mL are necessary to cause death [3]. Following sudden death, blood discharging from the blood vessels of the nose, mouth, and anus is commonly seen because the toxins released throughout the body prevent blood clotting; this bloody discharge subsequently continues the cycle of infection [10].

3.2 Morphology, Physiology and Taxonomy of *B. anthracis*

Bacillus anthracis is an endospore forming, gram-positive, rod-shaped bacterium approximately 1 μm wide by 4 μm long (a human hair is 75-100 μm wide). There are currently 89 characterized *B. anthracis* strains [24]. Gram-stained *B. anthracis* Sterne, shown in Figure 3.1, appear as violet rods containing colorless oval spores (also called endospores) that are resistant to adverse environmental conditions. When grown on 5 % SBA or TSA, the colonies are large (2-5 mm), slightly raised, gray-white in color that appear like ground glass, have irregular edges, are non-hemolytic, and are tacky when touched with a sterile loop. Typical *B. anthracis* Sterne morphology is shown in Figure 3.2. The complex surface of vegetative *Bacillus* is shown in Figure 3.3 [31]. The surface of *B. anthracis* begins for some strains with a poly-D-glutamic acid capsule

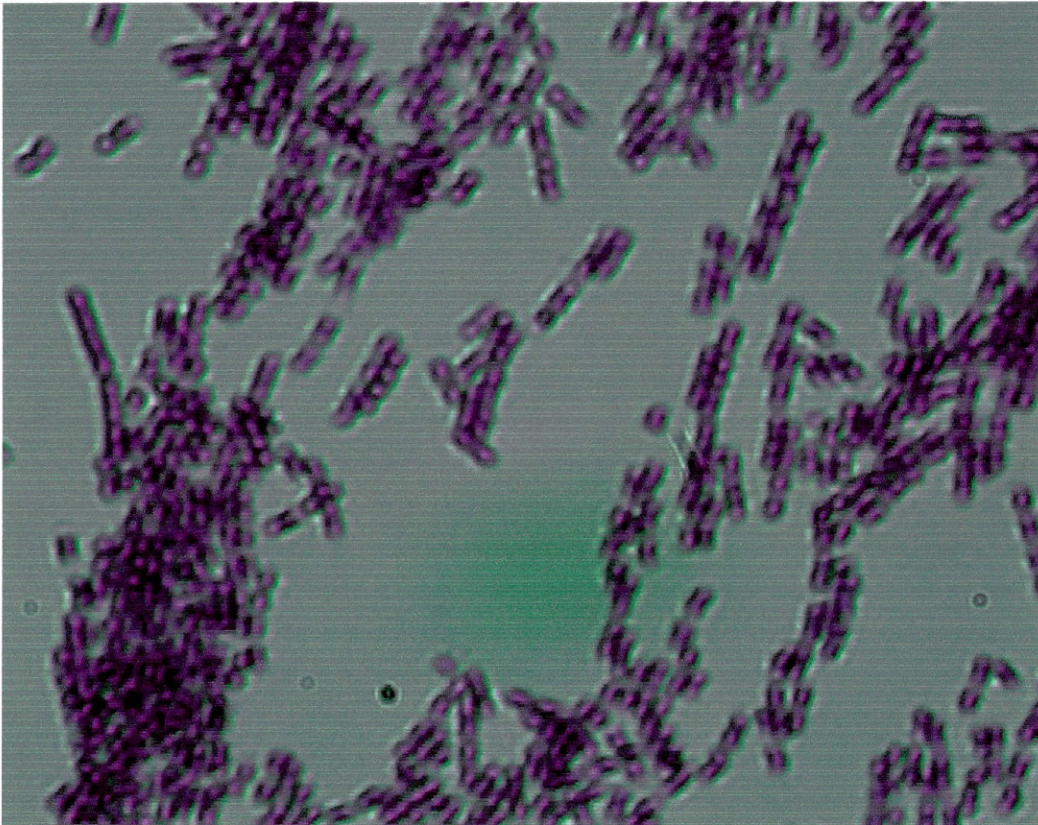


Figure 3.1 Gram stained colonies of *B. anthracis* Sterne from plate agar (CSM Leica microscope magnification 40x)

Bacillus Anthracis
Streak Plate
Start: 15 Feb 05 (1630L)
16 Feb 05 (0915L)

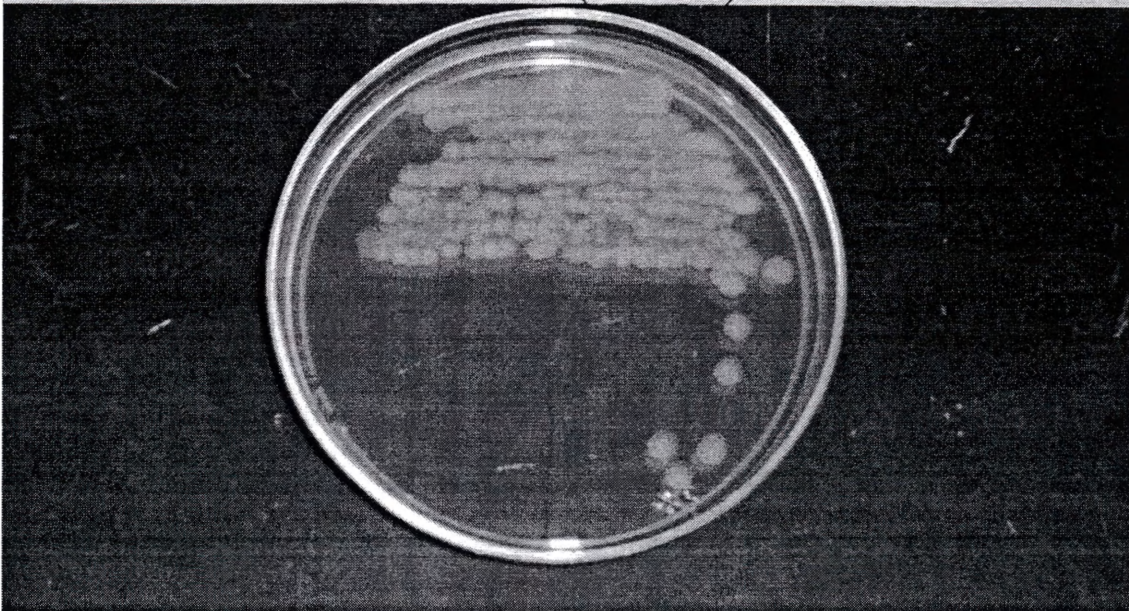


Figure 3.2 *B. anthracis* Sterne streak culture on TSA

(labeled “C” in Figure 3.3) that is one of the virulence factors because it makes the bacteria resistant to phagocytosis by macrophages [1]. The proteinaceous surface layer (labeled “S” in Figure 3.3) is next and seems to have a protective function and/or facilitate phage attachment. The peptidoglycan cell wall (labeled “P” in Figure 3.3) and cytoplasmic membrane, consisting mostly of imbedded proteins and phospholipids, make up the major environmental barrier and provide a layered structure that protects the cell from rupture. Three of the molecules embedded in the peptidoglycan layer are wall-associated proteins, teichoic acid, and lipoteichoic acid.

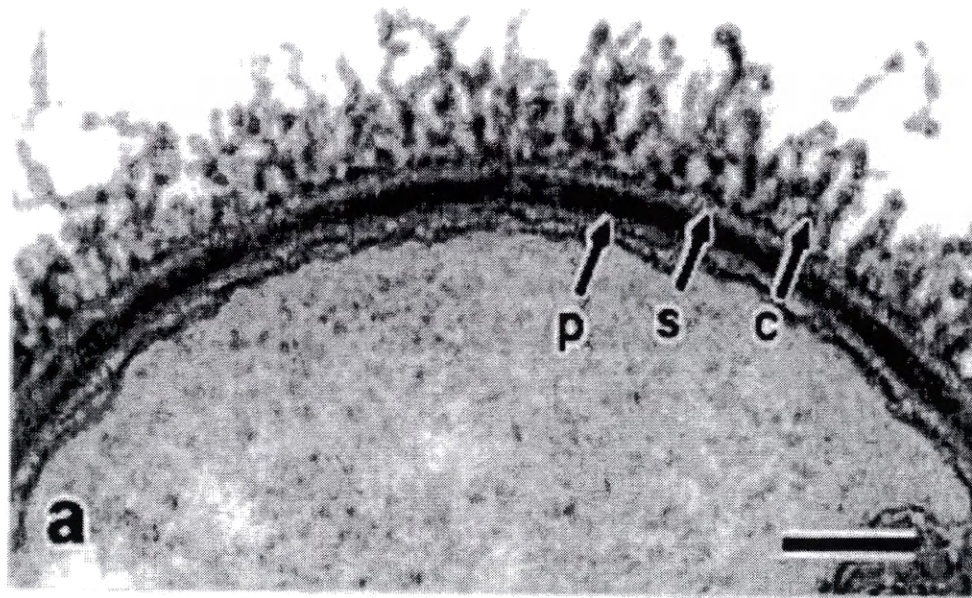


Figure 3.3 Pasteur Institute TEM of *Bacillus* surface

Bacillus anthracis is taxonomically aligned with *B. cereus*, *B. thuringiensis* and *B. mycoides*. It is most closely aligned with *B. cereus*, based on morphological, physiological, and DNA similarities [29]. *B. cereus* lives in the environment and is found in many foods, it produces toxins that lead to food poisoning within several hours of ingestion. *B. thuringiensis* is an insect pathogen while *B. mycoides* lives in the environment, but is nonpathogenic. *B. subtilis* looks similar to *B. anthracis* in culture and is commonly found in soil, but is not a human pathogen. The emergence of *B. anthracis* as an animal pathogen is associated with its acquisition of two large virulence plasmids that encode for anti-host toxins (110 MDa pXO1) and a capsular structure (60 MDa pXO2) [32].

3.3 Safe Handling Methods

Bacillus anthracis spores are extremely resistant to adverse environmental conditions such as extreme heat or cold, chemicals, irradiation, and large pH changes. Vaccination using killed whole pathogens, attenuated whole pathogens, or subunits of the pathogen is recommended for all workers being exposed to *B. anthracis*. An immune system that previously reacted to a specific antigen has immunological memory stored in white blood cells (called memory B and T-cells) and antibodies. When this antigen presents itself again, the cells respond in less than 24 hours instead of the minimum 7 to 10 days required for an antibody response on first exposure. The U.S. human anthrax vaccine called MDPH-AVA (Michigan Department of Public Health-Anthrax Vaccine Adsorbed), licensed by the FDA in 1970, is non-cellular and composed of the recombinant protective antigen (rPA) protein adsorbed to the adjuvant aluminum hydroxide [3]. The vaccination procedure calls for six injections followed by annual boosters and was ordered to be used on our active duty soldiers during the Gulf War in 1991 and mandated again in 1998.

For safety, nonpathogenic surrogates like *B. cereus*, *B. thuringiensis*, *B. mycoides*, and *B. subtilis* could be used. The type of study will determine whether or not a particular surrogate will simulate *B. anthracis* well enough. If the study cannot be done with surrogates, work might be able to be done with attenuated strains such as the Sterne strain 34F2 (pXO1⁺/pXO2⁻) and/or the Pasteur strain (pXO1⁻/pXO2⁺). If exposed to *B. anthracis*, antibiotics are typically prescribed as prophylactic treatment for 60 days because the longest known period between exposure and anthrax disease symptoms in humans is 43 days [7].

Samples potentially containing *B. anthracis* should be sent to at a Public Health laboratory in the LRN with at least biosafety level 3 (BSL-3) capabilities. All experimental work at CSM was done with the attenuated *B. anthracis* Sterne strain 34F2 (pXO1⁺/pXO2⁻) in BSL-2 facilities appropriate for work with moderate-risk agents. The identity of the *B. anthracis* Sterne strain was confirmed using RT-PCR tests done at the United States Air Force Academy (USAFA). These tests showed that the toxin encoding genes located on plasmid pXO1 for the PA and LF proteins that are secreted by *B. anthracis* were present, the γ small, acid-soluble spore protein (SASP) encoding gene located on the chromosomal DNA was present, and the poly-D-glutamic acid capsule encoding gene located on plasmid pXO2 was absent. These RT-PCR results confirmed that the previously unconfirmed bacteria were *B. anthracis* Sterne strain 34F2 (pXO1⁺/pXO2⁻).

3.4 Growth Conditions

3.4.1 Introduction

In vitro growth of *B. anthracis* can be done either in liquid growth media or on Petri dishes using solid agar growth media. During *in vitro* growth conditions, *B. anthracis* cells typically grow in long chains, spores are elliptic and located towards the

middle of the cell, and are encapsulated only when grown in bicarbonate (20 mM) and under elevated CO₂ (40 mm Hg). *In vivo* growth conditions tend to produce shorter chains of *B. anthracis* cells and the cells are encapsulated. The growth media contains all the required nutrients (salts, sugars, proteins, vitamins, and minerals) for the bacteria to grow and multiply; the only essential nutritional requirements for *B. anthracis* are methionine and thiamine. If sporulated, L-alanine acts as a germinating agent that causes spores to become vegetative. Optimal growth temperature for *B. anthracis* has been reported to be 37 °C with cell growth stopping above 43 °C [28].

Bacterial population growth curves are used to optimize growth conditions for specific bacteria and require some measure or estimation of cell number, or titer, when constructing them. Bacterial cell mass is proportional to its turbidity, or optical density (OD), measurement. A typical bacterial population growth curve is shown in Figure 3.4 [33]. The four phases of a standard bacterial population growth curve are: 1) lag phase: population remains unchanged as the cells increase their metabolic activity and synthesize required macromolecules; 2) exponential or log phase: the bacteria are growing exponentially expressed by the generation (doubling) time; 3) stationary phase: population growth becomes inhibited by inhibitory metabolites, lack of nutrients or lack of space; and 4) death phase: the number of viable cells decreases exponentially. Experiments were conducted at CSM to confirm both the optimal growth temperature and optimal growth media for *B. anthracis* using bacterial population growth curves. By experimentally determining the *B. anthracis* population growth curve, the generation (doubling) time can be calculated which allows an investigator to determine the time required for this bacteria to reproduce, under similar conditions, to detectable concentrations for a given detection method.

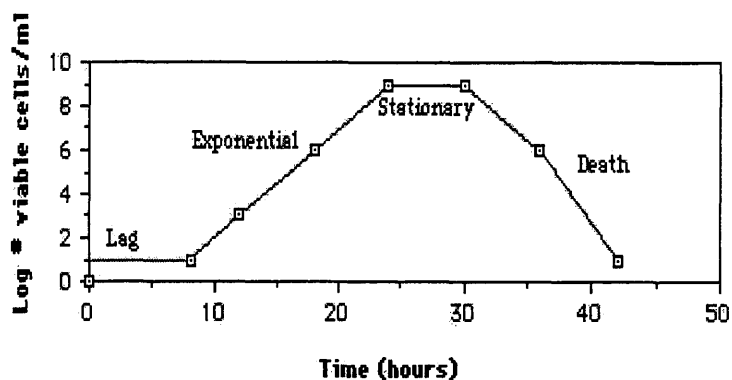


Figure 3.4 Typical bacterial population growth curve

3.4.2 Materials and Methods

The original *B. anthracis* Sterne sample was obtained from the Armed Forces Institute of Pathology (AFIP). “Master” stocks of *B. anthracis* were made from either fresh colonies on 5% SBA plates or from an exponentially growing liquid culture and were stored at $-80\text{ }^{\circ}\text{C}$ either on CryoBank™ glass beads (Mast Diagnostics, Bootle, U.K.) or with glycerol added as a cryoprotectant. A new bacterial sample was withdrawn from the frozen “master” stocks monthly to minimize the possibility of using bacterial variants (mutants).

A CryoBank™ glass bead of *B. anthracis* “master” stock was streaked on a 5% SBA plate and incubated at $37 \pm 2\text{ }^{\circ}\text{C}$. Sixteen to 20 hours later, one colony was removed from the 5% SBA plate and added to 10.0 mL of BHI (or TSB) broth using a 1.0 μL inoculating loop. This suspension was incubated overnight at $37 \pm 2\text{ }^{\circ}\text{C}$ on a shaker table. The next day, 100 μL of this bacterial suspension was added to 10 mL fresh BHI broth (or TSB) and incubated overnight at $37 \pm 2\text{ }^{\circ}\text{C}$ on a shaker table. The following

day, 8.5 mL of this overnight *B. anthracis* BHI (or TSB) culture was added to 125 mL of BHI (or TSB) that was heated in an incubator to 37 °C. An absorbance reading at 625 nm was taken at this time then approximately every 30 minutes for the next 3.5 hours using a ThermoElectron Corporation Nicolet evolution 300 UV/VIS spectrophotometer. The liquid culture was kept on a shaker table in an incubator at 37 ± 2 °C and aliquots of approximately 2 mL were removed into a 1.0 cm quartz cuvette for absorbance readings. After taking the absorbance reading, 100 µL was pipetted from the cuvette into a microcentrifuge tube holding 900 µL PBS for colony plate counts (see Section 3.5.2 for bacterial titer method). A 1 µL inoculating loop was used to streak this *B. anthracis* growth liquid from the cuvette on a 5% SBA plate to ensure there was no contamination. These purity plates were incubated overnight at 37 ± 2 °C and read the next day.

Bacillus anthracis was grown both in BHI broth (g/L: 27.5 g B/H extract from porcine and mixture meat and milk peptones, 2.0 g D(+) glucose, 5.0 g NaCl and 2.5 g disodium phosphate) and TSB (g/L: 17.0 pancreatic digest of caseine, 3.0 g enzymatic digest of soybean meal, 2.5 g dextrose, 5.0 g NaCl and 2.5 g dipotassium phosphate) from EMD that were autoclaved for 15 minutes at 121 °C.

Temperature studies were conducted at 27 °C, 37 °C, and 47 °C using TSB growth media. *In vitro* vegetative *B. anthracis* from a liquid TSB culture was Gram-stained as described in Section 2.3 and viewed on the CSM Leica microscope.

3.4.3 Results

Table 3.0 shows the results of *B. anthracis* grown at 27 °C, 37 °C, and 47 °C using TSB growth media. The higher OD values correlate to more *B. anthracis* cell mass being present. The faster the OD values increase, the more favorable the conditions were for *B. anthracis* growth. *B. anthracis* growth was almost nonexistent at 47 °C, slow growth was shown at 27 °C, and fastest growth was at 37 °C. Table 3.1 shows *B.*

anthracis growth in BHI at 37 °C which is improved from the growth shown in TSB at 37 °C.

Table 3.0 *B. anthracis* Sterne growth data in TSB at 27 °C, 37 °C, and 47 °C

Time (hr:min)	Optical Density @ 47 °C	Time (hr:min)	Optical Density @ 37 °C	Time (hr:min)	Optical Density @ 27 °C
3:01	.009	0:30	.035	2:58	.008
4:14	.008	0:58	.041	4:11	.021
5:27	.017	1:34	.058	5:24	.050
5:59	.017	2:05	.080	5:56	.080
6:49	.025	2:33	.127	6:46	.138
7:21	.030	3:16	.255	7:18	.190

Table 3.1 shows the results of the OD measurements and the plate count results (see Section 3.5.2 for the bacterial titer method) used to correlate OD values to *B. anthracis* cell count (cfu/mL) results. A graphical representation of Table 3.1 is shown in Figure 3.5. Using the growth data from OD .095 to .467, the generation time (or doubling time) for *B. anthracis* Sterne in BHI at 37 ± 2 °C was calculated at 34 minutes. Using the same data, the OD to *B. anthracis* Sterne concentration calibration equation is:

$$\text{Log}_{10}[\textit{B. anthracis Sterne}] = 3.62(\text{OD}) + 5.84 \quad (\text{equation 3.0})$$

Table 3.1 *B. anthracis* Sterne growth data in BHI at 37 °C

Time (hr:min)	Optical Density	[<i>B. anthracis</i>]_{average} (cfu/mL)
0	.087	$7.13 (\pm 1.48) \times 10^5$
:30	.089	No count
1:03	.095	$9.27 (\pm 3.87) \times 10^5$
1:30	.106	No Count
2:00	.130	$1.72 (\pm 0.50) \times 10^6$
2:34	.192	$5.08 (\pm 2.50) \times 10^6$
3:00	.276	$1.47 (\pm 1.08) \times 10^7$
3:37	.467	$2.20 (\pm 0.22) \times 10^7$

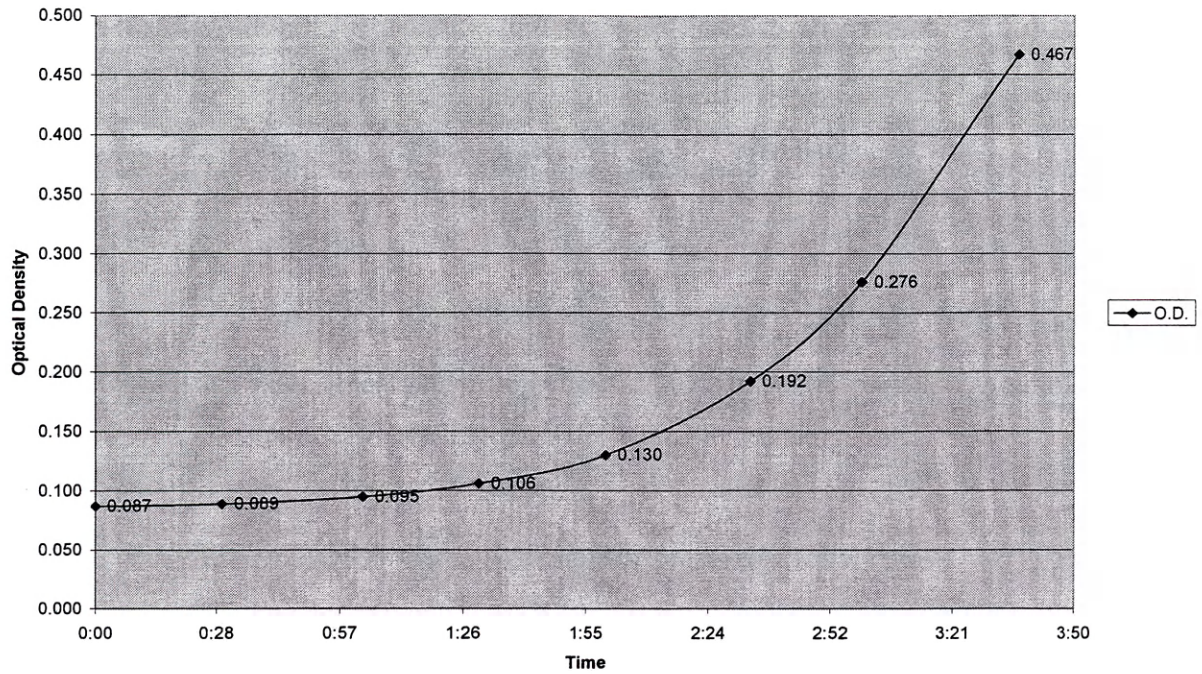


Figure 3.5 *B. anthracis* Sterne growth curve in BHI at 37 °C

Figure 3.6 shows vegetative *B. anthracis* grown *in vitro* using the CSM Leica microscope with 100x magnification using oil immersion.

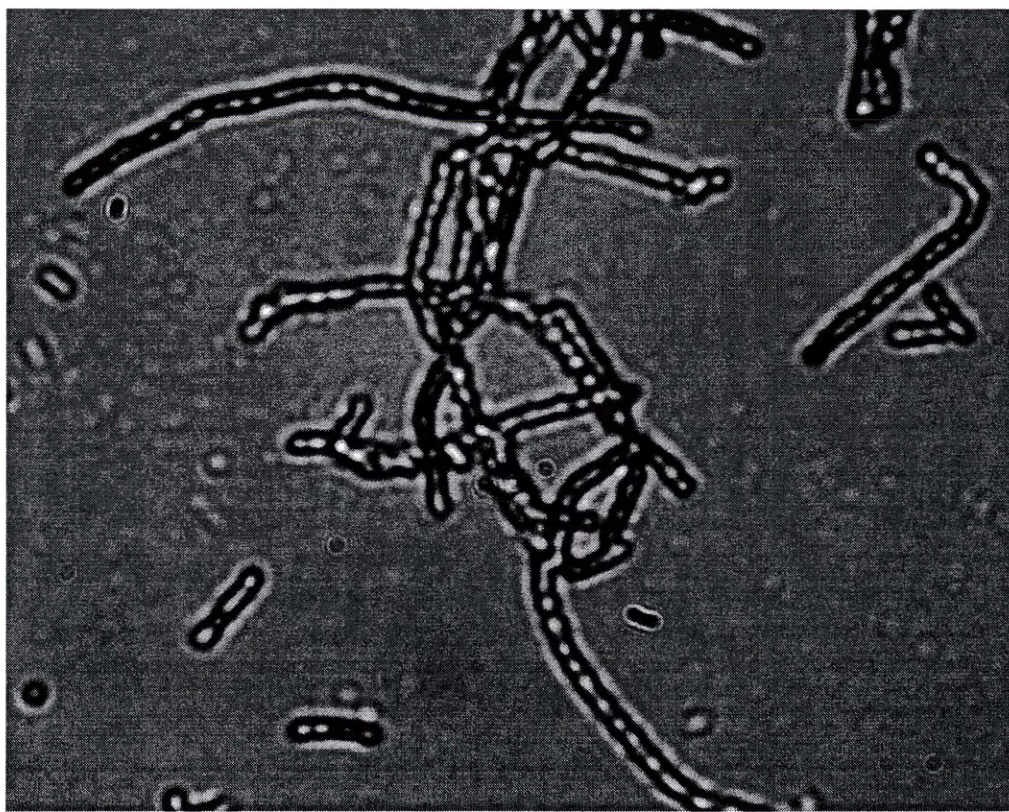


Figure 3.6 *In vitro* *B. anthracis* Sterne growth

3.4.4 Discussion and Conclusions

The *in vitro* growth of *B. anthracis* Sterne, shown in Figure 3.6, displayed the characteristic rod-shaped bacteria approximately 1 μm wide by 4 μm long growing in long chains that are typical of *in vitro* growth. This microscopic picture showed a morphology and growth pattern expected for *B. anthracis*. The growth curve data displayed in the Table 3.0 and 3.1 showed that *B. anthracis* Sterne optimally grew in BHI broth at 37 °C. Therefore the *B. anthracis* Sterne growth curve shown in Figure 3.5 was

constructed using BHI broth at 37 °C and is specific for these optimized growth conditions. The resulting growth curve could be different if another strain of *B. anthracis* was used or any growth conditions such as temperature or growth media were changed from those given above. The relationship between OD and viable bacterial cell counts now allows for quickly determining a bacterial titer (see Section 3.5) without always having to go through the labor intensive steps involved in performing colony plate counts (bacterial titer). It is very important to stress that the bacterial count is a viable bacterial count and that the conditions of growth should be replicated as closely as possible when using this conversion. These optimized growth conditions of 37 °C in BHI broth will now be used for all further experiments.

3.5 Determining Titer of *B. anthracis*

3.5.1 Introduction

Determining the concentration (titer) of viable *B. anthracis* is vitally important in studying phage/host interactions. Accurate bacterial counts are necessary to determine assay DLs and to set multiplicities of infection (MOIs) for bacteriophage amplification experiments. MOI is the ratio of phage concentration (or titer) to bacteria concentration. Turbidity measurements correlated to bacterial titer (growth curve) and/or colony plate counts were used for all experiments that required bacterial titers. A relatively accurate titer of bacteria (cell mass) is indirectly obtained by turbidity measurements that are then correlated to viable colony (cell) counts. Turbidity measurements are sensitive to bacterial strain and varying experimental conditions such as growth phase, growth media and temperature. Since the construction of a bacterial growth curve was shown in Section 3.4, the colony plate count method will be covered in this section.

3.5.2 Materials and Methods

One hundred μL of *B. anthracis* BHI liquid culture was serially diluted (eight total microcentrifuge tubes) in 900 μL of PBS (pH 7.32), and then each tube was vortexed to thoroughly mix. Ten μL aliquots of each dilution (8) were pipetted onto premarked lanes on plate count agar (this was done in triplicate), then the plates were tilted to allow the bacterial suspension to flow down the agar and the plates were incubated overnight at 37 ± 2 °C. The next day, the plates were removed and checked for purity. If no contamination was present on the purity plates or the plate count plates, the cfu's were visually counted on the Petri dishes taking into account the eight 10-fold dilutions. Equation 3.1 shows the calculation used to determine the starting *B. anthracis* titer.

$$\text{cfu/mL} = \text{cfu} \times 10^{(\text{lane \#} + 2)} \quad (\text{equation 3.1})$$

An average count was obtained using at least two lanes then the average of the triplicate counts was calculated. This represented the titer of *B. anthracis* cells at the OD it was sampled from.

3.5.3 Results

Figure 3.7 is a visual representation of how the *B. anthracis* colonies look after progressing down the dilution lane and being incubated overnight at 37 ± 2 °C. The morphology of the colonies indicates a pure sample. The increasing dilutions shown from left (Lane 1) to right (Lane 4) in Figure 3.7 allow for visual counting of the colonies (cfu's) by Lane 3. The colony plate counts would be 35 colonies in Lane 3 and four colonies in Lane 4. Table 3.2 shows the data for a *B. anthracis* colony plate count conducted on 6 January 2005 to determine the starting titer (before serial dilutions).

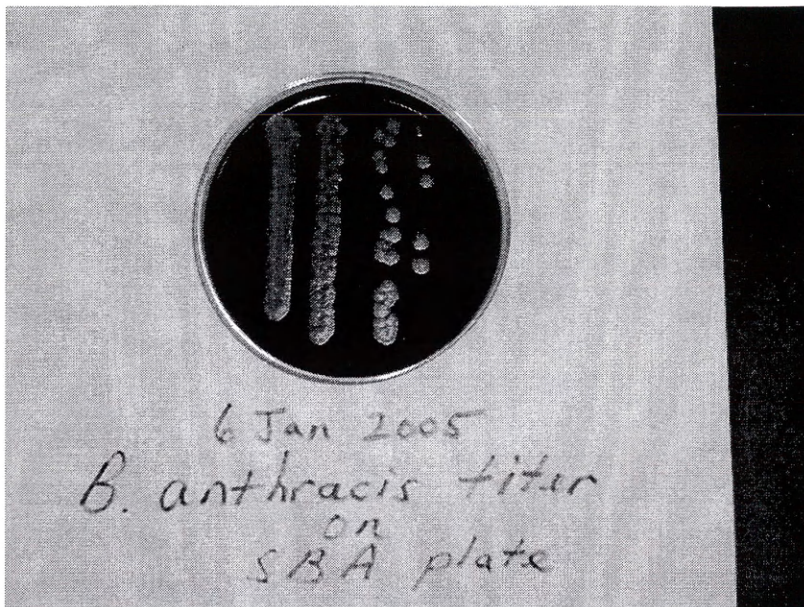


Figure 3.7 *B. anthracis* on 5% SBA to determine cfu/mL

Table 3.2 *B. anthracis* serial dilutions for viable plate count

Lane	Dilution Factor	Colonies (cfu)
1	10x	TMTC
2	100x	TMTC
3	1000x	35
4	10^4 x	4
5	10^5 x	0
6	10^6 x	0
7	10^7 x	0
8	10^8 x	0

When collecting the colony plate count data, “TMTC” stands for too many to count when counting the individual colonies on the 5% SBA plates. Taking into account the 10-fold dilutions from left to right in Figure 3.7 by using equation 3.1, the starting bacterial titer represented by Lane 3 would be 3.5×10^6 cfu/mL and Lane 4 would represent 4.0×10^6 cfu/mL. The average *B. anthracis* titer for this set of plates would be 3.75×10^6 cfu/mL.

3.5.4 Discussion and Conclusions

Using both the *B. anthracis* growth curve and conducting colony plate counts to titer bacteria not only provided extra confidence in the results, but also ensured that contamination was not present that could negatively affect the bacterial count. Culture contamination is endemic in any multi-use laboratory environment, so colony plate counts were conducted whenever very accurate titers were required to ensure bacterial purity. The results obtained by these two methods could vary from one another in that the growth curve method would also count dead bacterial cells and/or other bacterial cells that might be contaminating the culture; whereas the colony plate count method only counts viable cells and the purity can be visually confirmed. The possible variations between the methods were minimized by not using liquid cultures started directly from a colony grown on 5% SBA since they typically contain some dead cells. Liquid cultures used for *B. anthracis* growth curves were cultures that were twice removed from the inoculating colony as outlined in Section 3.4.2.

CHAPTER 4

CHARACTERIZATION AND AMPLIFICATION OF GAMMA PHAGE

4.1 Introduction to Bacteriophage

Viruses are particles with a genome that exist only to reproduce. Since viruses are pseudo-living particles that lack ribosomes and have no machinery for producing energy, they require living host cells in which to replicate. All viruses have an inner core of nucleic acid, either RNA or DNA, surrounded by a protein coat called a capsid while some viruses have an additional layer surrounding their capsid called an envelope. The capsid serves to protect the viral genome (replication instructions) and is commonly polyhedral in shape. Viruses produce diseases which generally do not respond to antibiotics, but may be responsive to antiviral compounds, of which there are few available. Although the concept of the virus was first developed in 1889 by Martinus Beijerinck, it would take the discovery of viruses that invade bacteria by Frederick Twort in 1915 and Félix d'Herelle, who called them "bacteriophage" meaning bacteria eaters, in 1917 that made studying viruses more practical. Viruses were found to infect plant, animal, and microbial cells; the term bacteriophage or "phage" stood for viruses that infect only bacteria. Studying bacteriophage had many practical advantages over studying plant and animal viruses such as having relatively small genomes, short replication cycles (hours versus days/weeks), being easily assayed, and ease of preparing host cells. A single phage particle or virion is a fragile particle that can be disassembled by vigorous shaking, and is susceptible to UV light around 260 nm and in the far UV region (DNA damage). Early phage research was involved in the identification of DNA as the genetic material, discovery of messenger RNA, identifying the transduction phenomenon, and deciphering the genetic code [34]. Initial phage applications called

“phage therapy” begun in the 1920’s centered on treatment and prevention of bacterial infections; however, bacteria mutations to resistant variants minimized the expected benefits and newly developed antibiotics rendered these treatments less necessary. There is currently renewed interest in “phage therapy” with better understanding of the viral/bacterial “life cycle” and antibiotic resistant bacteria on the rise.

A few of the many milestones in bacteriophage research follow below. Félix d’Herelle led research on phage as therapeutic agents and found the “host-range specificity of phages appeared to be characteristic of given ‘races’ of phages” [35]. Estimation of virus particle diameters through the use of filters with known pore sizes was done by Elford and Andrewes in 1932 [36]. After WWII, Seymour Cohen studied the infection of *E. coli* with T-even bacteriophages (7 virulent phages: T1, T2, T3, T4, T5 and T6); these T-phages served as lytic research organisms providing for comparison of data among different labs. Delbrück led an investigation into genes and gene functions; he and Baily discovered genetic recombination in bacteriophages in 1946 [37]. In 1945, Delbrück even organized a phage course held at Cold Spring Harbor Laboratories in New York. In 1950, Lwoff and Gutmann demonstrated lysogeny and named the latent phage “prophage” [38]. In 1959, Sinsheimer found single-stranded DNA phage; RNA-containing phage were discovered soon thereafter in 1961 by Loeb and Zinder [39].

4.2 Morphology, Physiology and Taxonomy of Gamma Phage

4.2.1 Introduction

Nonspecific bacteriophages active on *B. anthracis* were first described in 1931 by Cowles [40]. Another bacteriophage called “phage W” was isolated in 1951 by McCloy that was highly specific for 171 isolates of *B. anthracis*, but failed to lyse some *B. anthracis* strains plus it reacted with two *B. cereus* strains [41]. Then in 1955, Brown and Cherry isolated a variant of “phage W”, they called gamma (γ) phage, that lysed all

41 *B. anthracis* strains tested and did not react with any of the other 223 *Bacilli* tested [42]. As previously mentioned, this gamma phage is currently utilized by the CDC as a confirmatory *B. anthracis* identification method. The electron microscope has shown to be the most valuable tool for determining the fine structure of phages. In 1975, sodium dodecyl sulfate-polyacrylamide gel electrophoresis (SDS-PAGE) results implied gamma phage consisted of ten unique protein compositions ranging from 12 to 140 kDa and electron microscopy confirmed gamma phage had sheathless, noncontractile, long tails that were 185 nm long and 9.5 nm wide, and had hexagonal (icosahedral) heads that were 52 nm long [43]. The tailed phage (order Caudovirales) morphologies separate the three main families: 60% (Siphoviridae) have long flexible tails, 25% (Myoviridae) have double-layered contractile tails and 15% (Podoviridae) have short stubby tails [44]. Gamma phage belongs to the Siphoviridae family and its genome consists of linear double-stranded DNA (dsDNA) made up of between 37,373 and 40,864 base pairs depending on the variant [45].

4.2.2 Materials and Methods

Transmission electron microscopy (TEM) analysis was performed on a Philips CM-10 transmission electron microscope operated at 80 kV accelerating voltage, 3.50 μm diameter beam and magnification up to 300,000X (University of Colorado, Boulder). One μL of gamma phage suspension was pipetted on glow discharged (makes surface hydrophilic) 300-400 mesh copper EM grids with formvar backing and allowed to adsorb. After one minute, the suspension was blotted with filter paper then several drops of a 1% (w/v) solution of uranyl acetate in distilled water were applied to negatively stain the sample. After several seconds, the excess liquid was shaken off and the grids were allowed to air dry for several more minutes.

4.2.3 Results

The TEM pictures, an example of which is shown in Figure 4.0, confirmed the size of CSM gamma phage was consistent with the reported dimensions of gamma phage to within ± 8 nm.

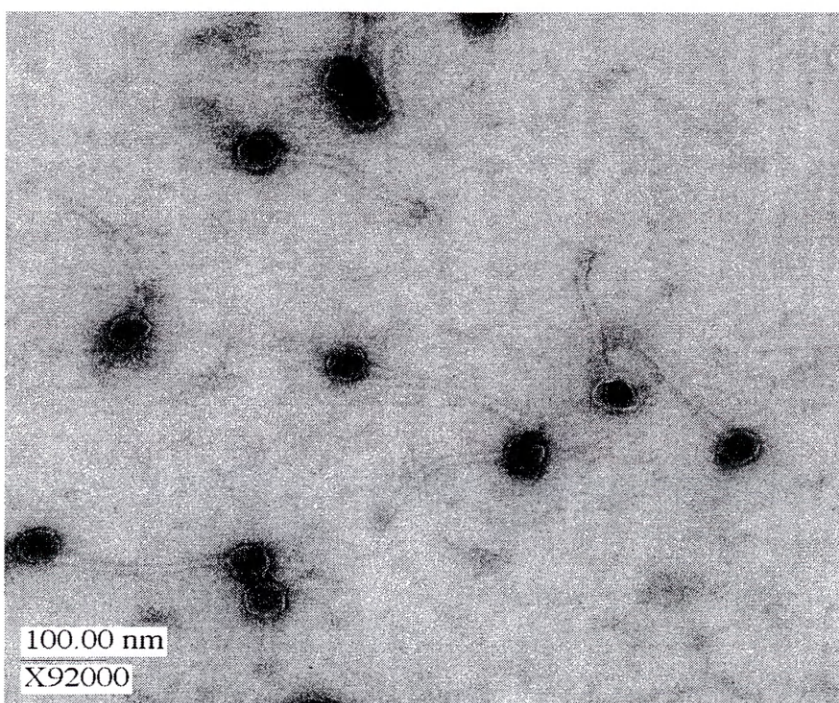


Figure 4.0 TEM of CsCl purified CSM gamma phage

4.2.4 Discussion and Conclusions

Both the analytical ultracentrifuge and the TEM proved to be powerful tools to study the fine structure of the nanometer-sized gamma phage. The analytical ultracentrifuge used with cesium chloride (CsCl) gradients, covered in Section 4.4,

provided a method to obtain highly purified gamma phage suspensions that were then used to obtain more accurate physical data with the TEM.

4.3 Propagation of Gamma Phage

4.3.1 Introduction

Understanding the phage/host life cycle is critical in optimizing growth conditions to maximize efficient and effective production of phage. Propagation of gamma phage, by the lytic replication cycle, requires healthy and actively growing *B. anthracis*. The five phases in the phage lytic replication cycle are phage adsorption, phage nucleic acid injection, synthesis of nucleic acids and proteins by cell metabolism, assembly of capsomers and packaging of nucleic acid into new phage (also called virions), and lysis of host cell with release of hundreds of progeny phage [1]. A single step bacteriophage growth curve is typically used to explore the efficiency of a phage's infectious cycle in a particular bacterium. When large quantities of phage are required, either multiple Petri dishes can be used or 500 mL liquid bacterial cultures at 10^7 cells/mL can be inoculated with phage at a MOI between 0.01 and 0.1 [46]. Propagating phage is an important process in maintaining reliable stocks for the LRN's *B. anthracis* plate lysis tests and is also a critical component of the RT-PCR, MALDI-TOF-MS, and hand-held immunoassay detection methods tested in this dissertation.

4.3.2 Materials and Methods

4.3.2.1 Gamma Phage Propagation [18]

One glass bead, obtained from a frozen "master" stock of *B. anthracis* Sterne on CryoBank™ glass beads, was streaked on a 5% SBA plate and incubated overnight

(minimum 12 hours) at 37 ± 2 °C. Five pure colonies were then transferred by a sterile 1.0 µL inoculating loop into 5 mL of autoclaved PBS and vortexed for 15 seconds. One hundred µL of this *B. anthracis* suspension was then inoculated onto each of 50 5% SBA plates and spread across the plate using a sterile glass rod spreader to produce a confluent lawn. These plates were then incubated for 15 minutes at 37 ± 2 °C. An electronic multichannel pipetter (RAININ 2-20 µL LTS EDP3-Plus) was used to dispense five µL aliquots of a previously sterilized gamma phage suspension in BHI in seven rows (49 total sites) on the plates containing the confluent bacterial lawn. The plates were then inverted and incubated overnight (minimum 12 hours) at 37 ± 2 °C. The next day, the plates were inspected for plaque formation, or circular clearings, of 5 to 10 mm in diameter.

4.3.2.2 Harvesting and Sterilizing Gamma Phage [18]

Gamma phage lysate was collected from the plates by adding two 5 mL aliquots of autoclaved BHI growth media to each plate followed by scraping the agar surface with a sterile glass rod spreader. The second 5 mL suspension scrapped from the previous plate was used as the first 5 mL addition to the next plate. The *B. anthracis*/gamma phage lysate from each plate was poured into Nalgene 85 mL Oak Ridge polycarbonate centrifuge tubes (Nalge Nunc International, Rochester, NY) and placed on ice. The centrifuge tubes were then vortexed for 15 seconds and the bacterial cells and debris were pelleted by centrifugation for 10 minutes at 10,000 x g at 4 °C (Marathon 22 KBR centrifuge). The supernatant gamma phage suspension was then sterilized by passage through a 0.8 µm filter followed by further filtration through a 0.2 µm filter (Pall Life Sciences Supor[®]800/200, 47 mm, Pall Corp., East Hills, New York). The resulting gamma phage suspension was titered as described in Section 4.5.2 and stored in the refrigerator at 4-10 °C.

4.3.3 Results

4.3.3.1 Gamma Phage Propagation

Circular clearings of 5 to 10 mm in the opaque bacterial lawn called plaques are the result of the specific lysis of *B. anthracis*. Figure 4.1 shows 49 such circular clearings made by gamma phage on 5% SBA plates.

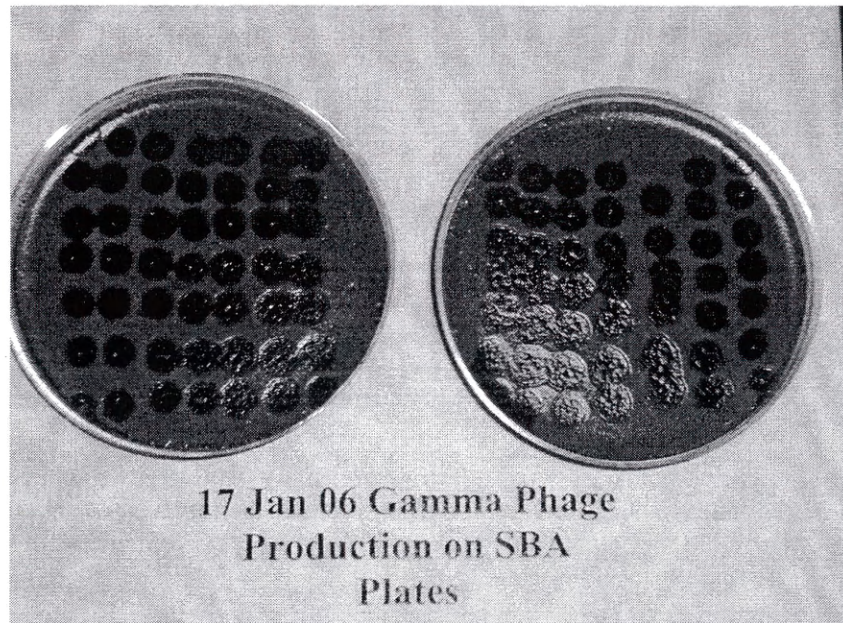


Figure 4.1 Propagation of gamma phage on 5% SBA plate

4.3.3.2 Harvesting and Sterilizing Gamma Phage

As one can see from Figure 4.1, there are many whole *B. anthracis* cells remaining after the gamma phage propagation as evidenced by the opaque lawn surrounding all the clearings. In addition, bacterial debris from the lysis process is present in the clearings. This is all scraped up in harvesting the gamma phage and is ultimately removed by centrifugation and filtration. Typical titers obtained by this propagation method are between 10^8 and 10^9 plaque forming units (pfu) per mL.

4.3.4 Discussion and Conclusions

Experiments showed that vegetative *B. anthracis* had to be early in its exponential growth phase to support gamma phage propagation, and that propagation could be done either on solid growth media or in liquid growth media. Growth on 5% SBA resulted in the most effective propagation results. Gamma phage titers were consistently at least one order of magnitude higher when the propagation was done on 5% SBA as compared with in liquid, BHI or TSB, growth media. Gamma phage propagation in liquid media resulted in titers between 10^6 and 10^7 pfu/mL. These lower gamma phage titers obtained in liquid media could negatively affect the ability to detect gamma phage amplification if the assay used has a high DL. Problems in getting consistent gamma phage lysis were encountered if the bacterial OD just before phage inoculation was ≥ 0.5 . The optimal *B. anthracis* cell density to support the gamma phage lytic replication cycle was determined to be at an OD between 0.2 and 0.4. This phenomenon was attributed to early stages of bacterial sporulation at OD values ≥ 0.5 that prevented the infectious process from fully taking place. Unlike non-spore producing bacteria, vegetative *B. anthracis* starts forming endospores based on sensed nutrient deficiencies or other environmental stresses; this phenomenon might start happening earlier than expected in its bacterial growth cycle.

4.4 Concentrating and Purifying Gamma Phage

4.4.1 Introduction

Concentrating and purifying phage propagation lysates, by precipitation with polyethylene glycol (PEG) followed by ultracentrifugation in CsCl gradients, proved to be important in obtaining pure high titers of gamma phage. Yamamoto *et al.* showed 100-fold increases in bacteriophage concentrations after the addition of 0.5 M NaCl and 10 % PEG 6000 followed by low speed centrifugation [47]. His procedures have become a mainstay in large-scale virus purification after he demonstrated minimal loss of viral infectivity. Ultracentrifugation in CsCl gradients further purifies the bacteriophage by removing other proteins and bacterial debris that might precipitate as well [48]. CsCl gradients separate phage particles based on their buoyant densities; tailed phages are composed equally of protein and DNA giving them a buoyant density between 1.45 and 1.52 g/mL [46]. The isolated phage bands can then be dialyzed in buffer solutions to facilitate long term storage and further analysis of the phage. Protein analysis of the resulting fraction required a sample free from bacterial debris and growth media typically present in large amounts after bacterial lysis. In addition, the two proposed hand-held immunoassay detection methods required gamma phage antibodies; these antibodies would be produced by inoculating rabbits with the highly purified gamma phage suspension.

4.4.2 Materials and Methods

Gamma phage suspensions were concentrated by polyethylene glycol precipitation and highly-purified by ultracentrifugation in CsCl gradients using methods detailed by Sambrook [48]. The starting suspension was the gamma phage containing filtrate obtained by the propagation and harvesting methods described in Sections 4.3.2.1

and 4.3.2.2 above. NaCl was added to a final concentration of 1 M (29.2 g per 500 mL of liquid) and PEG 8000 was added to the filtrate to a final concentration of 10% w/v (50 g per 500 mL); both were dissolved at room temperature by stirring. The NaCl promotes dissociation of bacteriophage particles from bacterial debris. The resulting suspension was placed on ice and refrigerated overnight to allow the bacteriophage particles to precipitate since highest recoveries were shown to occur after cooling for 16 hours [49]. The precipitated gamma phage was centrifuged using a Marathon 22 KBR centrifuge at 11,000 x g for 10 minutes at 4 °C and the supernatant was discarded. The gamma phage pellet was then resuspended (5 mL for each 500 mL of supernatant) in either PBS or SM (suspension medium: tris-HCl, MgSO₄, NaCl, and 2% glycerin solution). The PEG and cell debris was extracted by adding an equal volume of chloroform in a 30 mL Corex glass centrifuge tube (Corning Incorporated, Corning, NY) followed by vortexing for 30 seconds. The aqueous phase was recovered after separating the organic and aqueous phases by centrifuging at 3,000 x g for 15 minutes at 4 °C using a Marathon 22 KBR centrifuge. This chloroform extraction step was repeated two more times.

The PEG concentrated gamma phage samples were then purified using a CsCl density gradient. Four step density gradients using 62.5% CsCl in SM (25 g CsCl in 15 mL of SM) were prepared with 62.5% CsCl:SM ratios of 1:2, 1:1, 2:1 and 1:0. These gradients along with the PEG concentrated gamma phage suspension were placed in 35 mL polyallomer tubes (Beckman 1 x 3 ½ inch #326823) and ultracentrifuged (Beckman L8-M Ultracentrifuge, University of Colorado at Boulder) using a Beckman SW28 rotor at 25,000 rpm for 24 hours at 4 °C. A bluish band of gamma phage particles was collected around the 2:1 layer by puncturing the side of the tube with a 21-gauge needle and aspirating the suspension. The gamma phage suspension was dialyzed (Pierce Snakeskin™ 7,000 MWCO pleated dialysis tubing) in either Milli-Q water, SM, or PBS overnight then sterilized using 0.2 µm filters. The resulting buffered gamma phage suspension was stored in the refrigerator at 4-10 °C. The purity was confirmed by a

combination of MALDI-TOF-MS and TEM images. Gamma phage titers were obtained as described in Section 4.5.2.

4.4.3 Results

The following TEM picture series show the different stages of gamma phage propagation and harvesting, PEG concentration, and CsCl purification. Figure 4.2 shows sterile filtered (0.8 μm filter followed by further filtration through a 0.2 μm filter) gamma phage lysate from the propagation and harvesting procedures prior to the PEG concentration. Notice the two gamma phage among the stained bacterial debris and BHI growth media.

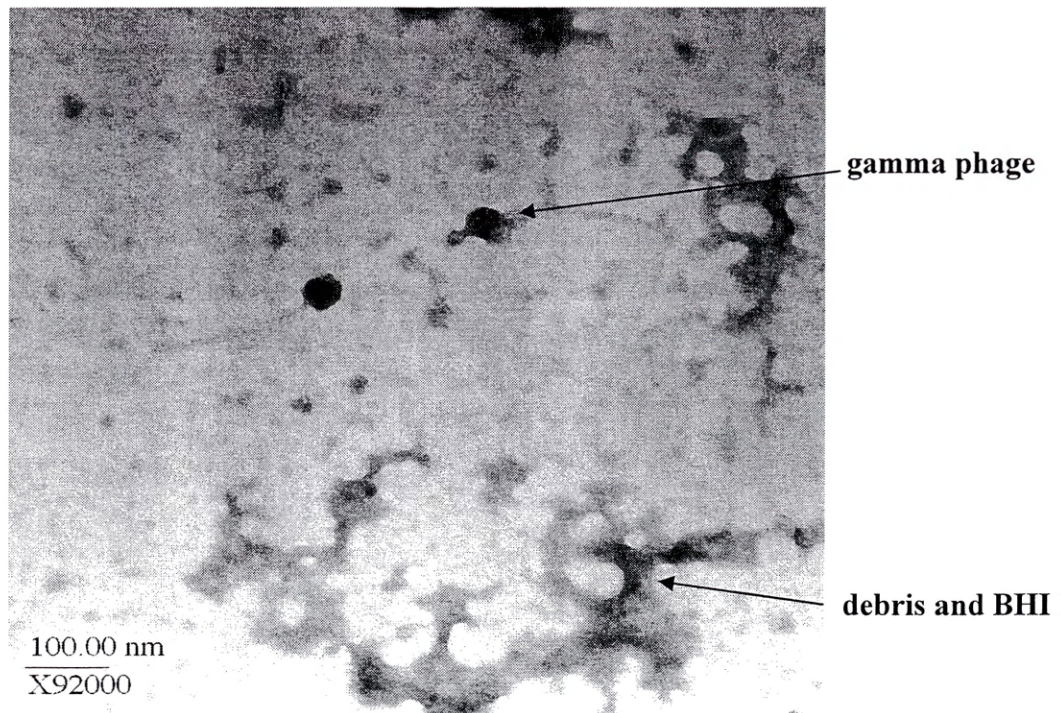


Figure 4.2 Sterile-filtered gamma phage

Figure 4.3 shows the gamma phage suspension after PEG concentration procedures were complete, but before the CsCl purification gradients were done. Notice the greater concentration of gamma phage, but with bacterial debris and BHI growth media still present.

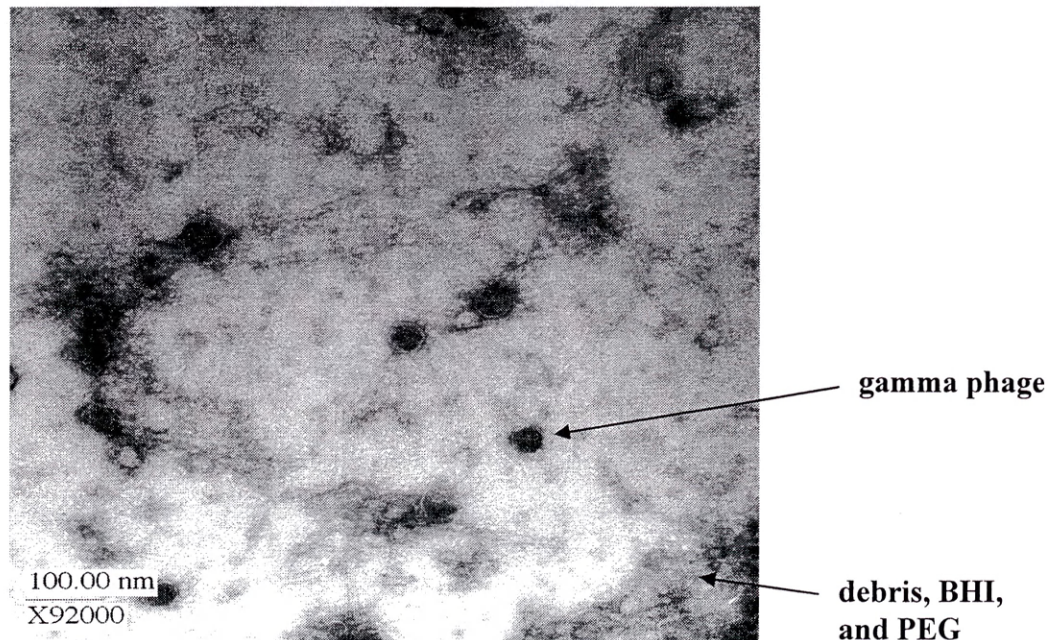


Figure 4.3 PEG purified gamma phage

Figure 4.4 shows the gamma phage suspension after being purified by ultracentrifugation using CsCl gradients. Notice the slight increase in gamma phage, but more importantly the noticeably clearer environment the phage are suspended in. The CsCl gradients appear to have highly purified the PEG concentrated gamma phage suspension.

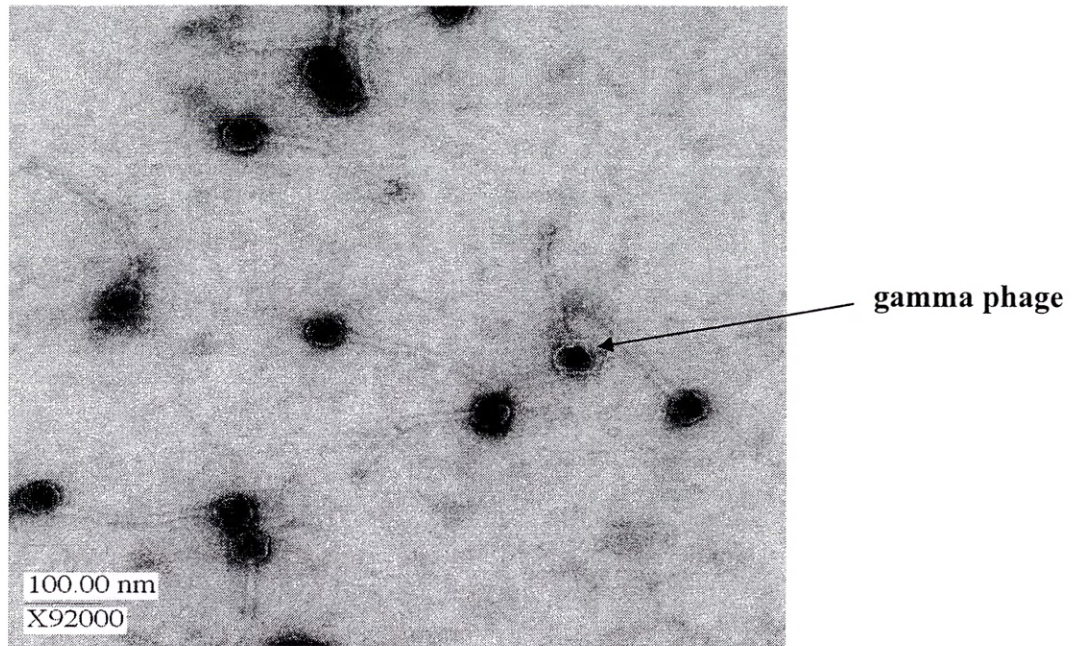


Figure 4.4 CsCl purified gamma phage

4.4.4 Discussion and Conclusions

The purpose of these gamma phage propagation, PEG concentration, and CsCl purification procedures was to obtain highly purified and high titer gamma phage suspensions for MALDI-TOF-MS protein analysis and for antibody development. A lack of gamma phage purity could be especially problematic for the antibody-based HHA if enough bacterial and/or growth media debris was present to induce an immunological response in the rabbits. As shown in Figures 4.2, 4.3, and 4.4 above, the PEG concentration and ultracentrifugation with CsCl gradients were both necessary to ensure high titer and pure gamma phage suspensions were produced. There was a noticeable improvement in titer and purity progressing from the harvested and filtered gamma phage suspension, to the PEG concentration, and on to the CsCl gradients. The gamma phage

suspension, according to both TEM and MALDI-TOF-MS analysis, looked very clean and concentrated so the suspensions were used for antibody development. The disadvantages of CsCl gradients are that they require overnight centrifugation, can lead to loss of phage infectivity, and making CsCl solutions is very expensive.

4.5 Determining Titer of Gamma Phage

4.5.1 Introduction

Determining the concentration (titer) of viable phage stocks is vitally important in studying phage/host interactions in the laboratory. Setting proper MOIs in bacteriophage amplification studies as well as determining gamma phage DLs for the tested phage-based detection assays required an accurate gamma phage count. In addition, antibody development required an accurate titer of gamma phage to ensure enough phage were present to illicit an immunological response in the rabbits. Phage stocks were kept refrigerated at approximately 4-10 °C, so phage under storage were warmed to 37 °C and carefully mixed before use since phage can aggregate together in storage. A “master” stock was kept since several rounds of propagation could produce variants that grow faster thereby increasing in numbers relative to the original phage [46].

The plaque assay is the most common method for counting phage and is similar to the gamma phage lysis confirmatory test used by the LRN to identify *B. anthracis* as well as the gamma phage propagation described in Section 4.3.2.1. At least 10-15 progeny phage (burst size) must be released by each infected cell to form a visible plaque [46]. Each plaque is caused by one original infecting phage particle that is then referred to as a pfu. Because of the large number of bacteria and phage involved in this lytic process, serial dilutions allow for a visual phage count. The number of pfu’s in a given solution volume is referred to as the phage titer (viable phage concentration).

4.5.2 Materials and Methods

Gamma phage suspensions were titered utilizing the traditional plaque assay method as described below. One glass bead, obtained from a frozen “master” stock of *B. anthracis* Sterne on CryoBank™ glass beads, was streaked on a 5% SBA plate and incubated overnight (minimum 12 hours) at 37 ± 2 °C. Five pure colonies were then transferred by a sterile 1.0 µL inoculating loop into 5 mL of autoclaved PBS and vortexed for 15 seconds. One hundred µL of this *B. anthracis* suspension was then inoculated on two (six for triplicate titers) 5% SBA plates and spread across the plates using a sterile glass rod spreader to produce a confluent lawn and incubated for 15 minutes at 37 ± 2 °C. Five µL of eight 10-fold gamma phage dilutions in PBS or SM were then pipetted onto the bacterial lawn using eight pre-marked locations (see Figure 4.5: the first dilution was applied on the top left clearing on the left plate, the next dilution to the right of the first dilution on the same plate, then the third dilution was applied on the bottom left clearing on the left plate, and so on until both plates had four applied dilutions each) on two plates as a reference to facilitate counting plaques (clear spots on the bacterial lawn). The Petri dishes were inverted, incubated overnight (at least 12 hours) at 37 ± 2 °C, and removed the next day to count plaques. Equation 4.0 shows the calculation used to determine the starting gamma phage titer in pfu/mL.

$$\text{pfu/mL} = 2 \times \text{pfu} \times 10^{(\text{sector} \# + 2)} \quad (\text{equation 4.0})$$

An average count was obtained using at least two sectors on a plate, then the average of the triplicate plate counts was calculated. This value in pfu/mL is the starting titer (before dilutions) of gamma phage particles.

4.5.3 Results

Figure 4.5 below visually displays one of the plaque assays that shows what a titer of 2.5×10^{10} pfu/mL looks like. The left 5% SBA plate shows large 5 to 10 mm clearings for gamma phage dilutions one (top left) through four (bottom right) that were pipetted from left to right in both rows. The right 5% SBA plate shows large 5 to 10 mm clearings for gamma phage dilutions five (top left) through six (top right) that were pipetted from left to right in both rows. Dilutions seven and eight had individual plaques that could be counted. The data from these plates is presented in Table 4.0.

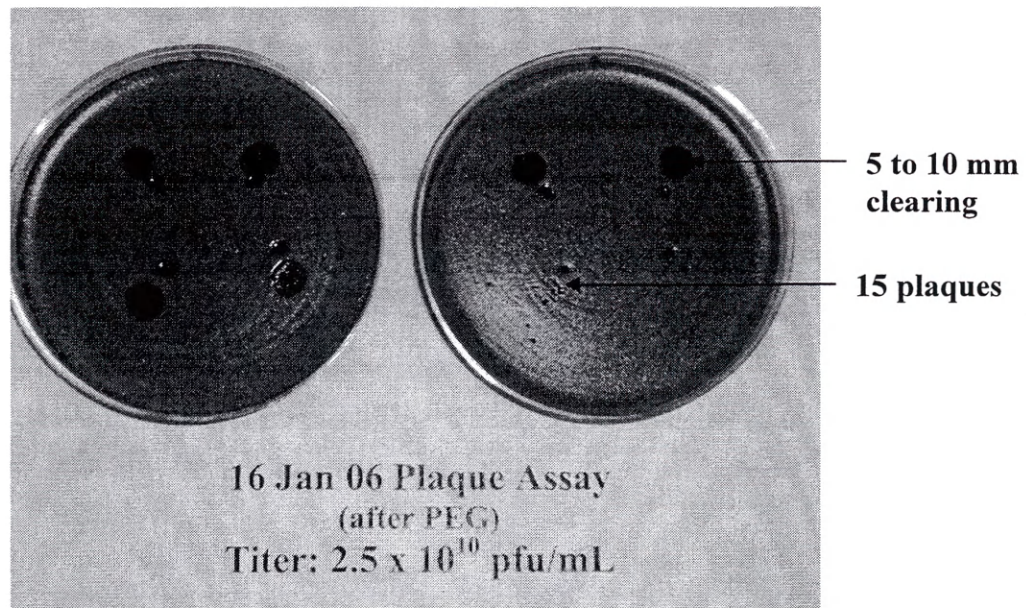


Figure 4.5 Gamma phage plaque assay

Table 4.0 Gamma phage serial dilutions for plaque assay

Sector	Dilution Factor	Plaques (pfu)
1	10x	Clearing
2	100x	Clearing
3	1000x	Clearing
4	10 ⁴ x	Clearing
5	10 ⁵ x	Clearing
6	10 ⁶ x	Clearing
7	10 ⁷ x	15
8	10 ⁸ x	1

When collecting the gamma phage plaque assay data for Table 4.0, “clearing” represents the large 5 to 10 mm clearing on the 5% SBA plates and signifies that too many gamma phage were present to count. Using the data from Table 4.0 in equation 4.0, the starting gamma phage titer represented by sector seven would be 3.0×10^{10} pfu/mL and sector eight would represent 2.0×10^{10} pfu/mL. The average starting gamma phage titer for this set of plates would be 2.5×10^{10} pfu/mL.

4.5.4 Discussion and Conclusions

To quantify or titer gamma phage, plaque assays were performed. Plating efficiency, the efficiency that gamma phage infects *B. anthracis*, is rarely 100%. When accurate titers were required, plaque assays were run in triplicate and average values were used. Very small clearings against an opaque bacterial background demonstrated the gamma phage lytic replication cycle had taken place and the surrounding *B. anthracis* had lysed. The large clearings of 5 to 10 mm represent the presence of more gamma

phage than could be counted, so 10-fold dilutions of the gamma phage suspensions allowed the number of individual plaques to ultimately be counted. These individual plaques could also be used to isolate pure gamma phage strains, since each plaque was the result of a single virus particle. Typical gamma phage titers obtained from 5% SBA plates after sterile filtration were 10^8 pfu/mL, and these titers became concentrated to 10^{10} pfu/mL after PEG concentration and CsCl gradients were performed. After a CsCl gradient, it had been reported that some phages do not form plaques unless in a broth with a high $MgCl_2$ concentration [46]. Experiments testing different solvents showed that gamma phage in water did not form consistent plaques, but that gamma phage in either PBS or SM formed consistent plaques. These two buffers were subsequently used to dilute gamma phage suspensions for plaque assays as well as for long term gamma phage storage. It was later discovered that SM totally suppressed MALDI signals and is discussed in Chapter 6.

4.6 Bacteriophage Amplification

Although Félix d'Herelle worked extensively with phage multiplication, it was Emory Ellis and Max Delbrück who received credit for the single-step growth experiment that detailed phage/host interactions [50]. When gamma phage are added to vegetative (actively growing) *B. anthracis*, they attach to peptidoglycan-anchored proteins (specific receptors referred to as GamR) on the cell wall and then inject their DNA [51]. During the phage replication cycle, progeny virions are assembled within the bacteria and subsequently release hydrolytic enzymes called lysins that attach to carbohydrate-binding sites and degrade the peptidoglycan bacterial cell wall [52]. The final result of the phage lytic replication cycle is bacterial lysis and subsequent release of up to 200 progeny gamma phage [53] that are fully capable of infecting additional susceptible bacteria. The number of phage in the growth media does not typically increase until after an eclipse period of 30 to 40 minutes; this can be longer when host cell densities are very low [54].

This bacteriophage amplification and subsequent virion release resulting from the gamma phage lytic replication cycle described above, is the basis of detection for the assays reported in this dissertation to indirectly detect *B. anthracis*. The exception was HHA 1 versions 1 and 2 which used the specific attachment of gamma phage to the bacterial cell wall as the basis of detection. Bacteriophage amplification required vegetative bacterial cells as opposed to sporulated ones. For *B. anthracis* spores, it has been reported that the proteinaceous *B. anthracis* spore coat porosity increases within 10 minutes of inducing germination and that germination can be accelerated with the addition of L-alanine [55]. Infecting bacteria with phage required an understanding of both the phage/host infectious cycle and MOI. The MOI used directly affected the required analysis time as did the method utilized to bring phage in contact with bacteria (in this case a shaker table). A model based on Brownian motion had been reported that effectively predicted bound phage after time t [54]:

$$\ln P/P_0 = -kCt \text{ or } P/P_0 = e^{-kCt} \quad (\text{equation 4.1})$$

$$P_{\text{bound}} = (1 - e^{-kCt}) P_0 \quad (\text{equation 4.2})$$

Where P/P_0 is the fraction of unbound phage at time t (in minutes); C is the concentration of host cells per cubic centimeter; and k is the adsorption rate constant (in cubic centimeters per minute). The adsorption rate constant can be experimentally determined since it depends on the number of binding sites per cell (T-even phages have up to 300), diffusion rates, and collision efficiencies. From the equation above, it can be seen that increasing the time, the adsorption rate constant, the concentration of bacterial cells, and the concentration of phage will all increase the phage adsorption events necessary to start the lytic replication cycle.

CHAPTER 5

INDIRECT DETECTION OF *BACILLUS ANTHRACIS* USING REAL-TIME POLYMERASE CHAIN REACTION (RT-PCR) TO DETECT GAMMA PHAGE DNA

5.1 Introduction

Real-time polymerase chain reaction (RT-PCR) allows the amplification of a target (or template) DNA to be monitored as it occurs through increased fluorescence of a reporter probe or dye. As discussed in Section 2.5, RT-PCR is currently used by the LRN to directly detect *B. anthracis* using three different DNA targets. In this study, RT-PCR using primers specifically designed for gamma phage was combined with the highly specific gamma phage amplification (described in section 4.6) into one simple assay to indirectly detect *B. anthracis* in real-time using SYBR green dye. Since gamma phage primers were not commercially available, they were designed in-house. By detecting the phage DNA, the bacteriophage amplification phenomenon should lead to improved assay sensitivity (or DL) over using RT-PCR to detect bacterial DNA. Since the amplification of gamma phage would only occur in the presence of a suitable host, the detection of increasing concentrations of progeny gamma phage DNA implied the presence of viable *B. anthracis*.

The potential advantages of using this combined RT-PCR/gamma phage amplification assay to indirectly detect *B. anthracis* compared with the direct detection of *B. anthracis* using RT-PCR or the CDC's gamma phage plate lysis method include: 1) less time to identify *B. anthracis* via gamma phage amplification; 2) increased assay sensitivity due to gamma phage amplification (production of progeny phage); 3)

improved specificity without having to develop multiple PCR targets; 4) no requirement for overnight bacterial culture; and 5) only viable *B. anthracis* is detected.

5.2 Materials and Methods

5.2.1 Design Gamma Phage Primers

Primers were designed in-house by first identifying a conserved DNA region within the major capsid protein putative region of *B. anthracis* phage gamma isolate d'Herelle (DQ289556) using the National Center for Biotechnology Information's (NCBI) nucleotide database (<http://www.ncbi.nlm.nih.gov/>). A Basic Alignment Search Tool (BLAST) was subsequently used to compare this DNA region with other viruses, bacteria, and organisms to minimize potential cross reactivity. A conserved DNA region between nucleotides 121 and 480 was selected and used in OligoPerfect™ Designer (Invitrogen Corp, Carlsbad, CA) to develop primers 20 nucleotides long (forward: 5'-ACTGGGGAAGATGGAGGACT-3'; reverse: 5'-ACGTGTACGCACTGGTTCAA-3'). A BLAST inquiry of the resulting 117 nucleotide amplicon was conducted to check cross homology with other organisms.

5.2.2 Gamma Phage Production

Gamma phage working suspensions for bacteriophage amplification experiments were prepared using *B. anthracis* Sterne 34F2 (pXO1⁺/pXO2⁻) as the propagation host in TSB. Liquid lysate was collected after three days of incubation at 37 ± 2 °C. Any remaining bacterial cells and debris were removed via centrifugation at 10,000 rpm for 10 minutes. The resulting phage containing supernatant was sterilized by passage through a 0.8 µm filter followed by further filtration through a 0.2 µm filter (Pall Life Sciences Supor®800/200, 47 mm, Pall Corp., East Hills, New York). The resulting gamma phage

suspension was quantified utilizing the traditional plaque assay method described in Section 4.5.2. Three independent plaque assays were used to determine the titer of gamma phage; the titer was $9 \pm 4 \times 10^7$ pfu/mL.

5.2.3 *Bacillus anthracis* (Host) Production

Several colonies of *B. anthracis* Sterne 34F2 (pXO1⁺/pXO2⁻) were scraped from a refrigerated 5% SBA Petri dish and inoculated into BHI broth. Optical density readings were taken at 625 nm (Pharmacia Biotech Ultrospec 2000 UV/VIS, Biochrom Ltd, Cambridge, UK) and additional BHI was added to reach an OD of 0.203. This OD reading ensured sufficient numbers of bacteria were present and sufficient nutrients were available to support additional bacterial growth. The concentration of *B. anthracis* was determined by colony plate counts described in Section 3.5.2. Three independent plate counts were used to determine the concentration of *B. anthracis*; concentration was $2.3 \pm 0.6 \times 10^7$ cfu/mL.

5.2.4 Sample Preparation

Extraction of DNA was performed by adding 200 μ L of PrepMan Ultra (Applied Biosystems, Foster City, CA) to 100 μ L of sample followed by 10 minutes in a boiling water bath. The resulting sample was further diluted with 900 μ L of deionized water (GIBCO Ultra Pure DNase RNase Free) to minimize the auto fluorescence signal and then spun at 8,000 rpm for three minutes to separate the DNA from cell debris. Two μ L of diluted DNA was then withdrawn from the supernatant to load the reaction capillaries. Twenty μ L of reaction components were pipetted into 20 μ L Roche LightCycler™ capillaries (Roche Diagnostics, Indianapolis, IN). The 20 μ L reaction components consisted of two μ L of extracted DNA sample, 10 μ L of QuantiTect SYBR Green PCR Kit master mix (QIAGEN Inc., Valencia, CA), 0.3 μ L each of forward and reverse

primers (20 pmol/ μ L), and 7.4 μ L of deionized water (GIBCO Ultra Pure DNase RNase Free). The capillaries were then capped and centrifuged for 3-5 seconds at 600 rpm to spin the sample into the lower portion of the capillary. Afterward, RT-PCR was run.

5.2.5 RT-PCR

Real-time amplification and detection of the amplified gamma phage PCR products was accomplished using Idaho Technology Inc.'s portable Ruggedized Advanced Pathogen Identification Device (R.A.P.I.D.[®]). Reactions were automatically monitored cycle-by-cycle via fluorescence of a double-strand specific fluorescent SYBR green dye incorporated into the QuantiTect SYBR green PCR kit. The cycle number at which fluorescence exceeded the baseline denoted positive samples. This value was recorded automatically for each sample and is called the threshold cycle (C_T).

Two different R.A.P.I.D.[®] instruments were used in all experiments and three independent sample runs were alternated between these two instruments. Average C_T 's were used for data analysis. Additionally, each RT-PCR run contained a no template control (NTC) consisting of the above components without the DNA sample (negative control), a positive control, and each DNA sample in duplicate. The RT-PCR cycle conditions were: melt at 95 °C for 10 minutes followed by 45 cycles of 1) 95 °C for 10 seconds, 2) 58 °C for 20 seconds, 3) 72 °C for 20 seconds, and 4) fluorescence acquisition.

5.2.6 Determination of Gamma Phage Detection Limit (DL)

Two stock solutions of PEG and CsCl gradient purified gamma phage in Milli-Q water were titered using the traditional plaque assay described in Section 4.5.2. The gamma phage titers were $4.60 \pm 3.14 \times 10^9$ pfu/mL (Sample A) and $1.53 \pm 0.46 \times 10^8$ pfu/mL (Sample B). DNA was extracted as described above, except 200 μ L of PrepMan

Ultra extracted DNA was diluted in 1.8 mL of deionized water (GIBCO Ultra Pure DNase RNase Free). The concentration of extracted DNA was spectrophotometrically determined at 260 nm to be 3.9 ng/ μ L and 2.3 ng/ μ L respectively. These phage DNA samples were then diluted with deionized water to one ng/ μ L in triplicate (independent samples) then 10-fold serially diluted in deionized water to concentrations of 1×10^8 ag/ μ L (ag = attogram) to 1×10^{-2} ag/ μ L. RT-PCR was then run on the serially diluted bacteriophage DNA samples to determine this assay's DL.

5.2.7 Determination of *B. anthracis* Detection Limit (DL)

Gamma phage was added to *B. anthracis* in BHI that was in five mL culture tubes at varying concentrations and MOIs to validate the combined RT-PCR/phage amplification capability to indirectly detect *B. anthracis* at concentrations as low as 2.07×10^2 cfu/mL. Three samples of $2.3 \pm 0.6 \times 10^7$ cfu/mL *B. anthracis* were each 10-fold serially diluted with BHI (2.3×10^6 to 2.3×10^2 cfu/mL) then 2.7 mL of each dilution was pipetted into five-5 mL culture tubes (in triplicate). A gamma phage working suspension ($9 \pm 4 \times 10^7$ pfu/mL) was 10-fold serially diluted with BHI (9×10^5 to 9×10^3 pfu/mL) then 300 μ L of gamma phage at each dilution was pipetted into five-5 mL culture tubes resulting in a three mL total sample volume. Table 5.0 shows the starting concentrations of *B. anthracis* and gamma phage in BHI contained in all five culture tubes. After vortexing each culture tube, 50 μ L of liquid was removed from each tube and frozen as time zero controls; these contain the starting gamma phage DNA concentrations prior to bacteriophage amplification. The culture tubes were then placed on their sides on a shaker at 120 rpm in an incubator at 37 °C for four hours. After four hours of incubation, the samples underwent sample preparation as described above except that 50 μ L of sample was withdrawn, 100 μ L of PrepMan Ultra added to extract DNA, and 400 μ L of deionized water was used to minimize auto fluorescence. RT-PCR was then run on each sample.

Table 5.0 Concentrations of *B. anthracis* (B) in cfu/mL and gamma phage (G) in pfu/mL in each five mL culture tube

	Tube 1	Tube 2	Tube 3	Tube 4	Tube 5
Sample 1	B: 2.07×10^6 G: 9×10^4	B: 2.07×10^5 G: 9×10^4	B: 2.07×10^4 G: 9×10^4	B: 2.07×10^3 G: 9×10^4	B: 2.07×10^2 G: 9×10^4
Sample 2	B: 2.07×10^6 G: 9×10^3	B: 2.07×10^5 G: 9×10^3	B: 2.07×10^4 G: 9×10^3	B: 2.07×10^3 G: 9×10^3	B: 2.07×10^2 G: 9×10^3
Sample 3	B: 2.07×10^6 G: 9×10^2	B: 2.07×10^5 G: 9×10^2	B: 2.07×10^4 G: 9×10^2	B: 2.07×10^3 G: 9×10^2	B: 2.07×10^2 G: 9×10^2

5.2.8 Primer Specificity Studies

DNA from a variety of bacteria (in-house), including gram-positive rods (*B. anthracis* and *B. cereus*), gram-positive cocci (*Staphylococcus aureus*), gram-negative rod (*Pseudomonas aeruginosa*), gram-negative cocci (*Neisseria gonorrhoea*) and yeast (*Candida albicans*) at a concentration of one ng/ μ L were analyzed by RT-PCR to test for primer cross reactivity. Human DNA, from both sterile (blood) and non-sterile (cheek) cells, were also tested for cross reactivity using RT-PCR. For cheek cells, two different individuals were cotton swabbed in four areas between their cheeks and gums. The swab was then vortexed in one mL of PBS (pH=7.2). For human blood cells, 900 μ L of Purogene™ was added to 100 μ L of blood and mixed well for three minutes to lyse the cells. All sets of cells were then spun for three minutes at 8,000 rpm, pelleted, and

underwent sample preparation as described above using the supernatant. RT-PCR was then run on each sample.

5.2.9 Check Purity of RT-PCR Amplification Products

A melting curve program (started at 50 °C and increased 0.2 °C/sec) and a Flash Gel™ Cassette-DNA Marker (Cambrex BioScience Rockland, Inc.) were run after a R.A.P.I.D.® run to confirm the purity of the PCR amplification products.

5.3 Results

5.3.1 Representative RT-PCR Spectrum

Figure 5.0 shows the real-time data displayed from the R.A.P.I.D.® instrument as the PCR amplification occurs on gamma phage DNA present in 10-fold dilutions of gamma phage DNA. The highest concentration of gamma phage DNA was 2.0×10^5 attograms and the lowest was 2.0×10^2 attograms. The x-axis contains the number of PCR cycles and the y-axis shows the fluorescence intensity. The NTC has all reaction components except the gamma phage and acts as a negative control. Because more time is required to PCR amplify lower concentrations of DNA to exceed the fluorescence baseline, increasing C_T values represent lower gamma phage DNA concentrations or lower number of gamma phage particles present. C_T differentiation for different gamma phage DNA concentrations is shown in Figure 5.0 below.

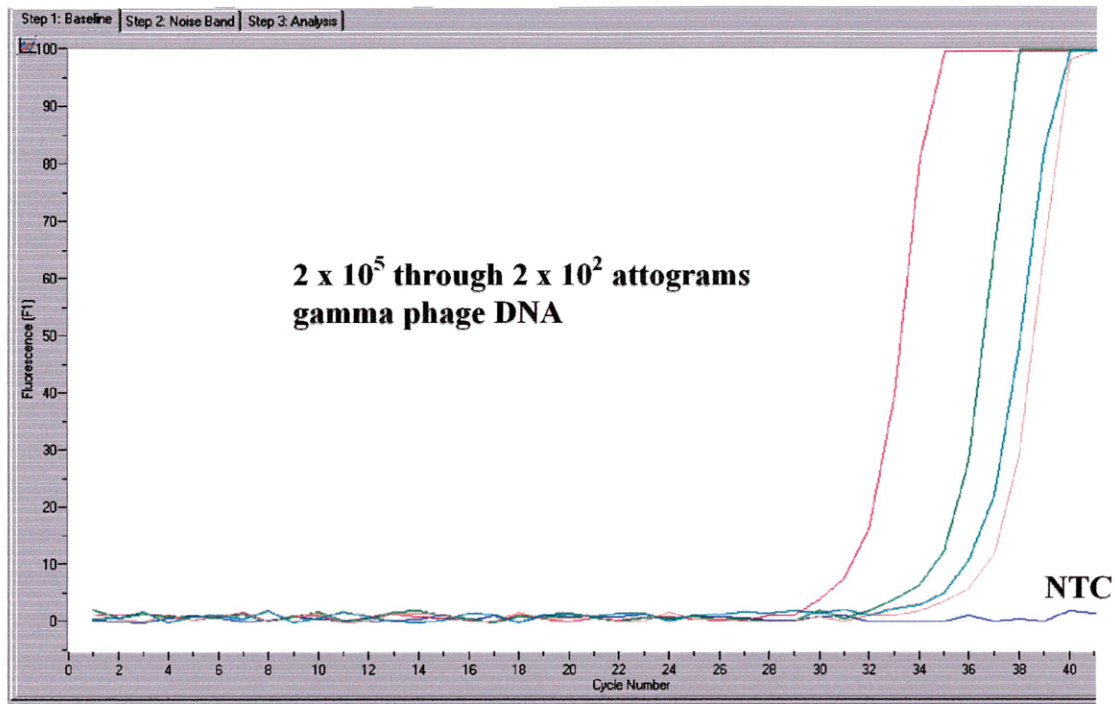


Figure 5.0 R.A.P.I.D.[®] RT-PCR spectrum of a pure gamma phage dilution series

5.3.2 Determination of Gamma Phage Detection Limit (DL)

Early experiments confirmed the feasibility of using C_T values lower than the NTC's to qualitatively detect gamma phage and using changes in C_T values to quantitatively detect different gamma phage concentrations. To determine gamma phage DL, a dilution series (three for two independent samples, A and B) was started at one ng/ μ L (2.0×10^9 ag in two μ L sample volumes) of gamma phage DNA. RT-PCR results are summarized for both independent samples in Table 5.1. Concentrations where average C_T 's showed increasing values with decreasing phage concentrations are shown as "QUAN" (quantitative); "QUAL" is where the C_T 's stopped increasing, but qualitative detection remained possible. The gamma phage quantitative DL (QDL) was 1.1×10^3 ag, which was determined by averaging the two independent samples shown above. Using

Table 5.1 Dilution series in attograms (ag) of gamma phage DNA.

Mass (ag) of gamma phage DNA	2.0 x 10³	2.0 x 10²	2.0 x 10¹
Sample A	QUAN	QUAL	QUAL
Sample B	QUAN	QUAN	QUAL

the average mass of DNA subunits (A-T = 1.0185×10^{-21} g, G-C = 1.0235×10^{-21} g) and counting A-T (26,458) and G-C (14,409) pairs in the gamma phage genome, the total DNA weight in one gamma phage is 4.16×10^{-17} g or 41.6 ag of DNA per gamma phage particle. Thus, this assay yielded a QDL of 26 gamma phage particles (or GEs) in 20 μ L (equivalent to 1.30×10^3 pfu/mL).

5.3.3 Determination of *B. anthracis* Detection Limit (DL)

Early experiments in this study showed that using bacteriophage amplification to indirectly detect *B. anthracis* was dependent on the ratio of bacteriophage to bacteria, or MOI. Therefore, a series of experiments was performed where the MOI was varied within each reaction tube. Table 5.2 shows gamma phage amplification results in indirectly detecting *B. anthracis*. See Table 5.0 for actual gamma phage and *B. anthracis* starting concentrations. A time equals zero or “starting” *B. anthracis* concentration of 207 cfu/mL was detected in Tube 5 at an MOI of 43.5; a starting *B. anthracis* concentration of 2,070 cfu/mL was detected in Tube 4 at an MOI of 4.35; and a starting *B. anthracis* concentration of 20,700 (2.07×10^4) cfu/mL was detected in Tube 3 at MOI’s of 0.043, 0.43 and 4.3. All *B. anthracis* samples at starting concentrations $\geq 2.07 \times$

10⁴ cfu/mL were detected at all MOI's tested. All sample C_T values stayed well below the NTC's. Thus, this assay yielded a DL of four *B. anthracis* cells in 20 µL (equivalent to 2.0 x 10² cfu/mL).

Table 5.2 Results of *B. anthracis* DL and MOI experiments (C_{T0} = time zero threshold cycle; C_{T4} = 4 hour phage amplification threshold cycle; INT = interpretation, where "POS" = amplification detected (lower C_T value) and "N.D." for amplification not detected).

	Tube 1	Tube 2	Tube 3	Tube 4	Tube 5
Sample 1	MOI = .043	MOI = .43	MOI = 4.3	MOI = 43.5	MOI = 435
	C _{T0} = 24.1	C _{T0} = 24.4	C _{T0} = 24.6	C _{T0} = 23.5	C _{T0} = 24.2
	C _{T4} = 13.4	C _{T4} = 18.1	C _{T4} = 23.4	C _{T4} = 24.5	C _{T4} = 25.4
	INT: POS	INT: POS	INT: POS	INT: N.D.	INT: N.D.
Sample 2	MOI = .0043	MOI = .043	MOI = .43	MOI = 4.35	MOI = 43.5
	C _{T0} = 29.2	C _{T0} = 29.6	C _{T0} = 29.8	C _{T0} = 29.3	C _{T0} = 28.6
	C _{T4} = 18.7	C _{T4} = 20.5	C _{T4} = 26.6	C _{T4} = 27.3	C _{T4} = 27.8
	INT: POS	INT: POS	INT: POS	INT: POS	INT: POS
Sample 3	MOI = .00043	MOI = .0043	MOI = .043	MOI = .435	MOI = 4.35
	C _{T0} = 29.0	C _{T0} = 29.6	C _{T0} = 28.8	C _{T0} = 28.6	C _{T0} = 28.0
	C _{T4} = 20.4	C _{T4} = 27.3	C _{T4} = 27.8	C _{T4} = 31.6	C _{T4} = 29.4
	INT: POS	INT: POS	INT: POS	INT: N.D.	INT: N.D.

5.3.4 Primer Specificity Studies

None of the DNA from bacteria (*B. anthracis*, *B. cereus*, *Staphylococcus aureus*, *Pseudomonas aeruginosa*, and *Neisseria gonorrhoea*), yeast, blood, or human cells underwent detectable PCR amplification within 38 RT-PCR cycles. These limited cross reactivity studies showed 100% primer specificity to gamma phage. In addition, a BLAST of the resulting 117 nucleotide amplicon showed it to be highly specific to gamma phage with only an approximate 40 nucleotide overlap with Zebrafish DNA and no cross homology with other organisms.

5.3.5 Check Purity of RT-PCR Amplification Products

Both the melting curve and the Flash Gel™ Cassette-DNA Marker (Figure 5.1) showed extremely clean amplification products. The DNA markers are located on both ends of the gel; the standard marker for 100 base pair (bp) is the uppermost bright mark. Two separate samples obtained from the RT-PCR amplified products were run on the gel and are represented by the two single bright marks to the left of the right DNA marker. The gel results showed one pure amplified product and confirmed the expected 117 bp amplicon size.

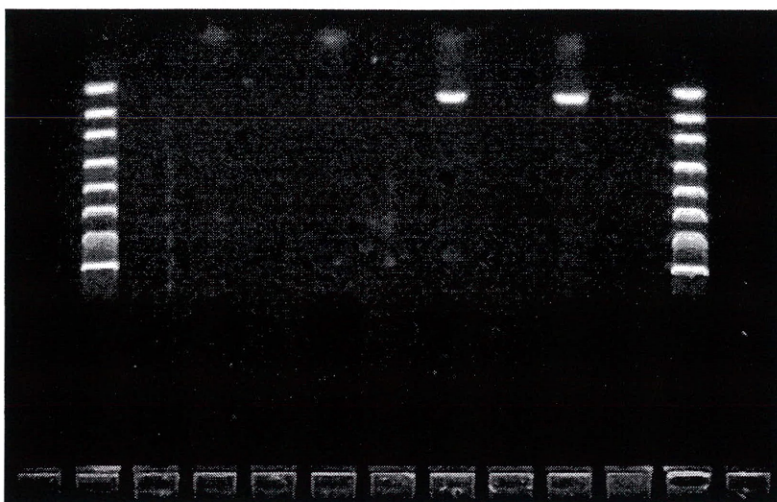


Figure 5.1 Flash Gel™ cassette-DNA marker of RT-PCR with standards (sizes 100/200/300/500/800/1250/2000/4000 bp) marking both ends

5.4 Discussion and Conclusions

In this combined RT-PCR/gamma phage amplification assay, gamma phage was inoculated into *B. anthracis* in BHI, the gamma phage suspension was incubated for four hours at 37 °C on a shaker to allow for bacteriophage amplification, DNA was extracted, and the sample analyzed by RT-PCR in less than five hours. The lower fluorescent C_T values compared with time zero C_T 's, monitored in real-time, signaled an increase in progeny gamma phage thereby implying the presence of viable *B. anthracis*. The CDC employed gamma phage plate lysis test for *B. anthracis* takes approximately 20 hours to complete, so this combined RT-PCR/gamma phage amplification detection method could be used for *B. anthracis* confirmatory testing and have the results in less than five hours.

A distinction was purposefully made between qualitative and quantitative DL when detecting gamma phage DNA using RT-PCR. This distinction emphasized that decreasing C_T values from time zero measurements (quantitative detection) reflected gamma phage amplification, and detection of this phage amplification implied the presence of viable *B. anthracis*. This assay yielded a QDL of 26 gamma phage particles (or GEs) in 20 μ L (equivalent to 1.30×10^3 pfu/mL). In contrast, C_T values less than the NTC but not measurably less than the time zero values (qualitative detection) meant that gamma phage was detected through the RT-PCR amplification of its DNA, but that gamma phage amplification prior to RT-PCR was not detected.

This method detected a starting *B. anthracis* concentration of 207 cfu/mL at an MOI of 43.5 and all *B. anthracis* samples starting $\geq 2.07 \times 10^4$ cfu/mL (equivalent to four bacterial cells in 20 μ L) were detected at all MOIs tested, thus indicating a sufficient DL to detect infectious doses of *B. anthracis*. In addition, RT-PCR qualitatively detected 20 ag of gamma phage DNA compared with 50 fg and 1 pg of *B. anthracis* DNA detected in other RT-PCR studies.

A MOI >3 typically results in infection of virtually all bacterial cells in exponential growth [46], thereby preventing additional bacterial growth along with progeny phage production. This could be detrimental in detecting extremely low concentrations of bacteria if the progeny phage produced are too few and the higher MOI does not allow for secondary infections to occur. A phage amplification event producing less than 1.30×10^3 pfu/mL would potentially be undetected using this assay at a MOI >3 ; however, given up to 200 gamma phage are produced in each infected *B. anthracis* cell, producing this scenario would require a *B. anthracis* starting concentration of about seven cfu/mL which is an extremely low bacterial concentration.

Using effective MOIs could present an additional level of difficulty when using this technique; however, the data shows two orders of magnitude differences in MOI did not negatively affect this assay's ability to detect the *B. anthracis*. Standard stocks of gamma phage could easily be made up and stored; allowing for a large sampling of

different MOIs. Thirty-two tubes available per run in the R.A.P.I.D.[®] would easily allow for this flexibility. Storage of gamma phage at 4 °C showed less than a log₁₀ drop in two years for one lot and in one year for another lot; thus storage of gamma phage with minimal loss of activity is reasonable [18].

Several important advantages were realized by using this combined RT-PCR/gamma phage amplification assay to indirectly detect *B. anthracis* instead of the direct detection of *B. anthracis* using RT-PCR or the CDC's gamma phage plate lysis method. First, this assay required less than five hours to obtain results compared with at least 20 hours to conduct the CDC's gamma phage lysis method. Second, this assay's *B. anthracis* DL was 2.07×10^4 cfu/mL or equivalent to approximately four cells in 20 µL, making it more sensitive than the direct detection of *B. anthracis* using RT-PCR (nine or 167 cells reported in previous studies). RT-PCR also proved to be more sensitive to gamma phage DNA (20 ag) than it was to *B. anthracis* DNA (50 fg and 1 pg reported in previous studies). Third, this method showed no primer cross reactivity within the small sample size tested here. Specificity is very important in any detection method because false positives and negatives result in ambiguity that could lead to hesitation, doubt, and ultimately poor decisions. The specificity of gamma phage towards *B. anthracis* is well documented [18], so it would be reasonable to expect this combined method would have similar excellent specificity without requiring the use of multiple DNA targets. Fourth, this assay was uniquely designed around the gamma phage amplification event which is totally dependent on the presence of a viable host. The importance of knowing the viability of potentially dangerous bacteria cannot be overstated from a treatment as well as a remediation perspective.

The combined RT-PCR/gamma phage amplification assay to indirectly detect *B. anthracis* detailed above could replace the current gamma phage plate lysis test for detecting *B. anthracis*. In addition, this assay could supplement other detection methods, to include RT-PCR, specifically to provide bacterial viability information not available with these other methods. This assay provides another tool to use in the fight for speed

and accuracy in identifying a suspected *B. anthracis* attack and in responding to a potential remediation situation.

CHAPTER 6

INDIRECT DETECTION OF *BACILLUS ANTHRACIS* USING MATRIX-ASSISTED LASER DESORPTION/IONIZATION TIME-OF-FLIGHT MASS SPECTROMETRY (MALDI-TOF-MS) TO DETECT GAMMA PHAGE PROTEINS

6.1 Introduction

Since the 1980's, matrix-assisted laser desorption/ionization time-of-flight mass spectrometry (MALDI-TOF-MS) has emerged as a powerful method in biological analysis. MALDI-MS is a soft ionization technique that uses a pulsed laser to vaporize/ionize a sample that is co-crystallized on a surface with a matrix; the matrix absorbs the laser energy thereby minimizing analyte ion decomposition [56]. When coupled with a TOF mass analyzer, ions become separated according to their mass-to-charge (m/z) ratios. To be useful for biological agent identification, MALDI-TOF-MS would have to unambiguously distinguish between different species, or possibly strains, of bacteria in complex matrices. Lysing bacterial cells to release macromolecules was a common sample preparation step until MALDI-TOF-MS was shown to be effective using intact bacteria [57]. Studies have since determined the minimum number of bacterial cells required for identification was fixed at 10^7 cells/mL or 10^4 cells in a μL sample volume [58].

MALDI-TOF-MS bacterial cell spectra are typically complex and can vary based on protein expression which constantly changes in response to cell growth cycles and environmental conditions [1]. Some MALDI-TOF-MS studies have shown spectra characterization of spores down to the *B. cereus* group of bacteria (*B. anthracis*, *B. cereus*, *B. mycoides* and *B. thuringiensis*) and small spectra distinctions between some

strains using corona plasma discharge or sonication prior to analysis; however, the spectra were influenced by different growth media [59]. A Pacific Northwest National Laboratory study found that despite visible differences in microorganism spectra generated under different growth conditions, they were able to identify microorganisms by concentrating on the common peaks in the m/z 2,000 to 20,000 range using their analysis algorithm [60]. Bacterial mixtures and different matrix components can further complicate the spectra.

The concept of using MALDI-TOF-MS for the indirect detection of bacteria using its very specific bacteriophage was first studied in the Voorhees group in 2002 [61, 62]. The advantages of such an approach potentially include simplified spectra, faster detection time than overnight bacterial culturing followed by gamma phage lysis, lower DLs and greatly improved specificity. The simplified spectra result from the simplistic nature of phage particles compared to the complex living bacterial cell. The bacteriophage amplification process works because of the infectious process (lytic replication cycle) between viable bacteria and its specific bacteriophage (see Section 4.6). To use MALDI-TOF-MS for the indirect detection of *B. anthracis*, an investigator must first identify and select one or more gamma phage biomarkers. The biomarkers must be highly specific to gamma phage and be consistently detectable at low DLs. Icosahedral double-stranded DNA viruses typically assemble their capsids from multiple copies (approximately 420) of a few type of protein subunits [63]. Four protein bands with molecular weights (MWs) estimated to be between 12 and 49 kDa were obtained using sodium dodecyl sulfate-polyacrylamide gel electrophoresis (SDS-PAGE) from gamma phage capsid rich preparations [43], so possible protein biomarkers might be found in this MW range. In assessing potential biomarkers, it is extremely important to start from a very pure bacterial or viral sample to ensure contaminant peaks are not being selected. This was done for gamma phage using the PEG concentration and CsCl gradients described in Section 4.4.2.

A hypothetical detection scheme would begin by environmentally sampling for *B. anthracis* spores, and then providing the growth conditions necessary for these spores to germinate and begin vegetative growth. Very early (OD between 0.2 and 0.4 at 625 nm) in exponential growth, the sample would be inoculated with a known titer of gamma phage just below the predetermined MALDI-TOF-MS DL. As time passes, larger quantities of progeny phage are produced and released (called bacteriophage amplification) ultimately producing a detectable MALDI-TOF-MS signal. Without the viable bacterial presence, no bacteriophage amplification would result and the concentration of the phage protein biomarker would remain below detectable amounts.

6.2 Materials and Methods

6.2.1 MALDI-TOF-MS Instrument Parameters

All spectra were obtained using a PerSeptive Biosystems Voyager-DE STR MALDI-TOF-MS (Applied Biosystems Inc., Foster City, CA) using a stainless steel 100 sample spot plate unless otherwise noted. MALDI spectra were obtained using the following parameters: 337 nm N₂ laser with laser intensity set just above ion generation threshold, positive ion, linear mode, 25 kV accelerating voltage, 80% grid voltage, 150 to 200 nsec delayed extraction, 2000 m/z low mass ion gate and 50 shots per spectrum. Mass spectra were averaged over 100 to 150 individual laser shots. The raw data from Data Explorer™ (PerSeptive Biosystems, Foster City, CA) was exported into SigmaPlot 2001 version 7.0 (SPSS Inc., Chicago, IL) for producing spectra.

6.2.2 Mass Calibration

The PerSeptive Biosystems Voyager-DE STR was calibrated using ProteoMass™ MALDI-TOF-MS standards (SIGMA, Saint Louis, MO). Ten µL of each apomyoglobin

(M+H)⁺= 16,952.27 Da, aldolase (M+H)⁺= 39,212.28 Da and albumin (M+H)⁺= 66,430.09 Da at 100 pmol/μL were mixed and used for instrument calibration.

6.2.3 Matrix and Sample Application

Ferulic acid (SIGMA, Saint Louis, MO) was used as the matrix based on a previous study comparing the efficiency of several potential matrices in analyzing whole cell bacterial peaks above 15 kDa [64]. 12.5 mg of ferulic acid (4-hydroxy-3-methoxy cinnamic acid) was dissolved in 170 μL of formic acid, 330 μL of acetonitrile, and 500 μL of deionized water. Samples and matrix was applied to the MALDI plate using a sandwich method that spotted 0.5 μL of matrix and allowed to air dry, then spotted 0.5 μL of sample, and quickly spotted another 0.5 μL of matrix on top.

6.2.4 Determine Gamma Phage Biomarkers

PEG concentrated and CsCl purified gamma phage suspensions in PBS and Milli-Q water were used to determine what protein peaks were the best biomarkers for gamma phage. Potential protein peaks were analyzed for their specificity to gamma phage and their MALDI signal characteristics.

6.2.5 Determine MALDI-TOF-MS Gamma Phage Detection Limit (DL)

Two independent PEG concentrated and CsCl gradient purified gamma phage stocks, 3.8×10^9 pfu/mL and 8.16×10^9 pfu/mL (determined by plaque assay described in Section 4.5.2), were ten-fold serially diluted using Milli-Q water to determine the MALDI-TOF-MS DL of gamma phage in Milli-Q water. Three independent gamma phage stocks of 3.8×10^9 pfu/mL, 2.6×10^9 pfu/mL, and 6.0×10^{10} pfu/mL (determined by plaque assay described in Section 4.5.2) were ten-fold serially diluted using PBS to

determine the MALDI-TOF-MS DL of gamma phage in PBS. A sandwich method, as described in Section 6.2.3, of sample application to the MALDI plate was used. MALDI-TOF-MS spectra were obtained on decreasing titers of gamma phage until the previously selected protein biomarker was no longer detected. The lowest detectable titers were then averaged to obtain the MALDI-TOF-MS DL for gamma phage.

6.2.6 Bacteriophage Amplification

Bacteriophage amplification experiments were conducted using two different methods. Method one kept MOIs constant while method two used different MOIs. In method one, a CryoBank™ glass bead of *B. anthracis*, from “master” stock in Section 3.4.2, was placed in a 15 mL culture tube containing 10 mL of BHI and incubated at 37 ± 2 °C. Two days later, nine mL of the *B. anthracis* culture was added to 36 mL of fresh BHI and incubated at 37 ± 2 °C for two hours. The OD of this culture at 625 nm was 0.30. Using the *B. anthracis* growth curve (equation 3.0 in Section 3.4.3), the expected *B. anthracis* titer was 8.4×10^6 cfu/mL. A bacterial titer was determined using the colony plate count procedures described in Section 3.5.2 since these growth procedures were slightly modified from the growth curve procedures. The *B. anthracis* titer was determined to be $5.62 \pm 3.35 \times 10^5$ cfu/mL and this value was used in all further calculations. A gamma phage titer was determined using the plaque assay method described in Section 4.5.2 and was $1.2 \pm .6 \times 10^8$ pfu/mL. Four different samples, shown in Table 6.0, were made containing *B. anthracis*, gamma phage, and BHI making up a total volume of 10 mL. A constant MOI of 0.21 was used for all four samples. These four samples were incubated at 37 ± 2 °C and 500 µL removed every two hours for a total of ten hours. Each 500 µL aliquot was filtered using an Acrodisc Syringe Filter 0.2 µm Supor® low protein binding membrane (PALL Gelman Laboratory, Ann Arbor, MI). Two hundred µL of this filtered aliquot was then dialyzed into Milli-Q water for two

hours using 20 μL to 250 μL sample size 8,000 MWCO Tube-O-Dialyzers (G-Biosciences, St. Louis, MO).

Table 6.0 Reaction components for gamma phage amplification (method one)

Sample	<i>B. anthracis</i> (μL)	Phage (μL)	BHI (μL)	[<i>B. anthracis</i>] in cfu/mL	[phage] in pfu/mL
1	9990	10	0	5.61×10^5	1.2×10^5
2	999	1	9000	5.61×10^4	1.2×10^4
3	99.9	0.1	9900	5.61×10^3	1.2×10^3
4	9.99	.01	9990	5.61×10^2	1.2×10^2

In method two, a CryoBank™ glass bead of *B. anthracis* was placed in a 15 mL culture tube containing 10 mL of BHI and incubated at 37 ± 2 °C. Three days later, 7 mL of the *B. anthracis* culture was added to 33 mL of fresh BHI and incubated at 37 ± 2 °C for two hours. The OD of this culture at 625 nm was 0.175. Using the *B. anthracis* growth curve (equation 3.0 in Section 3.4.3), the expected *B. anthracis* titer was 3.0×10^6 cfu/mL. A bacterial titer was determined using the colony plate count procedures described in Section 3.5.2 since these growth procedures were slightly modified from the growth curve procedures. The *B. anthracis* titer was determined to be $1.78 \pm .28 \times 10^6$ cfu/mL and this value was used in all further calculations. A gamma phage titer was determined using the plaque assay method described in Section 4.5.2 and was $1.2 \pm .6 \times 10^8$ pfu/mL. Four different samples, shown in Table 6.1, were made containing *B. anthracis*, gamma phage, and BHI making up a total volume of 10 mL. A different MOI was used for all four samples. These four samples were incubated at 37 ± 2 °C and 200 μL removed every two hours for a total of four hours. All samples from method one and two were refrigerated overnight and run on a Bruker Reflex 4 MALDI-TOF-MS (University of

Denver, CO) using the same instrument parameters outlined in Section 6.2.1 and the same matrix and sample application detailed in Section 6.2.3.

Table 6.1 Reaction components for gamma phage amplification (method two)

Sample	<i>B. anthracis</i> (μL)	Phage (μL)	MOI	[<i>B. anthracis</i>] in cfu/mL	[phage] in pfu/mL
1	9000	1000	7.5	1.60 x 10 ⁶	1.2 x 10 ⁷
2	9900	100	0.68	1.76 x 10 ⁶	1.2 x 10 ⁶
3	9990	10	0.07	1.78 x 10 ⁶	1.2 x 10 ⁵
4	9999	1	0.007	1.78 x 10 ⁶	1.2 x 10 ⁴

6.3 Results

6.3.1 Determine Gamma Phage Biomarkers

Three gamma phage protein MALDI peaks were identified at 11,075 Da, 22,779 Da, and 31,954 Da (see Figure 6.0). Two additional MALDI peaks appeared to be from doubly charged species of two of the gamma phage proteins identified above. The small peaks around 14,241 and 15,048 Da were attributed to proteins that were left over from the gamma phage propagation, concentration, and purification procedures. Since the most intense gamma phage peak was at 31,954 Da, this protein peak was selected as the MALDI biomarker for gamma phage. This peak was used to identify gamma phage in further studies to determine the gamma phage DL of MALDI and to conduct gamma phage amplification studies to indirectly detect *B. anthracis*.

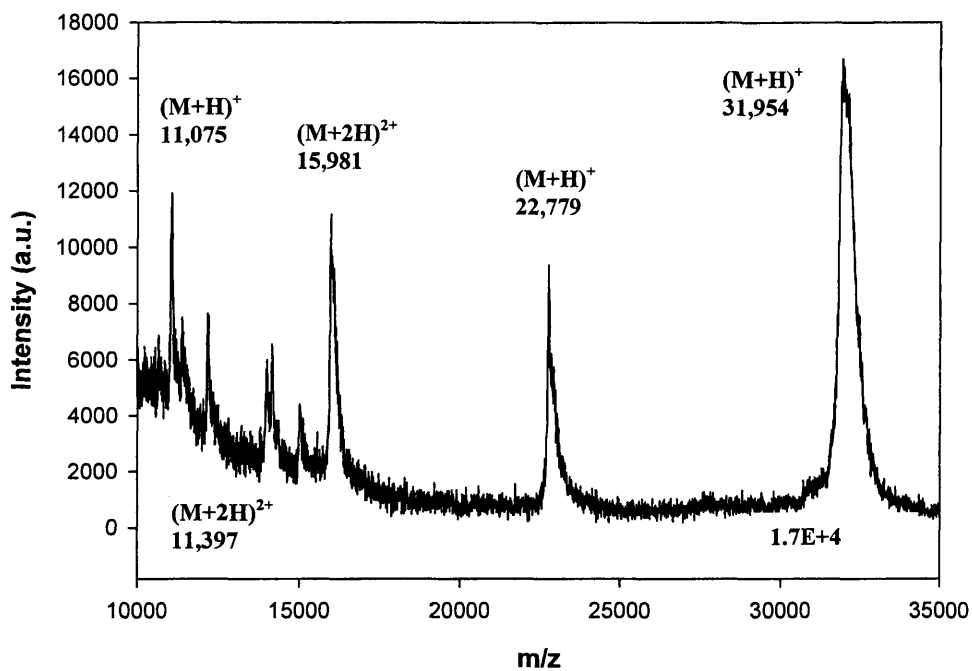


Figure 6.0 MALDI-MS spectrum of CsCl purified gamma phage in Milli-Q water

6.3.2 Determine MALDI-TOF-MS Gamma Phage Detection Limit (DL)

Figures 6.1 through 6.2 show the MALDI-MS spectra of a gamma phage 10-fold dilution series in Milli-Q water. The concentration of gamma phage in Figure 6.1 A. was 8.16×10^9 pfu/ml and Figure 6.1 B. was 8.16×10^8 pfu/ml. The concentration of gamma phage in Figure 6.2 A. was 8.16×10^7 pfu/ml and Figure 6.2 B. was 8.16×10^6 pfu/mL. The MALDI-TOF-MS DL when gamma phage was diluted in PBS was 1.55×10^8 pfu/mL. The MALDI-TOF-MS DL when gamma phage was diluted in Milli-Q water was 6.0×10^7 pfu/mL. The difference in DL was attributed to the salts present in PBS that can negatively affect ionization of the sample.

6.3.3 Bacteriophage Amplification

No MALDI gamma phage peak at 31,954 Da was detected using either method one or method two (see methods in Section 6.2.6). This would indicate that the gamma phage concentration from the bacteriophage amplification never went above either 1.55×10^8 pfu/mL or 6.0×10^7 pfu/mL, which are the DLs of gamma phage in PBS and Milli-Q water respectively. This result was not totally unexpected given that previous propagation of gamma phage in liquid growth media never produced a gamma phage concentration above 10^7 pfu/mL as outlined in Section 4.3.4.

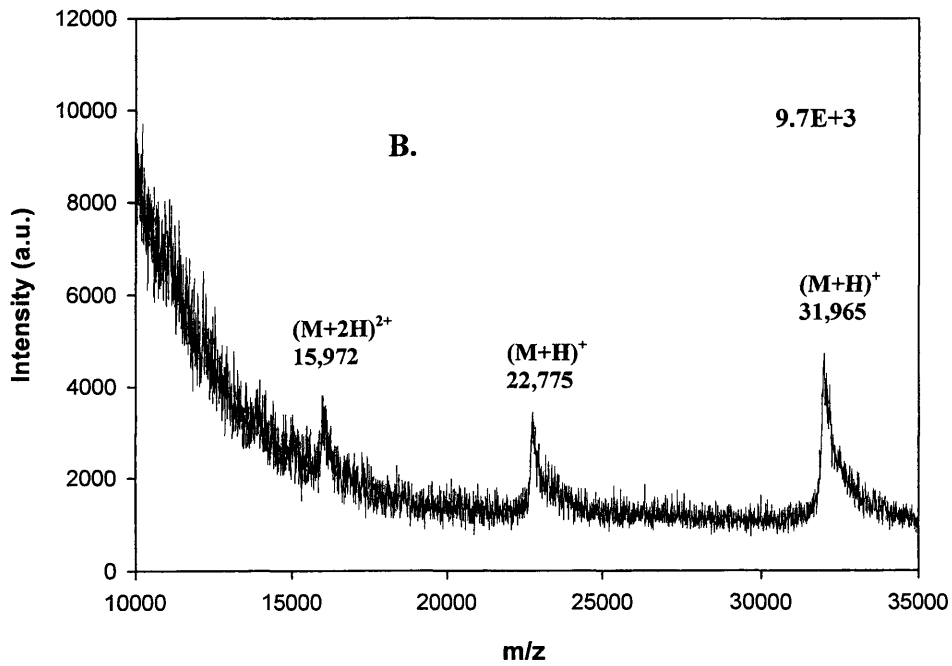
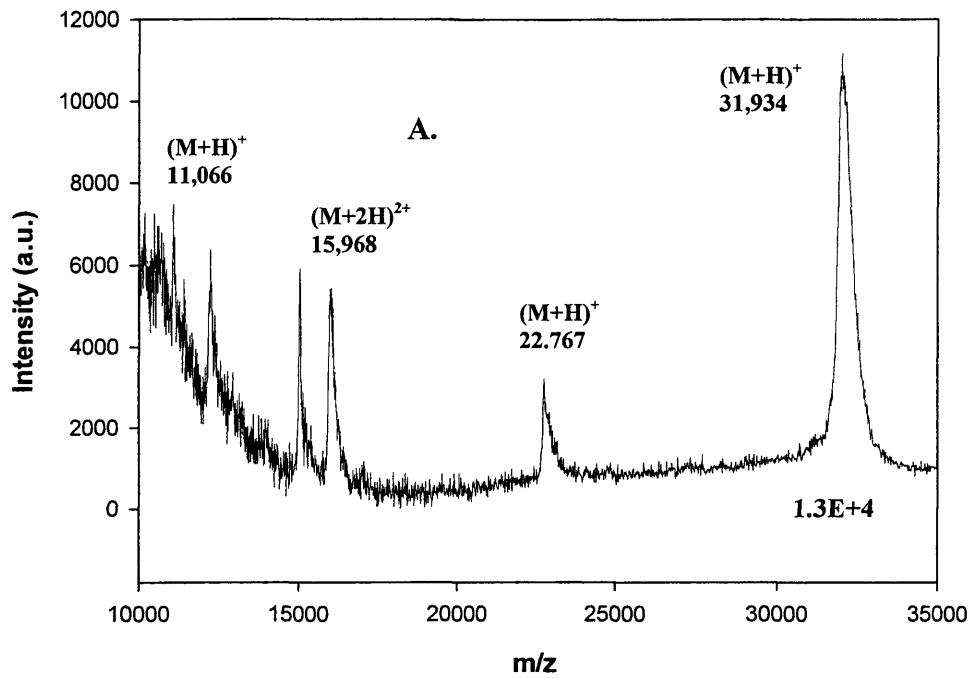


**Figure 6.1 MALDI-MS spectra of gamma phage dilution series for detection
 A. 8.16×10^9 pfu/mL and B. 8.16×10^8 pfu/mL**

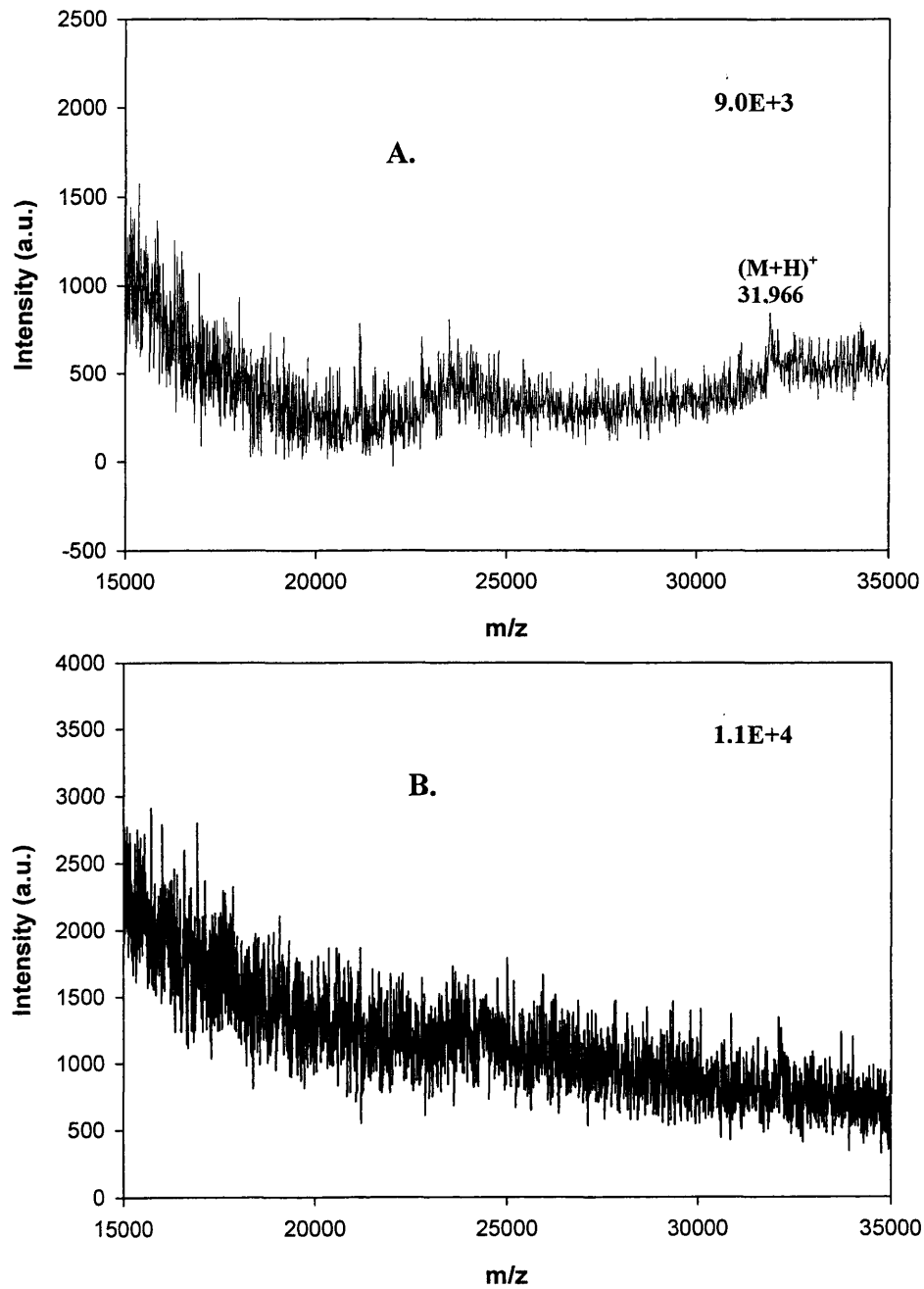


**Figure 6.2 MALDI-MS spectra of gamma phage dilution series for detection limit
A. 8.16×10^7 pfu/mL and B. 8.16×10^6 pfu/mL**

6.4 Discussion and Conclusions

MALDI-TOF-MS did not detect the amplified gamma phage proteins after gamma phage amplification in *B. anthracis*. The higher DL of the MALDI prevented detection of the gamma phage amplification event since the gamma phage propagation in liquid media was limited to titers no higher than 10^7 pfu/mL. This concentration is just at or below the determined DL of MALDI (1.55×10^8 pfu/mL in PBS or 6.0×10^7 pfu/mL in Milli-Q water). Another growth media, or the addition of other chemicals, could potentially support gamma phage amplification above 10^7 pfu/mL, but only if this titer limitation was not caused by an inherent property of *B. anthracis* like endospore formation.

Even though the MALDI DL was too high to detect the gamma phage amplification event, it could be an effective detection platform for any bacteriophage that will grow in its host in liquid growth media to concentrations above 10^8 pfu/mL. The strength of MALDI lies in being able to analyze high MW biomolecules without much sample preparation. In addition, MALDI typically produces singly charged species which greatly simplifies the analysis and makes MW determination and therefore molecular identification easier. The sample preparation and analysis steps using MALDI were straightforward and took approximately 15 to 20 minutes to complete. With an additional four hours dedicated the bacteriophage amplification event, the analysis and results could be available in less than five hours. The ability to spike unknown samples with a bacteriophage just below the DL, potentially makes the required amplification time much shorter. These advantages of MALDI detection make the search for another phage/host system that would be more amenable to MALDI detection worthwhile.

The choice of sample solvent did prove problematic for MALDI analyses. Most growth media and buffer solutions have high salts concentrations; these salts, especially magnesium was shown to suppress the MALDI ionization signal. The MALDI ionization signal was shown to be totally suppressed when SM (tris-HCl, MgSO₄, NaCl, and 2%

glycerin solution) was used as the solvent to store gamma phage. The DL of gamma phage was improved 2.6-fold by running the dilution series in Milli-Q water (6.0×10^7 pfu/mL or 3.0×10^4 particles) as compared with PBS (1.55×10^8 pfu/mL or 7.8×10^4 particles). These virus detection limits are comparable to those reported using whole bacterial cells (10^7 cfu/mL [58]), so it appears that the additional proteins in the gamma phage capsid did not provide the expected amplified MALDI signal.

CHAPTER 7

INDIRECT DETECTION OF *BACILLUS ANTHRACIS* USING HAND-HELD IMMUNOASSAYS TO DETECT GAMMA PHAGE

7.1 Introduction

The designs of hand-held immunoassays (HHAs), also referred to as lateral flow immunochromatography (LFI) strips, are based on the extreme molecular specificity that antibodies have for a specific antigen in potentially complex matrices. The mammal adaptive immune response starts when an infection produces enough antigens that the body starts producing specific white blood cells, B and T lymphocytes and macrophages, in the lymph system that recognize and destroy these foreign substances. Antigens are usually proteins or polysaccharides with molecular weights of at least 8,000 to 10,000 Daltons [65]. In the humoral immune response to antigens, signals provided by helper T-cells cause B-cells to produce soluble antigen-binding proteins called antibodies as early as 7 to 10 days after infection. The set of antibodies produced are collectively called immunoglobulins (Igs) and are present in blood serum, lymph fluid, gastric secretions, milk, and saliva.

Serum antibody concentrations are commonly determined using the “indirect” enzyme-linked immunosorbent assay (ELISA) [1]. “Indirect” ELISAs utilize two antibodies; one specific to the antigen and the second antibody specific to the first antibody. The second antibody is conjugated to an enzyme that fluoresces when a substrate is added. The amount of fluorescence is proportional to the amount of antibody specific to the antigen present (see Section 7.2.1.2 for the method used).

IgG antibody monomers (150 kDa) comprise approximately 80% of serum Ig and consists of four polypeptide chains, two identical light chains (25 kDa each) and two identical heavy chains (50 kDa each), formed into a Y-shape covalently bonded via interchain and intrachain disulfide (S-S) linkages between cysteine residues [1]. The Y-shaped IgG antibodies have two variable amino acid arms, made up of both heavy and light chains, that non-covalently (hydrogen bonds, ionic bonds, hydrophobic interactions and van der Waals forces) binds up to two antigens (determined by steric hindrances) at the two identical antigen-binding sites as shown in Figure 7.0 [65] below.

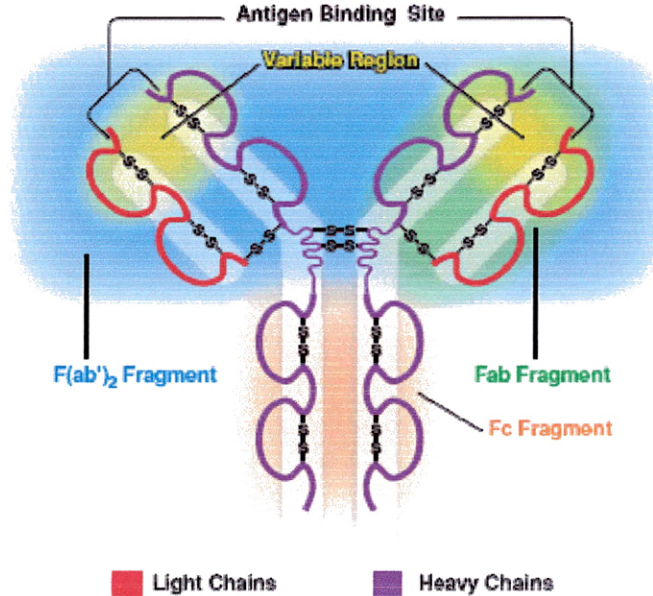


Figure 7.0 Characteristic Y-shape of IgG antibody

The Fc (Fragment, crystalizable) region is derived from the stem of the “Y” and is composed of two heavy chains made up of two constant domains each. Each domain is approximately 110 amino acids long. The Fab (Fragment, antigen binding) region is

composed of one constant and one variable domain of each the heavy and the light chains. The $F(ab')_2$ fragment would contain both Fab fragments along with the hinge region. The specific site on the antigen surface where the complementary antibody binds is called an epitope and is typically one to six monosaccharide or five to eight amino acid residues long [65]. The binding affinity of an antibody for an antigen is the strength of the non-covalent interaction between a single antigen-binding site on the antibody and its specific antigen epitope. Antibodies are very specific to each antigen, so their interaction in forming an antibody-antigen complex with one another has been described as a lock (antigen) and key (antibody).

In the humoral immune response, these antibodies attach to specific antigens and inactivate them while T-cells or macrophages move in to destroy the foreign invaders. Two types of antibodies can be produced by immunization of a suitable animal and are referred to as polyclonal antibodies (PABs) and monoclonal antibodies (MAbs). PABs are produced from many B-cell clones that recognize a variety of epitopes while MAbs are produced from a single B-cell clone that produces a homogeneous population of antibodies that recognize just one epitope. The antibodies are the single most important part of immunoassay detectors, so the type and quality of antibodies utilized directly affects the detection capabilities. Detector requirements such as specificity, sensitivity, time, and cost all need to be considered when deciding between PABs and MAbs.

Antigen affinity chromatography followed by Protein G chromatography can be performed on the serum (blood with clotting proteins and red blood cells removed) to enrich the target Ig and remove other background serum proteins present. The antigen affinity chromatography removes the bulk of non-specific Ig while enriching the specific Ig, but leaves many other serum proteins. These serum proteins could then be removed by Protein G purification that utilizes *Streptococcus aureus* Protein G's high affinity for the Ig Fc domain to remove serum proteins.

As described in Section 2.6, HHAs typically employ colloidal gold-conjugated MAbs stripped on the detector line to maximize specificity and PABs stripped on the

capture (or test) line to obtain high sensitivity. For signal amplification and detection purposes, the purified MAbs are typically conjugated to latex beads, radiolabels, enzymes, biotin, fluorophores, chemiluminescent substrates, or colloidal gold particles [65]. In this dissertation, PABs were used in the three HHAs studied mainly due to cost and time constraints, but also to test the feasibility of using the same antibodies on both the detector and capture (or test) lines. In addition, the three HHAs used colloidal gold-conjugated either to gamma phage or to rabbit anti-gamma phage PABs as the visual detection system. When concentrated along the capture or control lines, the 35 nm-sized colloidal gold particles form a red line that is visible with the naked eye.

7.2 Hand-Held Immunoassay 1 (HHA 1: Versions 1 and 2)

The adsorption of phage on a bacterial surface has been described as reversible binding to a recognition molecule followed by an irreversible step involving adsorption or DNA ejection [66]. Two versions of HHA 1 were designed, built, and tested based on a potentially quick and specific adsorption of gamma phage to the *B. anthracis* cell wall. When gamma phage are added to vegetative *B. anthracis*, they attach to peptidoglycan-anchored proteins (specific receptors referred to as GamR) on the cell wall then inject their DNA [51]. Figure 7.1 shows an electron microscopy (EM) binding picture of gamma phage particles adsorbed to the surface of *B. anthracis* Sterne [51]. The black lines are the bacterial cell wall and the hexagonal shapes are the capsids of the adsorbed gamma phage particles. Notice that many gamma phage appear to adsorb to the surface of *B. anthracis*. The potential signal amplification, in both versions of HHA 1, results from multiple gamma phage attaching to the bacterial cell wall during the adsorption phase of the replication cycle. Previous studies have shown a single bacterium can hold a large amount of phage particles on its surface [67, 68]. Although bacteriophage active

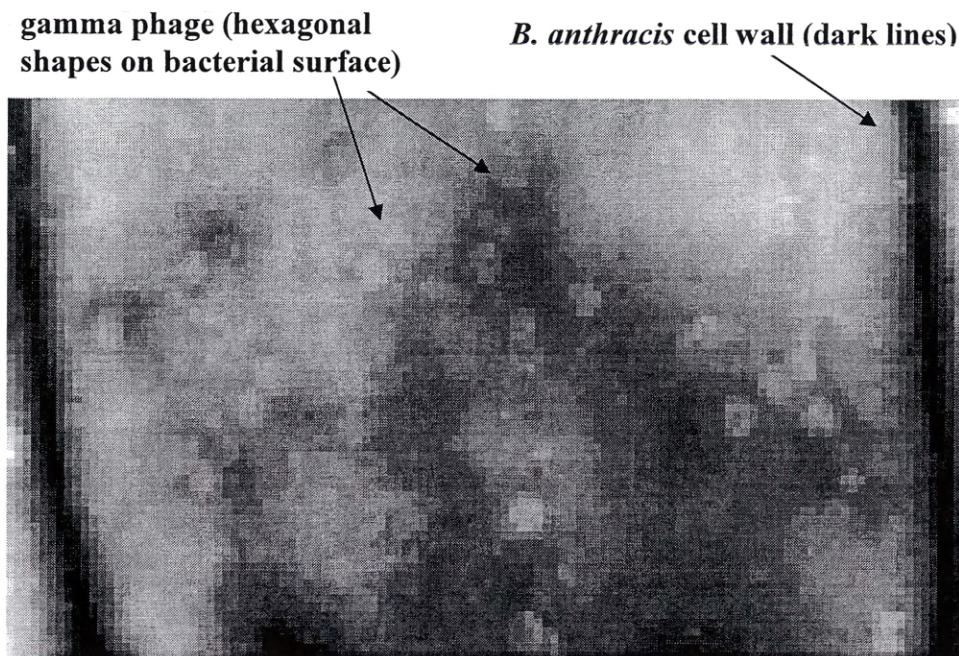


Figure 7.1 EM of gamma phage particles on *B. anthracis* Sterne surface

against *Escherichia coli* have shown 70 percent attachment in three minutes and 98 percent attachment in 10 minutes [50], the time required for gamma phage adsorption on *B. anthracis* has not been reported. Two different HHA 1 versions were conceived to account for this unknown adsorption time.

As shown in Figures 7.2 and 7.3, colloidal gold was conjugated (attached) directly to the phage by Millenia Diagnostics Inc. (San Diego, CA) to serve as the visual detection method. HHA 1 version 1 stripped the liquid conjugate onto the conjugate pad at the detector position while version 2 kept the liquid conjugate separate to mix with vegetative bacteria prior to application. Both HHA 1 versions were designed to capture

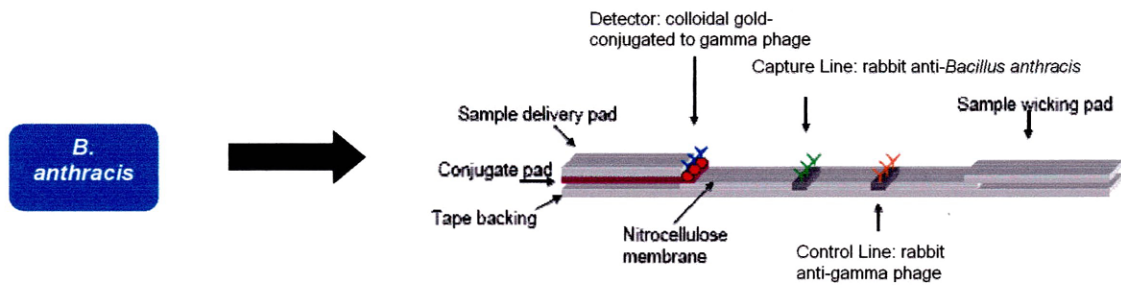


Figure 7.2 HHA 1 version 1

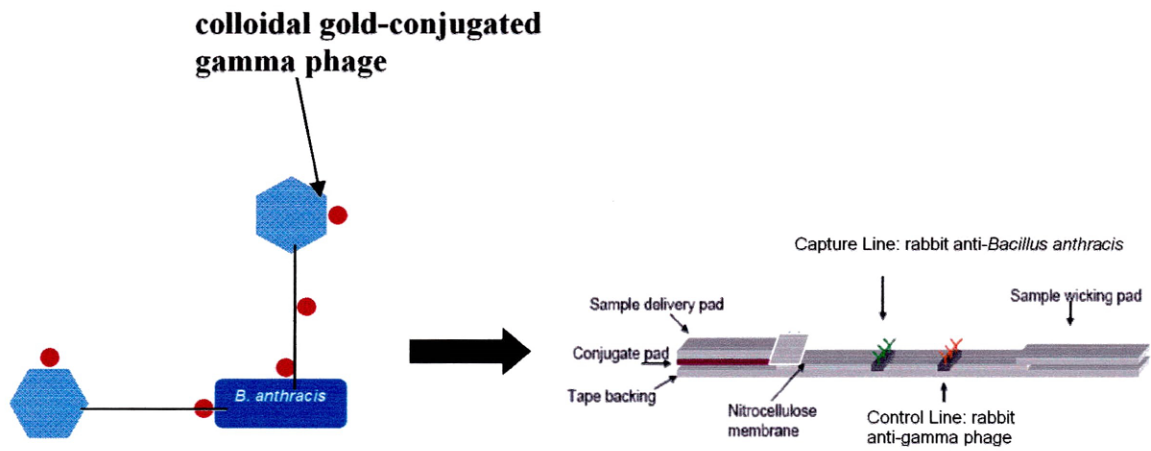


Figure 7.3 HHA 1 version 2

B. anthracis with gold-conjugated gamma phage attached; however, version 1 would require an immediate gamma phage adsorption while version 2 has a premixing step to allow for longer adsorption times. The capture line was stripped with rabbit anti-*B. anthracis* antibodies raised against a preparation of spores and vegetative antigen (1.6 mg from Tetracore Inc., Rockville, MD).

Preliminary studies along with the two versions of HHA 1 were used to answer the following questions: 1) Where does colloidal gold attach to gamma phage? 2) Does the colloidal gold conjugation affect gamma phage adsorption? 3) Is the colloidal gold gamma phage conjugate stable? 4) Is gamma phage adsorption fast? 5) Will the assays detect *B. anthracis*?

7.2.1 Materials and Methods

Methods outlined in Sections 7.2.1.1 through 7.2.1.6 were conducted by Harlan Bioproducts for Science, Inc. (Indianapolis, IN).

7.2.1.1 Production of Rabbit Anti-Gamma Phage Antibodies

The rabbit anti-gamma phage PABs used for all three HHAs were produced by using four immunizations of purified gamma phage (see Section 4.4.2 for purification procedures) in three different rabbits (R7214, R7215, and R7216) using Freund's adjuvant. Rabbit immunizations using the schedule in Table 7.0 were conducted using one mL inoculations for each rabbit using purified gamma phage titers between 1.50 and 2.35×10^{10} pfu/mL in SM.

Table 7.0 Polyclonal antibody production schedule

Day	Date	Procedure
0	02/24/06	Primary
21	03/17/06	1 st Boost
31	03/27/06	Test Bleed w/ELISA
42	04/07/06	2 nd Boost
52	04/17/06	Production Bleed
59	04/24/06	Production Bleed
63	04/28/06	3 rd Boost
73	05/08/06	Final Bleed w/ELISA

7.2.1.2 ELISAs on Rabbit Anti-Gamma Phage Antibodies

ELISAs were performed on the test bleed serum after 30 days (10 days after the second immunization) and on the final bleed serum after the 73-day schedule was complete to approximate the specific IgG concentrations.

Purified gamma phage was diluted in coating buffer at a concentration of 1 to 10 µg/ml. A multichannel micro-pipette was used to add 50 µL to each well of the 96-well Immulon-II, flat bottom ELISA plate(s). The plate(s) were sealed with plate sealers and incubated overnight at 4°C (plates were used within 24 hours of coating).

The excess antigen was removed from the wells by shaking the plate into a waste container followed by blotting the surface of the plate against several layers of absorbent wipes. A multichannel micro-pipette was used to add 100 µL of BSA₁₀ blocking solution

to each well. The plates were covered with an acetate plate sealer and incubated at room temperature for about 60 minutes.

The excess blocking solution was removed from the wells by shaking the plate into a waste container followed by blotting the surface of the plate against several layers of absorbent wipes. The plate(s) were washed three times with PBS-T washing solution using the 12-channel plate washer. The wash solution was removed from the plates by shaking and blotting as described above.

Fifty μL of test serum was added to each well. Two wells were set aside for a reagent blank well and a positive control well for each plate. The reagent blank well was 50 μL of PBS-T washing solution, and the positive control was 50 μL of a dilution of a positive serum. The plates were covered as above and incubated at room temperature for one hour.

The test material (gamma phage), reagent blank, and positive control serum were removed from the wells by shaking into a waste container. The plate(s) were washed three times with PBS-T as described above. Horseradish peroxidase (HRP)-goat anti-rabbit conjugate was diluted in BSA₅T at the manufacturer's recommended dilution. A multichannel micro-pipette was used to add 50 μL of diluted conjugate to each well. The plates were covered as above and incubated at room temperature for one hour.

Excess conjugate was removed from wells. The plate(s) were washed three times with PBS-T as described above. The enzyme substrate, 2,2'-azino-bis(3-ethyl-benzthiazoline-6-sulfonic acid) (ABTS), was a premixed stabilized solution. A multichannel micro-pipette was used to add 100 μL of fresh substrate to each well. The plates were covered and incubated at 37 °C for an hour and protected from direct light.

The plate(s) were read at 405 nm using an ELISA plate reader. The plate reader was programmed to subtract the reading of the reagent blank wells. The positive control wells on all plates gave a similar signal.

7.2.1.3 Antigen Affinity Column Preparation and Antigen Purification

Serums from two of the three rabbits (R7215 and R7216) were combined based on their higher Ig concentrations.

Gamma phage was dialyzed in coupling buffer (0.1 M MES, 0.9% NaCl, pH 4.7) to remove Tris which would interfere with the coupling reaction. The gamma phage (four mL at 1.9 mg/mL) was coupled to four ml of CarboxyLink Coupling Gel (Pierce) equilibrated with coupling buffer using 50 mg of 1-ethyl-3-(3-dimethylaminopropyl)-carbodiimide hydrochloride (EDC), at room temperature for about two hours. Unreacted sites were blocked with 0.1 M sodium acetate, pH 4.2, and the gel was washed with 1 M NaCl. Coupling efficiency was >96%.

Rabbit polyclonal serum was diluted 1:3 with antigen affinity binding buffer (50 mM sodium phosphate, 20 mM NaCl, pH 7.3), titrated to pH 7.3, filtered to 0.2 μ m, and loaded onto a 1 cm x 11 cm (8.64 mL) gamma phage antigen affinity column at 4 mL/min. The column was washed with 10 column volumes of binding buffer, and eluted with five column volumes of antigen affinity elution buffer (0.1 M glycine, 0.15 M NaCl, pH 2.5). The eluent was neutralized to approximately pH 7.3 with 2 M Tris, pH 9.0, dialyzed in 25 mM sodium phosphate, pH 7.2, and filtered to 0.2 μ m.

7.2.1.4 SDS-PAGE Purity Determination

An Invitrogen Novex 10% Tris-glycine gel 1.5 mm x 10 well (Cat.# EC6078BOX), 10x Tris-glycine SDS running buffer (Cat.# LC2675), 2x Tris-glycine SDS sample buffer (Cat.# LC2676) and 2% reducer (2-mercaptoethanol, Fisher Cat.# BP176-100) was used. Invitrogen Benchmark Protein Ladder (Cat.# 10747-012) was used to determine protein molecular weights.

The buffers were diluted to 1x prior to use (2x sample buffers were diluted with an equal volume of sample). SDS gel samples were heated at about 90 °C for about two

minutes and allowed to cool, loaded 40 μ L per well and ran at 125 V for 150 volt-hours (approximately 90 minutes).

7.2.1.5 Protein G Purification

The rabbit anti-gamma phage antibody was further purified by diluting 1:3 with PBS, pH 7.2, and loading onto a 1 cm x 9 cm (seven mL) Protein G column at 2 ml/min. The column was washed with two column volumes of PBS, and eluted with five column volumes of Protein G elution buffer (0.1 M glycine, pH 2.7). The eluent containing the antibodies was neutralized to pH 7.3 with 2 M Tris, pH 9.0, dialyzed in 25 mM sodium phosphate, pH 7.2, and filtered to 0.2 μ m.

7.2.1.6 Determine Rabbit Anti-Gamma Phage Isoelectric Point

A pH 3-7 isoelectric focusing (IEF) Invitrogen Novex gel 1.0 mm x 10 well (Cat.# EC6655B), 10x cathode buffer (Cat.# LC5370), 50x anode buffer (Cat.# LC5300), and 2x sample buffer (Cat.# LC5371) were used in determining the PAbs isoelectric point (pI). IEF samples were loaded 40 μ l per well, and ran at 125 V for 150 volt-hours (approximately 90 minutes).

7.2.1.7 Colloidal Gold Conjugation to Gamma Phage

Colloidal gold conjugation was done by Millenia Diagnostics with purified gamma phage (see Section 4.4.2 for purification procedures) and purified antibodies (provided by Harlan Bioproducts for Science, Inc.: nine mL of 2.45 mg/mL were dissolved in 25mM sodium phosphate, pH 7.2, filtered to 0.2 μ m and frozen).

Colloidal gold particles (reported to be 40 nm) in a suspension were adjusted to pH 9.0. Gamma phage was dialyzed in 10 mM borate buffer at pH 9.0 prior to

conjugation. Gamma phage was conjugated to the colloidal gold particles at pH 9.0 and blocked with 1% PEG. The conjugate was purified and concentrated by centrifugation at 7000 x g for 45 minutes at 4° C. The supernatant was removed and the conjugate pellet was then re-suspended in MDx conjugate stabilizer to OD₅₂₀=10. Further details were not released for proprietary reasons, but other sources detail the preparation of different size gold colloids and their attachment to proteins [69].

7.2.1.8 HHA 1 (Versions 1 and 2) Production (See Figures 7.2 and 7.3)

Prototype HHAs were constructed by Millenia Diagnostics using the following conditions: nitrocellulose membrane from Millipore catalog (HHA 1 version 1:HF 120, HHA 1 version 2:HF 090) was used as the solid phase for the assay. Test (or capture) line reagent was prepared and stripped with rabbit anti-*B. anthracis* (Lot: T090204-01) Tetracore, Inc. antibodies diluted in 25 mM potassium phosphate at pH 7.4 at a concentration of 0.5 mg/mL and stripped at 1.0 µL/cm. Control line reagent was prepared with rabbit anti-gamma phage (Lot: 56061608) antibodies diluted in 25 mM potassium phosphate at a concentration of 0.5 mg/mL and stripped at 1.0 µL/cm.

7.2.1.8.1 HHA 1 Version 1 (See Figure 7.2)

The colloidal gold-conjugated gamma phage was stripped at 4.0 µL/cm on blocked glass fiber and dried at 37 °C for 45 minutes. All stripping was done using a Kinematic Automation Reagent Dispensing Module model Matrix 1600. Stripped membranes were blocked using MDx lateral flow blocking solution and dried prior to assembling into the test cards. Membranes were prepared, as noted above, and stripped conjugate pads were assembled into test cards using sample pad Ahlstrom cytosep 1662 2.0 cm and absorbent pad Ahlstrom 222. The membranes were then cut into 4.5 mm

strips, using Kinematic Automation Programmable Shear model Matrix 2360, then assembled into cassettes, and pouched with desiccant.

7.2.1.8.2 HHA 1 Version 2 (See Figure 7.3)

Liquid colloidal gold-conjugated gamma phage (from method in Section 7.2.1.7) were stored at 2-8 °C prior to use. Typically 2-4 µL of conjugate is required for each test device. Membranes, prepared as noted above, were assembled into test cards using sample pad: Ahlstrom 8964 glass fiber treated with MDx blocking buffer, 2.2 cm and absorbent pad: Ahlstrom 222 1.7 cm. The membranes were then cut into 4.5 mm strips, using Kinematic Automation Programmable Shear model Matrix 2360, then assembled into cassettes, and pouched with desiccant.

7.2.1.9 HHA 1 Version 1 Testing

The test scale used for all HHA testing was: 0 = no test line, 1+ = very faint test line, 2+ = test line less intense than control line, 3+ = test line as intense as control line, and 4+ = test line more intense than control line.

B. anthracis cultures in BHI were grown as outlined in Section 3.4.2 except that the second day liquid culture was used for these tests. This liquid culture was incubated at 37 °C on a shaker until OD readings at 625 nm were 0.225, 0.45, and 0.825. Using equation 3.0 in Section 3.4.3, these OD values equate to *B. anthracis* titers of 4.51×10^6 cfu/mL, 2.94×10^7 cfu/mL, and 6.71×10^8 cfu/mL respectively. To test the device, 75 µl of sample at each OD was added to the sample pad, allowed to wick down the nitrocellulose membrane, and the results were read at 15 minutes.

7.2.1.10 HHA 1 Version 2 Testing

The *B. anthracis* cultures grown in BHI from Section 7.2.1.9 at OD readings of 0.225 and 0.45 were also used to test HHA 1 version 2. Using equation 3.0 in Section 3.4.3, these OD values equate to *B. anthracis* titers of 4.51×10^6 cfu/mL and 2.94×10^7 cfu/mL respectively. Seventy-five μ L of the liquid conjugate (colloidal gold-conjugated gamma phage suspension) was added to 150 μ L of the *B. anthracis* culture at each OD value into a 1.8 mL microcentrifuge tube. The tube was incubated at 37 °C on a shaker and samples were withdrawn at both 15 and 30 minutes after inoculation with the liquid conjugate. To test the device, 75 μ L of each sample at 15 and 30 minutes were added to the sample pad, allowed to wick down the nitrocellulose membrane, and the results were read at 15 minutes.

Further testing, allowing for longer adsorption time, was conducted after getting negative test results at both OD values. Fresh *B. anthracis* cultures were grown in BHI using the same method described in Section 7.2.1.9, but 400 μ L of *B. anthracis* at OD = 0.42 (2.30×10^7 cfu/mL) was added to 100 μ L of fresh BHI, 10 μ L of the liquid conjugate, and incubated at 37 °C on a shaker. Samples were withdrawn at 30, 60, and 90 minutes later and tested.

After determining negative test results at all three adsorption times, these three test strips along with several others were sent to Huffman Laboratories Inc. (Golden, CO) for further testing using inductively coupled plasma mass spectrometry (ICP-MS). The objective of this testing was to determine whether or not the gamma phage adsorption and HHA strips were working as planned. The detection scheme and strips could be functioning properly, but the amount of colloidal gold-conjugated gamma phage adsorbed to *B. anthracis* being captured might be insufficient for visual detection. The following procedures were conducted by Huffman Laboratories, Inc. The HHA nitrocellulose strips were removed from each plastic cassette and cut into three 0.2 inch pieces. Each piece either incorporated the control line, the test line, or an area of no

stripped antibodies between the test line and the sample application pad. All 0.2 inch nitrocellulose samples were transferred into Pyrex glass culture tubes and digested with a mixture of nitric and perchloric acids to fully oxidize the HHA strip material and other organics present on the strip. After refluxing with boiling perchloric acid, samples were cooled then reheated with 50% aqua regia in water to ensure complete dissolution of gold. Cooled samples were diluted to 20.0 mL total volume and analyzed for total gold by ICP-MS, monitoring Au¹⁹⁷ at mass 196.97 Da, using a Perkin-Elmer 6100-DRC Plus instrument.

7.2.2 Results

7.2.2.1 ELISAs on Rabbit Anti-Gamma Phage Antibodies

All three rabbits (R7214, R7215, and R7216) had good immunogenic responses to the gamma phage antigen as shown in Tables 7.1 and 7.2 ELISA results. Increasing emission numbers in arbitrary units (a.u.) at a particular dilution from the pre-bleed to the 1st test bleed show that the rabbits are producing antibodies. Any ELISA emission number above 1.000 is considered an excellent amount (or titer) of antibodies. Table 7.1 shows the pre-bleed and test bleed ELISAs done on the rabbit anti-gamma phage polyclonal antibodies produced by Harlan Bioproducts for Science. Very low numbers for the pre-bleeds indicate that the rabbits had not been previously exposed to gamma phage. All three rabbits produced an excellent concentration of antibodies towards gamma phage at an antibody dilution of 1: 62,500. At the first test bleed, rabbits R7215 and R7216 seem to be producing more antibodies than R7214. By the final bleed, rabbits R7215 and R7216 have produced an excellent concentration of antibodies towards gamma phage at an antibody dilution of 1: 312,500. Rabbit R7214 was slightly behind the others. Based on this ELISA data, rabbit final bleed serum from R7215 and R7216 were combined and used for further purification.

Table 7.1 ELISA results on rabbit anti-gamma phage antibodies (pre and 1st bleeds)

Type of Collection	Pre-Bleed	1st Test Bleed	Pre-Bleed	1st Test Bleed	Pre-Bleed	1st Test Bleed
Date of Collection	2/20/06	3/27/06	2/20/06	3/27/06	2/20/06	3/27/06
Rabbit Number	R7214	R7214	R7215	R7215	R7216	R7216
Serum Dilution						
1:100	0.251	1.843	1.695	2.065	0.970	1.863
1:500	0.120	1.847	0.897	1.773	0.319	1.719
1:2,500	0.071	1.732	0.321	1.654	0.145	1.627
1:12,500	0.068	1.626	0.114	1.559	0.068	1.550
1:62,500	0.059	1.272	0.070	1.403	0.062	1.371
1:312,500	0.090	0.630	0.067	0.876	0.069	0.667
1:1,562,500	0.064	0.214	0.061	0.356	0.071	0.221
1:7,812,500	0.090	0.085	0.057	0.123	0.057	0.086

**Table 7.2 ELISA results on rabbit anti-gamma phage antibodies
(final bleeds)**

Type of Collection	Final Bleed	Final Bleed	Final Bleed
Date of Collection	05/08/06	05/08/06	05/08/06
Rabbit Number	R7214	R7515	R7216
Serum Dilution			
1:100	1.866	1.868	1.989
1:500	1.916	1.885	1.950
1:2,500	1.878	1.903	2.001
1:12,500	1.778	1.798	1.798
1:62,500	1.515	1.606	1.561
1:312,500	0.899	1.083	0.982
1:1,562,500	0.304	0.448	0.356
1:7,812,500	0.099	0.133	0.111

7.2.2.2 Antigen Affinity Purification

Rabbit anti-gamma phage antibodies (72 x 1 mL at 3.07 mg/mL) were recovered from approximately 150 mL of serum from rabbits R7515 and R7216. Purity was >31% determined by reduced SDS-PAGE. This is about 221 mg of protein at 31% purity, which results in 69 mg of antibody directed against the gamma phage. Isoelectric point was not determined by IEF gel due to the lack of purity. The pre-bleed material, production bleeds, and one final bleed (R7214) were not included in this purification.

7.2.2.3 SDS-PAGE Purity Determination

Lane 1 in Figure 7.4 shows the amount of antibodies and other proteins that were present before the antigen affinity purification column was run. By comparing Lane 1 with Lanes 3 through 8, it is apparent that many non-specific proteins were removed from the serum. Lane 2 shows the proteins that were subsequently removed by the antigen affinity column. The protein ladder in Figure 7.5 provides some additional information about the molecular weights of the proteins removed and those still present. The reported purity of >31% after the affinity purification column signified that there were many other proteins, other than the gamma phage antibodies of interest, still present. Further purification would be required, so a Protein G purification step was added.

7.2.2.4 Protein G Purification

After the Protein G purification, the final protein titer was 2.45 mg/mL determined by light absorbance at 280 nm using a one cm light path and extinction

HARLAN BIOPRODUCTS FOR SCIENCE

SDS-PAGE Gel

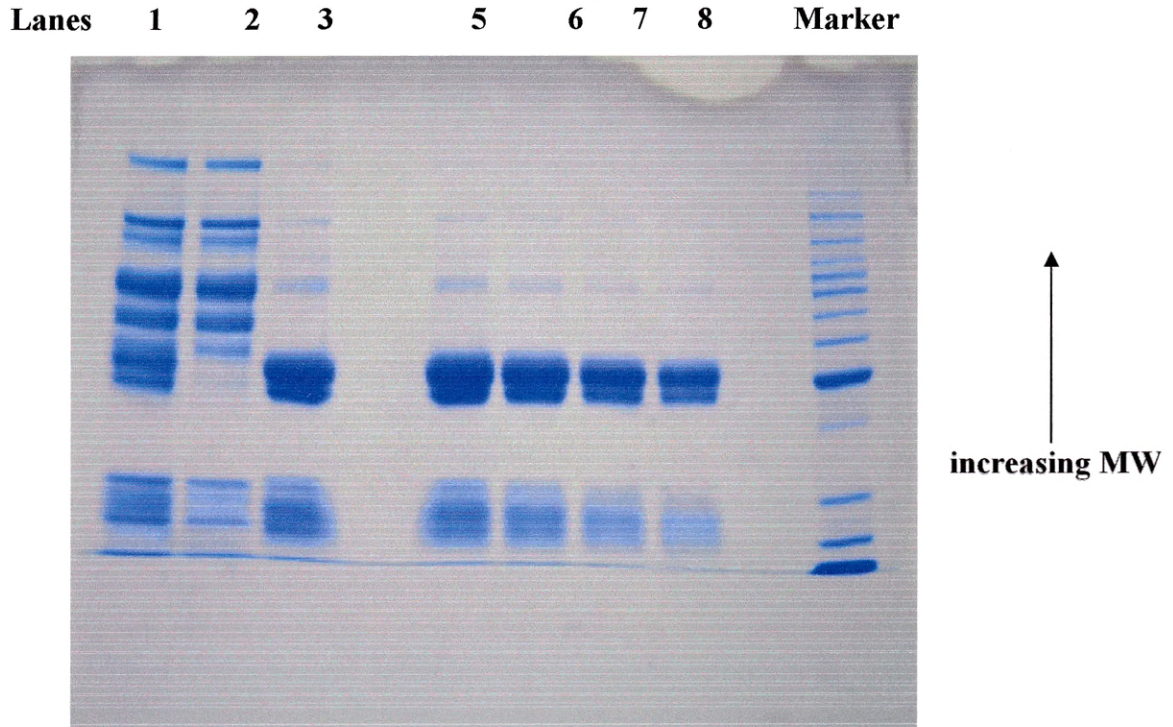


Figure 7.4 SDS-PAGE on rabbit-anti gamma phage antibodies

Legend:

Lane 1: Gamma Phage, Lot # S6061608 (S6071623 Pre-Column)

Lane 2: Gamma Phage, Lot # S6071623, Void & Wash

Lane 3: Gamma Phage, Lot # S6071623, Eluent

Lane 5: Gamma Phage, Lot # S6071623, Final Product diluted 2x

Lane 6: Gamma Phage, Lot # S6071623, Final Product diluted 3x

Lane 7: Gamma Phage, Lot # S6071623, Final Product diluted 4x

Lane 8: Gamma Phage, Lot # S6071623, Final Product diluted 6x

Marker: Protein ladder MWM, Invitrogen, Lot #1317882



Figure 7.5 Protein ladder (standards) used in SDS-PAGE

coefficient of 1.0. Protein G purification resulted in about 25 mg of total protein in about 10 mL. Purity was > 98% by PAGE. The Protein G purification was very effective at removing additional proteins that could have potentially interfered with the colloidal gold conjugation to the antibodies.

7.2.2.5 Determine Rabbit Anti-Gamma Phage Isoelectric Point

The pI of the purified antibodies provided the approximate pH at which Millenia Diagnostics Inc. should conjugate them to colloidal gold. Since the antibodies were polyclonal, the pI would actually be determined as a range since the PABs are made up of different antibodies to different epitopes. The range provided was between 8.0 and 8.5 as shown in Figure 7.6.

HARLAN BIOPRODUCTS FOR SCIENCE

IEF Gel

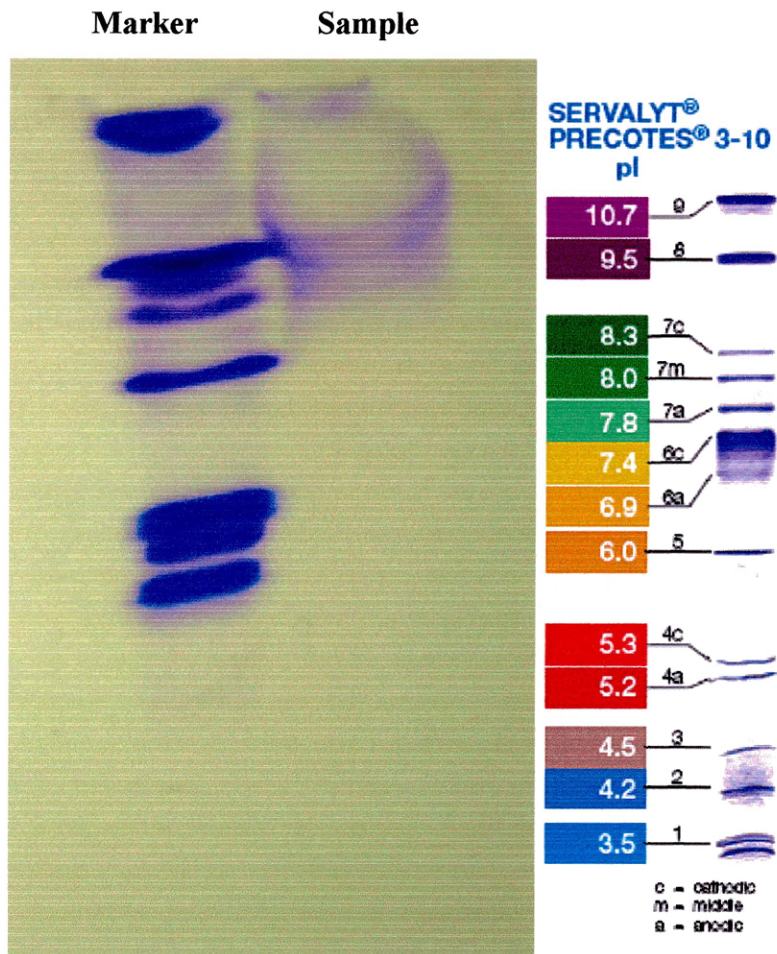


Figure 7.6 Isoelectric focusing gel on rabbit-anti-gamma phage antibodies

7.2.2.6 Colloidal Gold Conjugation to Gamma Phage and Rabbit Anti-Gamma Phage

Millenia Diagnostics Inc. had not previously conjugated colloidal gold to phage particles, so normal antibody-colloidal gold complex procedures were followed and the liquid conjugate sent to CSM for TEM analysis. TEM pictures were used to determine the proper pH and best blocking substance for colloidal gold conjugation to gamma phage; pH 9.0 was selected for conjugation and PEG was used in place of bovine serum albumin (BSA) to block remaining active sites on the colloidal gold. Average colloidal gold particle size, shown as dark black spheres, was determined to be approximately 35 nm from the TEM picture shown in Figure 7.7. In addition, it was shown that colloidal gold preferentially attached both at the tip of the gamma phage tail and at the capsid. Plaque assays conducted as described in Section 4.5.2 showed that the colloidal gold-conjugated gamma phage were still infective with the colloidal gold particles attached.

7.2.2.7 HHA 1 Version 1 Testing

The results of this testing showed no visual signal at the test line for all three ODs of 0.225, 0.45, and 0.825. The lower two ODs were representative of vegetative *B. anthracis*, so it was expected that the gamma phage would have attached to the *B. anthracis* cell wall. Possibly, there was not sufficient time for enough gamma phage particles to attach as the *B. anthracis* wicked down the membrane. All strips produced a strong positive control signal showing that gamma phage was successfully conjugated to colloidal gold particles.

7.2.2.8 HHA 1 Version 2 Testing

The results of this testing showed no visual signal at the test line for the two ODs of 0.225 and 0.45 after allowing up to 30 minutes for gamma phage adsorption to take place.

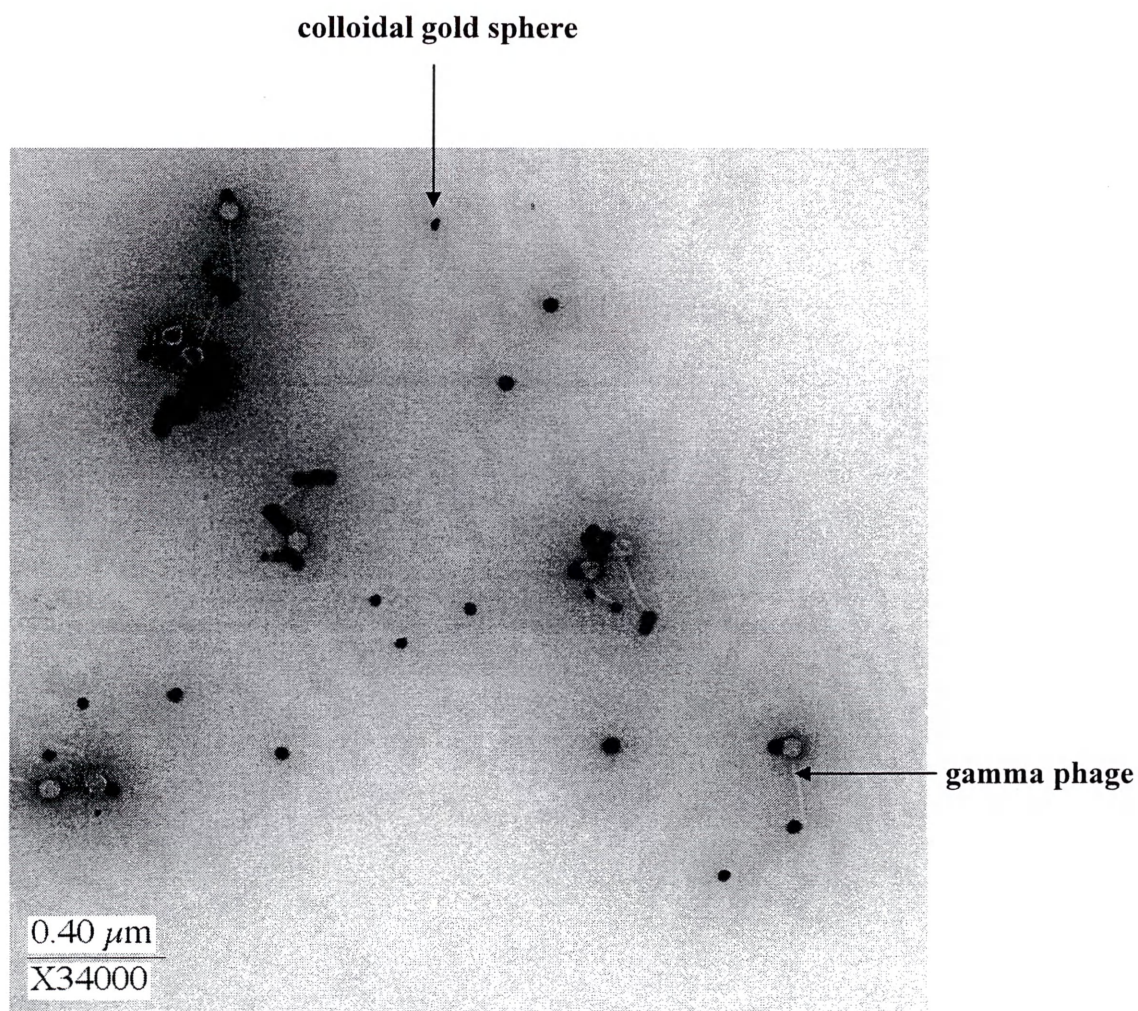


Figure 7.7 Colloidal gold-conjugated to gamma phage

The additional tests allowing for up to 90 minutes for gold-conjugated gamma phage adsorption to *B. anthracis* also tested negative. This could be a result of few gamma phage adsorption events taking place thereby not concentrating enough on the test line to be visible. All strips produced a strong positive control line signal showing that gamma phage was successfully conjugated to colloidal gold particles and in sufficient amounts to be seen. Table 7.3 shows the ICP-MS results from Huffman Laboratories Inc. and descriptions for the sample labels follow. An unused HHA 1 version 2 was used as a negative control and was labeled LCB-C, LCB-T, and LCB-S for liquid conjugate blank. The letter after the dash represented the 0.2 inch section of nitrocellulose removed as a sample; the “C” for the control line area, the “T” for the test line area, and the “S” for the area with no antibody stripping. The LC30, LC60, and LC90 labels represent HHAs that were tested as described in Section 7.2.1.10 for 30, 60, or 90 minutes. The gamma light and heavy labels represent HHA 2 gamma phage detectors that tested positive with a score of 1+ and 3+ respectively. These HHA 2 results should provide an estimate of the number of gold particles, or gold mass, required for positive assay results. From Table 7.3, the sample sections containing the control line all had Au values of 167 ng or higher. It appeared from the gamma light-T results, that any concentrated amount of gold of at least 38 ng would produce a positive test result (1+). The LC30-T, LC60-T, and LC90-T amounts of gold detected with ICP-MS showed no apparent concentration of gold along the test lines. This meant either the gold-conjugated gamma phage was not adsorbing to the *B. anthracis* as expected or that the rabbit anti-*B. anthracis* antibodies were not capturing the bacteria with adsorbed gamma phage along the test line.

Table 7.3 ICP-MS Au analysis of HHA strips

Sample	Au mass (in ng)	Au fraction (Au on 0.2 inch section/ total Au on all three sections)
LCB-C	<1	0.41
LCB-T	<1	0.30
LCB-S	<1	0.29
LC30-C	167	0.76
LC30-T	9	0.04
LC30-S	43	0.20
LC60-C	198	0.82
LC60-T	6	0.02
LC60-S	38	0.16
LC90-C	207	0.87
LC90-T	6	0.02
LC90-S	24	0.10
gamma light-C	190	0.81
gamma light-T	38	0.16
gamma light-S	6	0.02
gamma heavy-C	294	0.63
gamma heavy-T	132	0.28
gamma heavy-S	44	0.09

7.2.3 Discussion and Conclusions

Unfortunately, neither HHA 1 version 1 nor version 2 detected *B. anthracis* in several stages of vegetative growth using the adsorption of colloidal gold-conjugated gamma phage to the bacterial cell wall. The rabbit anti-gamma phage PABs were used only for the control line in the two versions of HHA 1 that were tested. Rabbit anti-*B. anthracis* PABs against both the spore and vegetative forms were used on the capture (or test) line. Because Millenia Diagnostics did not possess *B. anthracis*, they were not able to optimize the concentration of antibodies used along the capture line. Based on the results obtained, the rabbit anti-gamma phage antibodies appeared to work properly at the control line. However, testing of HHA 2 showed that the rabbit anti-gamma phage antibodies cross reacted significantly with autoclaved growth media (TSB and BHI). This cross reactivity was not as harmful on the control line as it would have been on the test line because the rabbit anti-gamma phage antibodies are just validating the proper operation of the HHA when used on the control line.

The kinetics of gamma phage adsorption as well as the quantity of adsorbing phage are key to this type of detection scheme. The results from HHA 1 version 1 suggest that the gamma phage adsorption to *B. anthracis* is not an immediate phenomenon or at least not in large enough numbers to produce positive test results. The additional tests using HHA 1 version 2, showed that gamma phage did not attach to *B. anthracis* in sufficient quantities to produce positive test results after 90 minutes. The Huffman Laboratories ICP-MS results indicated that the gold was not concentrating along the test line. The results mean either the gamma phage was not adsorbing to the *B. anthracis* or the rabbit anti-*B. anthracis* capture antibodies produced by Tetracore Inc. were not capturing the *B. anthracis* cells with gamma phage attached.

The ELISA results on the final rabbit bleeds, shown in Table 7.2, indicated that the rabbits had excellent immunogenic responses to the gamma phage antigen and that a good concentration of antibodies was demonstrated in R7515 up through a 1:312,500

antibody dilution. The oxidation of ABTS (substrate) by hydrogen peroxide catalyzed by the HRP enzyme produced a soluble blue-green colored product that could be measured at 405 nm with a conventional plate reader. The intensity of the developed color correlates to the concentration of the primary antibody (rabbit anti-gamma phage). Any OD reading above 1.0 is considered to be a good Ig titer. Based on the results of the final bleed ELISAs shown in Table 7.2, rabbit serum from R7215 and R7216 were combined and further purified. These ELISA results showed that the serum from rabbit R7214 could also have been used, but was not because of the additional costs that would be incurred with further purification.

The SDS-PAGE results in Figure 7.4 show many Igs and other proteins initially present (shown in Lane 1) that were later washed from the affinity purification column (shown in Lane 2). The SDS-PAGE results in Lanes 3 through 8 showed that the antigen affinity purification column did an effective job removing many other Igs from the final bleed serum that were non-specific towards the gamma phage attached on the inner walls of the column. A Protein G purification step was added after a purity of >31% was estimated from the SDS-PAGE results. The extra higher molecular weight proteins that eluted with the antibody are mostly due to non-specific binding to the unreacted coupling gel. This is difficult to control because it is hard to know exactly how much coupling gel to use so that it binds all of the antigen without having excess coupling gel which will be unreacted, and therefore will bind proteins non-specifically. Antigen affinity columns can often bind proteins non-specifically, resulting in varying degrees of purity. The additional proteins could interfere with the colloidal gold-conjugating to the rabbit anti-gamma phage antibodies, so a Protein G column was then run to remove these high molecular weight proteins from the Igs. Protein G purification of the rabbit anti-gamma phage resulted in an Ig purity of 98.7 % measured by PAGE. Although this data showed highly pure antibodies, it is important to realize that the amount of antibody which is specific for the gamma phage antigen will still only be a fraction of the total purified antibody.

The antibody pI was used to set the pH in the colloidal gold conjugation procedures. PAbs consist of many different Igs, so the IEF gel will not be able to determine a single pI. The IEF results narrowed the pI down to a range between 8.0 and 8.5.

Initial TEM results showed problems conjugating colloidal gold directly to the gamma phage using procedures typically used by Millenia Diagnostics to conjugate gold to antibodies. The presence of BSA, used by Millenia Diagnostics to block reactive gold sites, appeared to impede the conjugation process as did the pH of 8.0. Through additional TEM studies varying both the pH and the blocking agent, PEG was substituted as the blocking agent and a pH of 9.0 was selected. TEM pictures, like in Figure 7.7, showed that colloidal gold preferentially attached at the capsid and the tail of the phage. The colloidal gold conjugation to phage did not seem to affect adsorption of the phage to *B. anthracis* based on positive plaque assays, represented by 5 to 10 mm plaques or clearings, done with the liquid gamma phage colloidal gold conjugate.

7.3 Hand-Held Immunoassay 2 (HHA 2)

Hand-held immunoassay 2 (HHA 2) was designed and built to detect gamma phage amplification. Gamma phage at a concentration below the predetermined DL of HHA 2 would be added to a sample suspected of containing *B. anthracis*. Since *B. anthracis* would typically be found in the sporulated state, BHI growth media along with other nutrients would be added to promote the germination of the spores. Germination of *B. anthracis* spores can start to happen as quickly as 10 minutes after appropriate growth conditions are provided as reported in Section 4.6. The vegetative *B. anthracis* would increase the amount of gamma phage present from its initial amount to beyond the DL, and thereby implying the presence of *B. anthracis*. Colloidal gold, used as the visual detection method, was conjugated (attached) directly to the rabbit anti-gamma phage antibodies by Millenia Diagnostics and stripped on the detector line. The test (or capture) line was stripped with unconjugated rabbit anti-gamma phage antibodies. The control

line was stripped with goat anti-rabbit antibodies. A schematic of HHA 2 is shown in Figure 7.8.

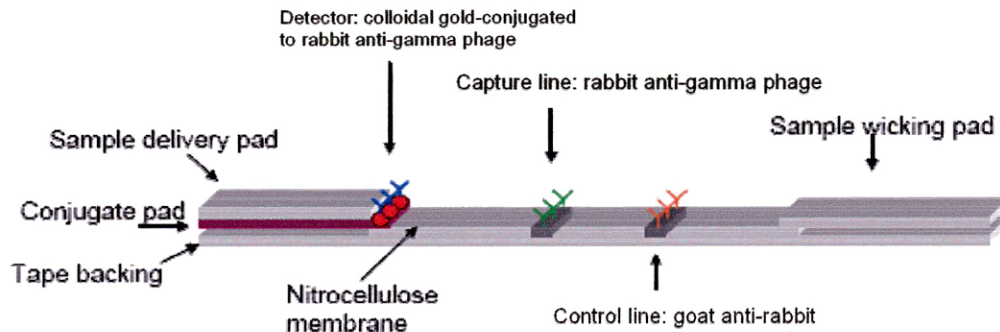


Figure 7.8 Design of HHA 2

This detector was being built to answer the following questions: 1) Is this detection assay specific for *B. anthracis*? 2) Can the same polyclonal antibodies be used for both the detector and test (or capture) lines? 3) Can the viability of *B. anthracis* be proven? 4) How reproducible are the results? 5) Is there an improvement in DL from directly detecting *B. anthracis*?

7.3.1 Materials and Methods

7.3.1.1 HHA 2 Production (See Figure 7.8)

Prototype test devices for gamma phage were constructed using the following conditions: nitrocellulose membrane from Millipore catalog (HF 120) was used as the solid phase for the assay. The test (or capture) line reagent was prepared and stripped

with rabbit anti-gamma phage (Lot: S6071623) antibodies from Harlan Bioproducts for Science diluted in 25 mM potassium phosphate at pH 7.4 at a concentration of 0.75 mg/mL and stripped at 1.0 μ L/cm. The control line was prepared with goat anti-rabbit IgG (Lot: 100997) antibodies diluted in 25 mM potassium phosphate at a concentration of 0.5 mg/mL and stripped at 1.0 μ L/cm. All stripping was done using a Kinematic Automation Reagent Dispensing Module model Matrix 1600. Stripped membranes were blocked using MDx lateral flow blocking solution and dried prior to assembling into test cards. Membranes and stripped conjugate pads were assembled into test cards using sample pad Ahlstrom cytosep 1662 2.0 cm and absorbent pad Ahlstrom 222. The membranes were then cut into 4.5 mm strips, using Kinematic Automation Programmable Shear model Matrix 2360, assembled into cassettes and pouched with desiccant.

7.3.1.2 Colloidal Gold Conjugation to Rabbit Anti-Gamma Phage Antibodies

Colloidal gold particles (reported to be 40 nm) in a suspension were adjusted to a pH of 8.4. Rabbit anti-gamma phage antibodies were dialyzed in 10 mM potassium phosphate at pH 7.4 prior to conjugation. Rabbit anti-gamma phage antibodies were conjugated to the colloidal gold particles at pH 8.4 and blocked with MDx conjugate blocking solution at pH 8.6. The conjugate was purified and concentrated by centrifugation at 7000 x g for 45 minutes at 4 °C. The supernatant was removed and the conjugate pellet was then resuspended in MDx conjugate stabilizer to OD₅₂₀=10. The conjugate was stripped at 6.0 μ L/cm on blocked glass fiber and dried at 37 °C for 45 minutes.

7.3.1.3 HHA 2 Testing

To test the device, 75 μ l of sample was added to the sample pad, allowed to wick down the nitrocellulose membrane, and the results were read at 15 minutes. The previously defined test scale that was used for all HHA testing is: 0 = no test line, 1+ = very faint test line, 2+ = test line less intense than control line, 3+ = test line as intense as control line, and 4+ = test line more intense than control line. Negative controls were tested first. Liquids tested included: autoclaved and unautoclaved BHI, autoclaved and unautoclaved PBS, autoclaved and unautoclaved TSB, unautoclaved nutrient broth, deionized water, and Milli-Q water.

In an effort to obtain gamma phage DL information, three independent gamma phage solutions that had previously been purified by CsCl gradients and dialyzed in Milli-Q water were used. The gamma phage titers (5.8×10^8 pfu/mL, 2.3×10^7 pfu/mL, and 5.6×10^7 pfu/mL) were determined by plaque assays described in Section 4.5.2. These gamma phage suspensions were then 10-fold serially diluted in Milli-Q water and run twice each on HHA 2 to determine the gamma phage DL.

7.3.2 Results

7.3.2.1 HHA 2 Testing

Negative controls were evaluated using 75 μ L of test sample. Autoclaved BHI gave positive results (3+), unautoclaved BHI gave positive results (1+), autoclaved BHI diluted 1:1500 in running buffer gave positive results (1+), autoclaved PBS gave positive results (3+), unautoclaved PBS gave positive results (2+), autoclaved TSB gave positive results (3+), unautoclaved TSB gave positive results (2+), unautoclaved nutrient broth gave positive results (1+), Milli-Q water gave negative results (0) and deionized water gave negative results (0). These tests confirmed that HHA 2 was experiencing serious

cross reactivity problems. All strips produced a strong positive control signal showing that rabbit anti-gamma phage was successfully conjugated to colloidal gold particles in detectable amounts. Because of the positive results obtained with the negative controls, three different gamma phage samples that were CsCl purified and dialyzed into Milli-Q water were 10-fold serially diluted in Milli-Q and run on HHA 2. The gamma phage concentrations tested on HHA 2 are shown in Tables 7.4, 7.5, and 7.6.

Table 7.4 Test HHA 2 with gamma phage dilution series (5.8×10^8 pfu/mL)

[gamma phage]	HHA 2 Results
5.8×10^7 pfu/mL	2+
5.8×10^6 pfu/mL	2+
5.8×10^5 pfu/mL	1+
5.8×10^4 pfu/mL	1+
5.8×10^3 pfu/mL	0

Table 7.5 Test HHA 2 with gamma phage dilution series (2.3×10^7 pfu/mL)

[gamma phage]	HHA 2 Results
2.3×10^7 pfu/mL	2+
2.3×10^6 pfu/mL	2+
2.3×10^5 pfu/mL	2+
2.3×10^4 pfu/mL	1+
2.3×10^3 pfu/mL	0

Table 7.6 Test HHA 2 with gamma phage dilution series (5.6×10^7 pfu/mL)

[gamma phage]	HHA 2 Results
5.6×10^7 pfu/mL	2+
5.6×10^6 pfu/mL	2+
5.6×10^5 pfu/mL	2+
5.6×10^4 pfu/mL	1+
5.6×10^3 pfu/mL	0

The average gamma phage DL determined from three independent gamma phage dilution series was 4.6×10^4 pfu/mL (equivalent to 3.4×10^3 gamma phage particles in 75 μ L).

7.3.3 Discussion and Conclusions

The simplicity of the HHA is its biggest advantage. Although it was well known that PABs are subject to cross reactivity problems, the strong positive (3+) HHA 2 test result with autoclaved BHI media was not expected. Because gamma phage amplification through the lytic replication cycle requires vegetative *B. anthracis*, BHI growth media could not be eliminated unless a suitable growth media replacement could be found. Unfortunately, two other common growth medias (TSB and nutrient broth) tested positive as well. One explanation for the positive BHI test result, given the decrease in unautoclaved BHI signal, was that a denatured protein from autoclaved BHI was the culprit. If the CsCl purified gamma phage contained some denatured BHI proteins left over from the gamma phage propagation and purification procedures, these proteins could have produced an antigen immunological response in the rabbits. If this happened, antibodies specific towards the denatured proteins would have developed and

would lead to an undesirable specific binding event. Another feasible explanation is that a very strong non-specific binding is taking place with the BHI media. This explanation is potentially supported by the strong positive test results using PBS. PBS contains nothing big enough to produce an immunological response, so a non-specific problem with the antibodies seems possible. This non-specific binding problem could be the direct result of using the same PAb for both the detector and capture antibodies on HHA 2.

Bacteriophage amplification experiments to determine the *B. anthracis* detection limit were not done because of the cross reactivity HHA 2 had with growth media. Vegetative bacterial growth, hence bacteriophage amplification, can not be supported without growth media. CsCl purified gamma phage that was dialyzed into Milli-Q water was used to demonstrate a DL for gamma phage using HHA 2. These tests resulted in an excellent DL of 4.6×10^4 pfu/mL (3.4×10^3 particles) compared with HHAs that directly detect *B. anthracis* with reported DLs of 10^5 to 10^8 cfu/mL. The CsCl gradients must remove enough of the contaminant that it no longer is detected with HHA 2; however, running difficult and time consuming CsCl gradients with every sample was not practical.

Although good specificity was not demonstrated with this HHA, the use of a conjugated MAbs for the detector line would have eliminated the cross reactivity of the BHI growth media. Antibody combinations should be “matched pairs”, that is they should recognize different epitopes on the antigen so they do not hinder each other’s binding [65]. Reproducibility of HHA 2 was demonstrated as all tests were run at least in duplicate and gave the same results each time. Different preparations of growth media all produced the same reproducible results. After eliminating the cross reactivity problem, this type of HHA has the capability to replace or at least supplement the current HHAs being used to directly detect *B. anthracis*. The increased sensitivity for gamma phage, the bacterial viability required for gamma phage amplification, and the ability to spike the sample with gamma phage just below the HHA 2 DL makes this method extremely attractive.

CHAPTER 8

PROJECT ASSESSMENT AND FOLLOW-ON WORK

8.1 Project Overview

The overall goal of the research described in this dissertation was to design, develop, and assess gamma phage amplification assays to indirectly identify *B. anthracis*. The objectives used to achieve this goal were: 1) to characterize the gamma phage/*B. anthracis* system in terms of morphology, physiology and optimal growth conditions; 2) to propagate and highly purify gamma phage for antibody development; 3) to design and develop assays using the gamma phage amplification phenomenon to indirectly identify *B. anthracis*; and 4) to assess the gamma phage-based assays in terms of simplicity of use, cost, speed, specificity, DL, and reproducibility. As more questions were raised than answered, my research grew into a project that ultimately involved four different detection schemes. One scheme, using HHA 1 version 1 and version 2, was designed to detect the highly specific gamma phage adsorption to *B. anthracis*. The other three schemes using RT-PCR, MALDI-TOF-MS, and HHA 2 were designed to detect amplified amounts of gamma phage produced through the highly specific gamma phage lytic replication cycle using *B. anthracis* as the host. RT-PCR had been used to detect and identify both bacteria and viruses, but it had not been used to indirectly identify the bacteria through the detection of its bacteriophage amplification. In addition to the RT-PCR studies, experiments were conducted using MALDI-TOF-MS to detect the amplified gamma phage through the use of protein biomarkers. Although MALDI-TOF-MS is currently a relatively expensive laboratory-based technique, its ability to rapidly analyze samples without complex sample preparation steps made it an attractive platform

to study for this application. Lastly, an HHA was designed, developed, and evaluated for its ability to indirectly detect *B. anthracis* through detecting gamma phage amplification. HHAs are known for their simplicity of use and ability to get quick results; they are commonly being used in the field for pathogen detection, but the bacteriophage amplification detection method studied here would provide a totally different way of using them.

8.2 Assessment of Project

The overall goal of designing, developing, and assessing gamma phage amplification assays to indirectly identify *B. anthracis* was achieved with varying degrees of success obtained in reaching the specific objectives. The gamma phage/*B. anthracis* system is better understood with the optimum growth conditions for *B. anthracis* and gamma phage amplification determined to be at 37 °C in BHI growth media. The gamma phage was effectively propagated on 5% SBA plates and thought to be highly purified using the CsCl gradients. Unfortunately, some BHI growth media proteins that remained after the purification steps might have produced an immune response in the rabbits when developing antibodies against gamma phage. This unexpected antibody development towards growth media proteins could explain the cross reactivity problem experienced with HHA 2 against several different growth medias. RT-PCR has been used extensively in pathogen detection, but using RT-PCR to indirectly detect a pathogen through its bacteriophage was something not found in my literature searches. To use RT-PCR to detect the gamma phage, the gamma phage DNA primers were designed from scratch since none were commercially available. RT-PCR was used to detect a starting *B. anthracis* concentration of four cells in less than five hours using gamma phage amplification. RT-PCR used in this manner could replace the currently used CDC gamma phage lysis method of confirming *B. anthracis*. At the very least, RT-PCR to detect gamma phage DNA could be used to provide bacterial viability information not

normally obtained when using other detection methods. The RT-PCR aspect of this project was deemed successful based on these positive results. MALDI-TOF-MS was used to detect gamma phage proteins, but not very effectively. The experimentally determined MALDI gamma phage DL of 10^7 to 10^8 pfu/mL was too high to be used with the gamma phage/*B. anthracis* system. Gamma phage amplification in liquid BHI media only produced gamma phage titers between 10^6 and 10^7 pfu/mL. This concentration is just at the detection limit of MALDI, so MALDI was not an effective detection platform for the gamma phage/*B. anthracis* system. Other phage/host systems might work better. HHA 1 versions 1 and 2 were unable to demonstrate any detection of the attachment of gold-conjugated gamma phage on *B. anthracis*. Although not successful in the ultimate detection goal, conjugation of colloidal gold to gamma phage and adsorption of gamma phage to *B. anthracis* were demonstrated by electron microscopy. HHA 2 had problems with cross reactivity, but also showed great potential in its low gamma phage DL of 4.6×10^4 pfu/mL. With MAbs being used as the detector antibodies, the cross reactivity problem could be fixed and this detection scheme could exceed the detection capabilities of the HHAs currently being used. Some of the greater successes of this project were found in characterizing and understanding the gamma phage/*B. anthracis* system that was fundamental to all the detection schemes. Experimenting with a living microorganism added a complexity and variability that had to be thoroughly studied and managed. Seemingly small perturbations to the growth conditions were shown to have large consequences to the overall gamma phage/*B. anthracis* system. The success of bacteriophage amplification was totally dependent on healthy and actively growing bacteria. Only when the gamma phage/*B. anthracis* system was optimized, could these detection schemes have any chance of success.

8.3 Recommended Follow-on Work

For all the detection assays, but especially for MALDI, additional growth medias should be studied to maximize the amount of gamma phage produced in the fastest time. Additional chemical components, like blood or amino acids, added to BHI could make this media even more effective at supporting additional gamma phage growth. The propagation of gamma phage on 5 % SBA plates produced higher titers of gamma phage compared with propagating gamma phage in liquid media. The solid agar media or the 5 % blood could be the critical contributor. Follow-on studies are currently planned to test this RT-PCR assay's specificity against other bacteriophages and to test this assay using environmental and clinical samples without prior isolation cultures. Since other bacteriophages are present in the environment, it is very important to ensure they do not cross react with the gamma phage DNA primers and produce a false positive RT-PCR result. Host range studies should also be conducted, but would require BSL-3 workspace and clearances to work with these select agents. Since the gamma phage DNA primers were very specific and the phage DNA samples did not have to be purified prior to amplification by RT-PCR, this method should be very amenable to non-culture identification of *B. anthracis*. Isolation cultures are typically used with many *B. anthracis* detection methods, but they add an additional 18 to 24 hours to the analysis time. In addition, RT-PCR can quantify the gamma phage. If the amount of DNA per phage particle is known, RT PCR can quantify the amount of phage DNA present and then the number of phage can be calculated [70]. Concentration information on both the gamma phage and the *B. anthracis* would be valuable additional information that should be pursued. For the HHAs, MAbs should be produced against gamma phage to eliminate the cross reactivity problems experienced and greatly improve the HHA detection capabilities. Additional testing using *B. anthracis* spores should also be done. Since bacteriophage amplification depends upon the presence of vegetative bacterial cells, finding ways to accelerate the germination of *B. anthracis* spores is critical to minimizing

the testing time. Dugway Proving Grounds has a chamber for generating known spore concentrations [6] that might be utilized for these additional studies. Finally, assay optimization to include standardizing and validating sampling, extraction, testing, and analysis protocols needs to be done for all the methods described in this dissertation. To validate these protocols, they should be subjected to reproducibility and accuracy studies conducted by different laboratories with different analysts using a known concentration of *B. anthracis*. Since 2001, laboratory studies have shown that pre-moistened cotton and macrofoam swabs worked best, compared with polyester and rayon, in surface sampling to recover *B. anthracis* spores; they had a mean recovery of 43.6% after vortexing [71]. Findings such as these could easily be incorporated into sampling protocols developed for the four detection methods studied in this dissertation.

REFERENCES CITED

1. Madigan, M.T. and J.M. Martinko, *Brock Biology of Microorganisms*. 11th ed. 2006, Upper Saddle River: Pearson Education, Inc.
2. Popovic, T., A. Hoffmaster, J.W. Ezzell, T.G. Abshire, and J.E. Brown, *Validation of Methods for Confirmatory Identification of Presumptive Isolates of Bacillus anthracis*. Journal of AOAC International, 2005. **88**(1): p. 175-177.
3. Saffer, B., *Anthrax*. Diseases and Disorders. 2004, San Diego: Lucent Books.
4. Meselson, M., J. Guillemin, M. Hugh-Jones, A. Langmuir, I. Popova, and A. Shelokov, *The Sverdlovsk Anthrax Outbreak of 1979*. Science, 1994. **266**: p. 1202-1208.
5. Frist, B., *When Every Moment Counts: What You Need to Know about Bioterrorism from the Senate's Only Doctor*. 2002, Boulder: Rowman & Littlefield Publishers, Inc.
6. Congress, U.S., *Assessing Anthrax Detection Methods*, U.S. Congress, Editor. 2005, U.S. Government Printing Office. p. 1-242.
7. Decker, J., *Anthrax*. Deadly Diseases and Epidemics. 2003, Philadelphia: Chelsea House.
8. Congress, U.S., *Proliferation of Weapons of Mass Destruction: Assessing the Risks*. 1993, Government Printing Office.
9. Bush, G.W., *The National Security Strategy of the United States of America*, President, Editor. 2002, White House. p. 4.
10. Thompson, M.W., *The Killer Strain: Anthrax and a Government Exposed*. 2003, New York: HarperCollins Publishers Inc.
11. Matsumoto, G., *Anthrax Powder: State of the Art?*, in *Science*. 2003. p. 1492-1497.

12. Weis, C., A. Intrepido, A. Miller, P. Cowin, M. Durno, and J. Gebhardt, *Secondary Aerosolization of Viable Bacillus anthracis Spores in a Contaminated U.S. Senate Office*. JAMA, 2002. **288**(22): p. 2853-2858.
13. Vitko, J., D.R. Franz, M. Alper, P. Biggins, L.D. Brandt, C. Bruckner-Lea, and H.A. Burge, *Sensor Systems for Biological Agent Attacks: Protecting Buildings and Military Bases*. 2005, National Research Council of the National Academies: Washington. p. 1-196.
14. CDC. *Select Agent Program*. 2006 [cited 2006 2006/04/15]; Available from: <http://www.cdc.gov/od/sap/>.
15. CDC. *Bioterrorism Agents/Diseases*. 2006 [cited 2006 2006/04/15]; Available from: <http://www.bt.cdc.gov/agent/agentlist-category.asp>.
16. CDC. *Facts about the Laboratory Response Network*. 2005 [cited 2006; Available from: <http://www.bt.cdc.gov/lrn/factsheet.asp>.
17. CDC (2001) *Use of Onsite Technologies for Rapidly Assessing Environmental Bacillus anthracis Contamination on Surfaces in Buildings*. Morbidity and Mortality Weekly Report **Volume**, 1087
18. Abshire, T.G., J.E. Brown, and J.W. Ezzell, *Production and Validation of the Use of Gamma Phage for Identification of Bacillus anthracis*. Journal of Clinical Microbiology, 2005. **43**(9): p. 4780-4788.
19. CDC, *Basic Diagnostic Protocols for Level A Laboratories for the Presumptive Identification of Bacillus anthracis*. 2002. p. 1-22.
20. Turnbull, P.C.B. *Guidelines for the Surveillance and Control of Anthrax in Humans and Animals. 3rd Edition*. 1998 [cited 2006 04/28/2006].
21. De, B.K., S.L. Bragg, G.N. Sanden, K.E. Wilson, L.A. Diem, C.K. Marston, A.R. Hoffmaster, G.A. Barnett, R.S. Weyant, T.G. Abshire, J.W. Ezzell, and T. Popovic, *Two-Component Direct Fluorescent-Antibody Assay for Rapid Identification of Bacillus anthracis*. Emerging Infectious Disease, 2002. **8**(10): p. 1060-1065.

22. Kubista, M., J.M. Andrade, M. Bengtsson, A. Forootan, J. Jonák, K. Lind, R. Sindelka, R. Sjöback, B. Sjögreen, L. Strömbom, A. Ståhlberg, and N. Zoric, *The Real-Time Polymerase Chain Reaction*. Molecular Aspects of Medicine, 2006. **27**: p. 95-125.
23. Christensen, D.R., L.J. Hartman, B.M. Loveless, M.S. Frye, M.A. Shipley, D.L. Bridge, M.J. Richards, R.S. Kaplan, J. Garrison, C.D. Baldwin, D.A. Kulesh, and D.A. Norwood, *Detection of Biological Threat Agents by Real-Time PCR: Comparison of Assay Performance on the R.A.P.I.D., the LightCycler, and the Smart Cycler Platforms*. Clinical Chemistry, 2006. **52**(1): p. 141-145.
24. Hoffmaster, A.R., R.F. Meyer, M.P. Bowen, C.K. Marston, R.S. Weyant, K. Thurman, S.L. Messenger, E.E. Minor, J.M. Winchell, M.V. Rassmussen, B.R. Newton, J.T. Parker, W.E. Morrill, N. McKinney, G.A. Barnett, J.J. Sejvar, J.A. Jernigan, B.A. Perkins, and T. Popovic, *Evaluation and Validation of a Real-Time Polymerase Chain Reaction Assay for Rapid Identification of Bacillus anthracis*. Emerging Infectious Diseases, 2002. **8**(10): p. 1178-1182.
25. Edwards, K.A., H.A. Clancy, and A.J. Baeumner, *Bacillus anthracis: Toxicology, Epidemiology and Current Rapid-Detection Methods*. Analytical and Bioanalytical Chemistry, 2006. **384**: p. 73-84.
26. Tetracore[®], *RedLine Alert[™] Test: An Immunochromatographic Test Kit for the Presumptive Identification of Bacillus anthracis Colonies from Culture Plates* 2004: Gaithersburg. p. 1-15.
27. Bellenir, K., ed. *Infectious Diseases Sourcebook*. 1st ed. 2004, Omnigraphics, Inc.: Detroit.
28. Thorne, C.B., *Bacillus subtilis and other Gram-positive Bacteria: Biochemistry, Physiology, and Molecular Genetics*. *Bacillus anthracis*, ed. R. Losick. 1993, Washington, D.C.: American Society for Microbiology. 113-124.
29. Fischetti, V.A., R.P. Novick, J.J. Ferretti, D.A. Portnoy, and J.I. Rood, *Gram-Positive Pathogens*. 2000, Washington: ASM press.
30. Wesche, J., J.L. Elliot, P.O. Falnes, S. Olsnes, and R.J. Collier, *Characterization of Membrane Translocation by Anthrax Protective Antigen*. Biochemistry, 1998. **37**: p. 15737-15746.

31. Todar, K. *The Genus Bacillus*. Todar's Online Textbook of Bacteriology 2005 [cited 2006 19 November 2006]; Available from: <http://textbookofbacteriology.net/Bacillus.html>.
32. Schuch, R. and V.A. Fischetti, *Detailed Genomic Analysis of the $W\beta$ and γ Phages Infecting Bacillus anthracis: Implications for Evolution of Environmental Fitness and Antibiotic Resistance*. Journal of Bacteriology, 2006. **188**(8): p. 3037-3051.
33. Todar, K. *Growth of Bacterial Populations*. Todar's Online Textbook of Bacteriology 2002 [cited 2006 17 May 2006]; Available from: <http://textbookofbacteriology.net/growth.html>.
34. Cairns, J., G.S. Stent, and J.D. Watson, *Phage and the Origins of Molecular Biology*. 1966, Cold Spring Harbor, New York: Cold Spring Harbor Laboratory.
35. Summers, W.C., *Bacteriophage Research: Early History*. Bacteriophages Biology and Applications, ed. E. Kutter and A. Sulakvelidze. 2005, Washington, D.C.: CRC Press.
36. Elford, W.J. and C.H. Andrewes, *The Sizes of Different Bacteriophages*. Brit. J. Exp. Pathol., 1932. **13**: p. 446.
37. Delbrück, M. and W.T. Bailey, *Cold Spring Harbor Symp. Quant. Biol.*, 1946. **11**: p. 33.
38. Lwoff, A. and A. Gutmann, *Recherches sur un Bacillus megathérium lysogène*. Ann. Inst. Pasteur, 1950. **78**: p. 711.
39. Loeb, T. and N.D. Zinder. in *Proc. Natl. Acad. Sci.* 1961. U.S.
40. Cowles, P.B., *A Bacteriophage for B. anthracis*. Journal of Bacteriology, 1931. **21**: p. 161-169.
41. McCloy, E.W., *Studies on a Lysogenic Bacillus Strain. I. A Bacteriophage Specific for Bacillus anthracis*. J. Hyg., 1951. **49**: p. 114-125.
42. Brown, E.R. and W.B. Cherry, *Specific Identification of Bacillus anthracis by Means of a Variant Bacteriophage*. Journal of Infectious Diseases, 1955. **96**: p. 34-39.

43. Watanabe, T., A. Morimoto, and T. Shiomi, *The Fine Structure and Protein Composition of γ Phage of Bacillus anthracis*. Canadian Journal of Microbiology, 1975. **21**: p. 1889-1892.
44. Guttman, B., R. Raya, and E. Kutter, *Basic Phage Biology*. Bacteriophages Biology and Applications, ed. E. Kutter and A. Sulakvelidze. 2005, Washington, D.C: CRC Press.
45. Fouts, D.E., D.A. Rasko, R.Z. Cer, L. Jiang, N.B. Fedorova, A. Shvartsbeyn, J.J. Vamathevan, L. Tallon, R. Althoff, T.S. Arbogast, D.W. Fadrosh, T.D. Read, and S.R. Gill, *Sequencing Bacillus anthracis Typing Phages Gamma and Cherry Reveals a Common Ancestry*. Journal of Bacteriology, 2006. **188**(9): p. 3402-3408.
46. Carlson, K., *Appendix: Working with Bacteriophages: Common Techniques and Methodological Approaches*. Bacteriophages Biology and Applications, ed. E. Kutter and A. Sulakvelidze. 2005, Boca Raton: CRC Press. 437-490.
47. Yamamoto, K.R., B.M. Alberts, R. Benzinger, L. Lawhorne, and G. Treiber, *Rapid Bacteriophage Sedimentation in the Presence of Polyethylene Glycol and its Application to Large-scale Virus Purification*. Virology, 1970. **40**: p. 734-744.
48. Sambrook, J. and D.W. Russell, *Molecular Cloning: A Laboratory Manual*. 3rd ed. 2001, Cold Spring Harbor: Cold Spring Harbor Laboratory Press.
49. Kohno, T., S. Mohan, T. Goto, C. Morita, T. Nakano, W. Hong, J.C.E. Sangco, S. Morimatsu, and K. Sano, *A New Improved Method for the Concentration of HIV-1 Infective Particles*. Journal of Virological Methods, 2002. **106**: p. 167-173.
50. Ellis, E.L. and M. Delbrück, *The Growth of Bacteriophage*. Journal of General Physiology, 1939. **22**: p. 365-384.
51. Davison, S., E. Couture-Tosi, T. Candela, M. Mock, and A. Fouet, *Identification of the Bacillus anthracis γ Phage Receptor*. Journal of Bacteriology, 2005. **187**(19): p. 6742-6749.
52. Schuch, R., D. Nelson, and V.A. Fischetti, *A Bacteriolytic Agent that Detects and Kills Bacillus anthracis*. Nature, 2002. **418**: p. 884-889.
53. Brown, A.E., *Benson: Microbiological Applications Lab Manual*. 8th ed. 2001: The McGraw-Hill Companies. 120-124.

54. Kasman, L.M., A. Kasman, C. Westwater, J. Dolan, M.G. Schmidt, and J.S. Norris, *Overcoming the Phage Replication Threshold: a Mathematical Model with Implications for Phage Therapy*. Journal of Virology, 2002. **76**(11): p. 5557-5564.
55. Santo, L.Y. and R.H. Doi, *Ultrastructural Analysis during Germination and Outgrowth of Bacillus subtilis Spores*. Journal of Bacteriology, 1974. **120**: p. 475-481.
56. Trauger, S.A., T. Junker, and G. Siuzdak, *Investigating Viral Proteins and Intact Viruses with Mass Spectrometry*. Topics in Current Chemistry, 2003. **225**: p. 265-282.
57. Holland, R.D., J.G. Wilkes, F. Rafii, J.B. Sutherland, C.C. Persons, K.J. Voorhees, and J.O. Lay, *Rapid Identification of Intact Whole Bacteria Based on Spectral Patterns using Matrix-assisted Laser Desorption/Ionization with Time-of-flight Mass Spectrometry*. Rapid Communications in Mass Spectrometry, 1996. **10**: p. 1227-1232.
58. Evason, D.J., M.A. Claydon, and D.B. Gordon, *Exploring the Limits of Bacterial Identification by Intact Cell-Mass Spectrometry*. Journal of the American Society of Mass Spectrometry, 2001. **12**: p. 49-54.
59. Ryzhov, V., Y. Hathout, and C. Fenselau, *Rapid Characterization of Spores of Bacillus Cereus Group Bacteria by Matrix-assisted Laser Desorption-Ionization Time-of-Flight Mass Spectrometry*. Applied and Environmental Microbiology, 2000. **66**(9): p. 3828-3834.
60. Valentine, N., S. Wunschel, D. Wunschel, C. Petersen, and K. Wahl, *Effect of Culture Conditions on Microorganism Identification by Matrix-Assisted Laser Desorption Ionization Mass Spectrometry*. Applied and Environmental Microbiology, 2005. **71**(1): p. 58-64.
61. Madonna, A.J., S.V. Cuyk, and K.J. Voorhees, *Detection of Escherichia coli using Immunomagnetic Separation and Bacteriophage Amplification Coupled with Matrix-assisted Laser Desorption/Ionization Time-of-Flight Mass Spectrometry*. Rapid Communications in Mass Spectrometry, 2003. **17**: p. 257-263.

62. Rees, J.C. and K.J. Voorhees, *Simultaneous Detection of two Bacterial Pathogens using Bacteriophage Amplification Coupled with Matrix-Assisted Laser Desorption/Ionization Time-of-Flight Mass Spectrometry*. *Rapid Communications in Mass Spectrometry*, 2005. **19**: p. 2757-2761.
63. Tuma, R., H. Tsuruta, J.M. Benevides, P.E. Prevelige, and G.J. Thomas, *Characterization of Subunit Structural Changes Accompanying Assembly of the Bacteriophage P22 Procapsid*. *Biochemistry*, 2001. **40**: p. 665-674.
64. Madonna, A.J., F. Basile, I. Ferrer, M.A. Meetani, J.C. Rees, and K.J. Voorhees, *On-Probe Sample Pretreatment for the Detection of Proteins above 15 kDa from Whole Cell Bacteria by Matrix-assisted Laser Desorption/Ionization Time-of-Flight Mass Spectrometry*. *Rapid Communications in Mass Spectrometry*, 2000. **14**: p. 2220-2229.
65. Chemicon. *Introduction to Antibodies*. [cited September 24, 2006]; 2nd:[Available from: <http://www.chemicon.com/resource/litlibrary/ant101.pdf>].
66. Adams, M.H., *Bacteriophages*. 1959, New York: Interscience Publishers.
67. Burnett, F.M., E.V. Keogh, and D. Lush, *Australian J. Exp. Biol. and Med. Sc.*, 1937. **15**(Supplement to Part 3): p. 227.
68. Krueger, A.P., *Journal of General Physiology*, 1931. **14**: p. 493.
69. Beesley, J., *Colloidal Gold: A New Perspective for Cytochemical Marking*. 1989: Oxford University Press. 1-58.
70. Edelman, D.C. and J. Barletta, *Real-Time PCR Provides Improved Detection and Titer Determination of Bacteriophage*. *Biotechniques*, 2003. **35**: p. 368-375.
71. Rose, L., B. Jensen, A. Peterson, S.N. Bonerjee, and M.J. Ardvino, *Swab Materials and Bacillus anthracis Endospore Recovery from Surfaces*. *Emerging Infectious Diseases*, 2004. **10**(6): p. 1023.